geosciences

MDPI

Review

The Alpine Geological History of the Hellenides from the Triassic to the Present—Compression vs. Extension, a Dynamic Pair for Orogen Structural Configuration: A Synthesis

Adamantios Kilias

Department of Geology, Aristotle University of Thessaloniki, 54124 Thessaloniki, Greece; kilias@geo.auth.gr

Abstract: In this paper, the Hellenic orogenic belt's main geological structure and architecture of deformation are presented in an attempt to achive a better interpretation of its geotectonic evolution during Alpine orogeny. This study was based not only on recent research that I and my collaborators conducted on the deformational history of the Hellenides but also on more modern views published by other colleagues concerning the Alpine geotectonic reconstruction of the Hellenides. The structural evolution started during the Permo–Triassic time with the continental breaking of the supercontinent Pangea and the birth of the Neotethyan ocean realm. Bimodal magmatism and A-type granitoid intrusions accompanied the initial stages of continental rifting, followed by Triassic–Jurassic multiphase shallow- and deep-water sediment deposition on both formed continental margins. These margins were the Apulian margin, containing Pelagonia in the western part of the Neotethyan Ocean, and the European margin, containing continental parts of the Serbo-Macedonian and Rhodope massifs in the eastern part of the Neotethyan ocean. Deformation and metamorphism are recorded in six main deformational stages from the Early–Middle Jurassic to the present day, beginning with Early–Middle Jurassic Neotethyan intra-oceanic subduction and ensimatic island arc magmatism, as well as the formation of a suprasubduction oceanic lithosphere. Compression, nappe stacking, calc-alkaline magmatism, and high-pressure metamorphic events related to subduction processes alternated successively over time with extension, orogenic collapse, medium- to high-temperature metamorphism, adakitic and calc-alkaline magmatism, and partial migmatization related to the uplift and exhumation of deep crustal levels as tectonic windows or metamorphic core complexes. A S- to SW-ward migration of dynamic peer compression vs. extension is recognized during the Tertiary Alpine orogenic stages in the Hellenides. It is suggested that all ophiolite belts in the Hellenides originated from a single source, and this was the Neotethyan Meliata/Maliac-Axios/Vardar ocean basin, parts of which obducted during the Mid–Late Jurassic on both continental margins, Apulian (containing Pelagonia) and European (containing units of the Serbo-Macedonian/Rhodope nappe stack), W-SW-ward and E-NE-ward, respectively. In this case, the ophiolite nappes should be considered far-traveled nappes on the continental parts of the Hellenides associated with the deposition of Middle–Late Jurassic ophiolitic mélanges in basins at the front of the adjacent ophiolite thrust sheets. The upper limit of the ophiolite emplacement are the Mid–Upper Jurassic time(Callovian–Oxfordian), as shown by the deposition of the Kimmeridgian–Tithonian Upper Jurassic sedimentary carbonate series on the top of the obducted ophiolite nappes. The lowermost Rhodope Pangaion unit is regarded as a continuation of the marginal part of the Apulian Plate (External Hellenides) which was underthrust during the Paleocene–Eocene time below the unified Sidironero–Kerdylia unit and the Pelagonian nappe, following the Paleocene–Eocene subduction and closure of a small ocean basin in the west of Pelagonia (the Pindos–Cyclades ocean basin). It preceded the Late Cretaceous subduction of the Axios/Vardar ocean remnants below the European continental margin and the final closure of the Axios/Vardar ocean during the Paleocene–Eocene time, which was associated with the overthrusting of the European origins Vertiskos–Kimi nappe on the Sidironero–Kerdylia nappe and, subsequently, the final collision of the European margin and the Pelagonian fragment. Subsequently, during a synorogenic Oligocene–Miocene extension associated with compression and new subduction processes at the more external orogenic parts, the Olympos–Ossa widow and the

Citation: Kilias, A. The Alpine Geological History of the Hellenides from the Triassic to the Present—Compression vs. Extension, a Dynamic Pair for Orogen Structural Configuration: A Synthesis. *Geosciences* **2024**, *14*, 10. https://doi.org/10.3390/geosciences14010010

Academic Editors: Ilias Lazos, Emmanouil Steiakakis, George Xiroudakis, Sotirios Sboras and Jesus Martinez-Frias

Received: 25 October 2023
Revised: 9 December 2023
Accepted: 14 December 2023
Published: 27 December 2023

Cyclades, together with the lower-most Rhodope Pangaion unit, were exhumed as metamorphic core complexes.

Keywords: Hellenides; subduction; obduction; compression; extension; geotectonics; mélanges

1. Introduction

Today, the Hellenides show an arcuate orogenic belt extending from Dinarides in the north to the Taurides, Menderes, and Sakarya massifs in the east, traditionally subdivided into the External and Internal Hellenides zones (Figures 1 and 2). These form a branch of the broader Alpine orogenic belt in Eurasia resulting from the convergence and final continental collision of the European and Apulian plates in a complicated, multiphase Alpine deformational regime in which subduction processes, compression, and nappe stacking have alternated successively with extension, tectonic denudation, and crustal exhumation from the Permo–Triassic to the present day (e.g., [1–24]). In any case, in this tectonic framework, some questions about the structural and geotectonic evolution of the Hellenides remain under debate today, or several controversial interpretations have been proposed for them. For instance, there is a debate about how many Mesozoic Tethys ocean basins, one or more, existed between the European and Apulian continents. Additionally, there are discussions about the origin and the obduction directions of the ophiolite nappes on the continental segments (e.g., Meliata/Maliac-Axios/Vardar ocean, Pindos/Mirdita ocean, etc.). Furthermore, the paleogeographic and tectonic origins of the old Paleozoic, pre-Alpine crystalline Pelagonian, and Serbo-Macedonian/Rhodope continental segments with their Triassic–Jurassic sedimentary cover incorporated in the Hellenides are also open questions (e.g., a critical element of these questions is the geotectonic and paleo-geographic position of the tectonically lowermost Rhodope Pangaion unit and the other geological units constituting the Serbo-Macedonian/Rhodope nappe stack).

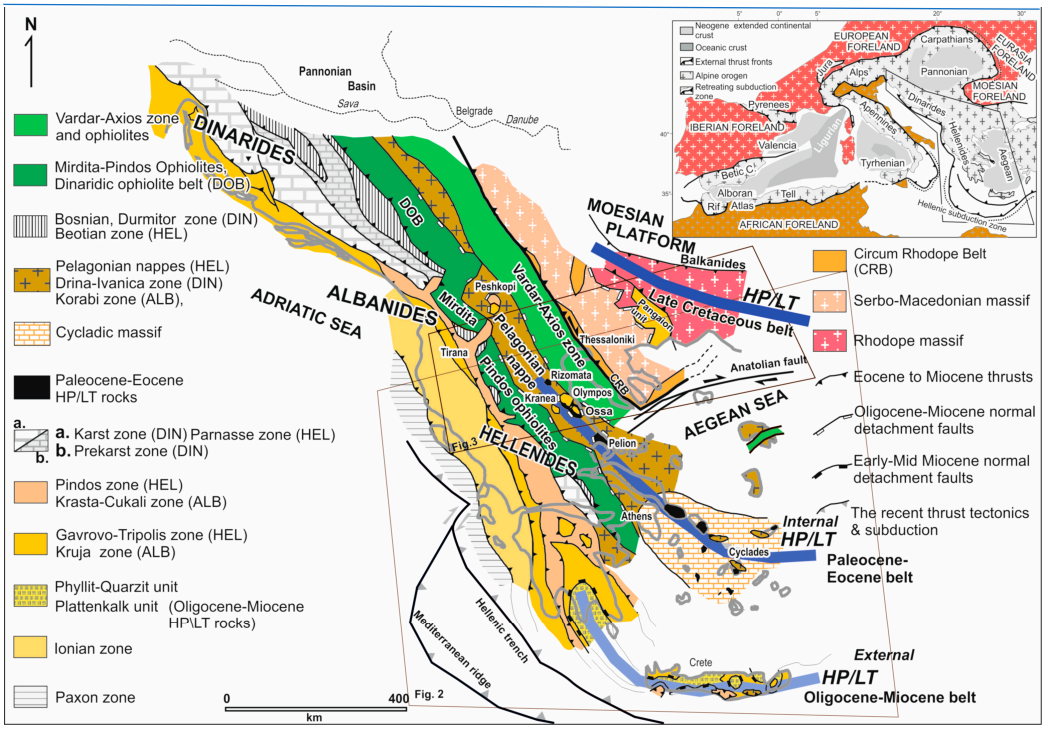

Figure 1. The main structural domains of the Dinarides and Hellenides as parts of the broader Alpine orogenic belt in Europe. Insert: The Alpine orogenic belt in Europe. Modified after [7].

Several geotectonic models with controversial conclusions have been suggested to explain the geotectonic evolution and paleogeographic conditions of the Hellenides (e.g., [1–24]). More specifically, some authors suggest that the Axios/Vardar ocean basin was a basin between the Pelagonian micro-continent in the west and the Serbo-Macedonian/Rhodope continental province in the east, operating almost simultaneously during the Triassic–Jurassic with a second Pindos/Mirdita ocean that was situated west of the Pelagonian micro-continent and east of the Apulian Plate, e.g., [1–3,8–10,14–16,19]. Alternatively, the Axios/Vardar basin is also viewed as just a small ocean, part of a series of narrow ocean domains extending in the middle of small continental blocks between Apulia and the European continent, e.g., [4,18,19,21]. In any case, according to any of these scenarios, the Hellenides' ophiolite belts derive from more than one ocean basin with different Late Jurassic to Early Cretaceous emplacement directions, mainly top to the west and/or top to the east. However, other researchers propose that only one main ocean basin opened during the Triassic–Jurassic time, situated east of the Apulian (including the Pelagonian) and west of the European (including the Serbo-Macedonian and the Rhodope nappes) continental margins, and this corresponds to the Neotethyan Meliata-Axios/Vardar ocean basin. In this case, all ophiolite belts that crop out in the Hellenides, east and west of the Pelagonian and the Serbo-Macedonian/Rhodope provinces, originated from the Meliata-Axios/Vardar ocean basin. They were obducted on the Pelagonian and Serbo-Macedonian continental margins during the Late Jurassic with W-ward and E-ward movement, respectively, e.g., [5–7,11–13,20]. Additionally, Papanikolaou (2009,2013) [22,23] describes a different geodynamic evolution for the Hellenides according to which a number of Triassic–Jurassic to Cretaceous Tethys oceanic terranes existed between several continental terranes of Gondwanan origin and various dimensions drifting to the north. The timings of the opening and closure of each oceanic terrane and the tectonic emplacement of the ophiolites were different. The oceans' closure and the ophiolite obduction procedures on top of the pre-Alpine continental terranes become younger from the northeast towards the southwest (Mid–Late Jurassic to Late Eocene–Oligocene), with a main ophiolite emplacement direction towards the SW. Recent works, e.g., [17,24] suggest a new theory, the so-called "maximum allochthony hypothesis". According to this, all the ophiolite belts of the Hellenides are allochthonous, originating from one main Triassic–Jurassic ocean rooted along the northeastern border of the Rhodopes and the southwestern margin of Europe. The Axios/Vardar ocean closed finally during the Late Cretaceous–Paleocene, subducted totally under the European margin and the Late Cretaceous Sredna–Gora magmatic arc. Furthermore, the Pindos ocean is regarded as a narrow ocean basin operating west of the Pelagonian block during the Late Cretaceous and closed in the Paleocene–Eocene, when subducted completely under the Pelagonian segment. The lowermost Rhodope Pangaion unit belongs to the External Hellenides and the Apulian Plate, exhumed during the Oligocene–Miocene as a metamorphic core complex below the overthrust European nappes. These controversial views are also presented in detail below in descriptions of the isopic geological units or zones and the structural evolution of the Hellenides.

The goal of this work was to present the Alpine structural architecture and geodynamic evolution of the Hellenides in the context of the several contradicting proposed models, finally adding my point of view regarding the geotectonic reconstruction of the Hellenides. For example, I consider how many oceanic basins developed during the Alpine orogeny, the emplacement direction of the obducted ophiolites, and the paleogeographic origin of the pre-Alpine continental blocks incorporated in the Hellenic orogenic belt. This will be based on recent studies and experience not only from me and my collaborators but also on more modern works published by other colleagues concerning the Hellenides' geology. Furthermore, sedimentary, magmatic, and metamorphic processes during the Alpine orogeny also constitute important data for this work's proposals.

2. Geological Setting

Maintaining the old subdivision of the Hellenides into isopic zones (i.e., [25–27]), the External and Internal Hellenides are composed, from west to the east, of the following main tectonostratigraphic domains:

1. External Hellenides: I. Paxos zone, II. Ionian zone, III. Gavrovo zone, and IV. Pindos zone, possibly including the Koziakas unit.

2. Internal Hellenides: I. Pelagonian zone or nappe and ?Parnassos zone, II. ?Sub-Pelagonian zone, III. Axios/Vardar zone, IV. Cycladic massif, V. Circum-Rhodope belt, VI. Serbo-Macedonian massif, and VII. Rhodope massif.

The External Hellenides are mainly built up of Mesozoic and Cenozoic deep-sea and shallow-water sedimentary rocks, characterized by continuous sedimentation processes that terminated in the Paleocene to Miocene flysch deposition. They form a complicated, SW- to SSW-verging, thin-skinned thrust and fold belt from the Paleogene to the Neogene age without any important metamorphisms (Figures 3 and 4; [25,26,28–30]). Due to Oligocene–Miocene internal underthrusting between the litho-stratigraphic domains of the External Hellenides, a high-pressure/low-temperature metamorphic belt (HP/LT) was developed. It is recorded in the Plattenkalk, Phyllite-Quartzite, and Tripali units exhumed in the southern Peloponnese and on Crete island (Figures 1–5; [31–35]).

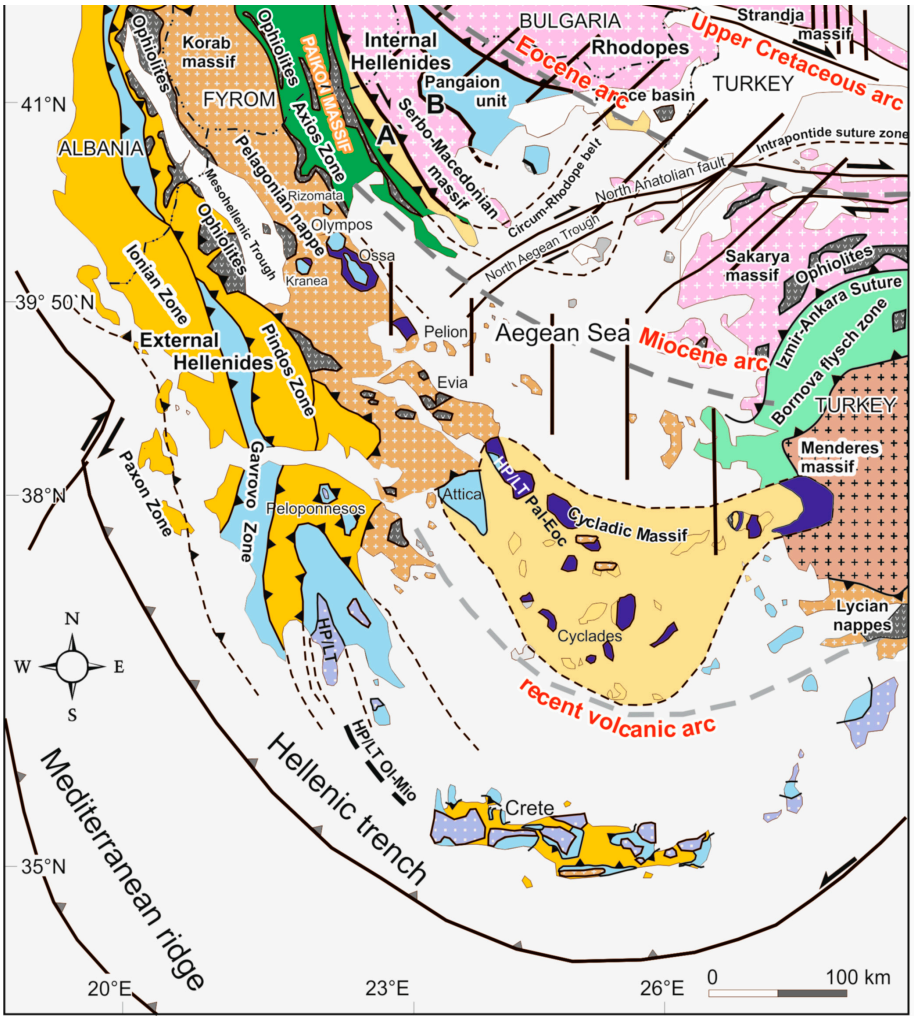

Figure 2. Geological map of the Hellenides with the main tectonic zones and their possible continuation to the east in Turkey. Modified after [7,9,12].

On the other hand, the Internal Hellenides are composed of Paleozoic and older basement rocks covered by Triassic–Jurassic carbonate platform sediments, as well as outer shelf and shelf-edge sedimentary series, on which the Neo-Tethyan ophiolite realms were initially obducted during the Mid–Late Jurassic. The Internal Hellenides are characterized by a multiphase tectonic history and metamorphism during the Alpine orogeny, from the Jurassic to the Tertiary (D1 to D6 events; they are described in detail in the chapter "Architecture of deformation and structural evolution"). The Internal Hellenides overthrusted the External Hellenides during the Eocene–Oligocene (Figures 3–5; [6,18,19,21,30,36–43]).

A Paleocene–Eocene high-pressure belt characterizes the tectonic contact between the External and Internal Hellenides zones exhumed in the Olympos-Ossa and Cyclades provinces directly under the Internal Hellenides Pelagonian nappe (Figures 1–4; [38,39,44–49]). Additionally, the high- to ultra-high-pressure metamorphic conditions of the Jurassic–Cretaceous and Paleocene–Eocene ages are also described for the Serbo-Macedonian/Rhodope metamorphic province of the Internal Hellenides [50–57]. Recent works recognize a Late Cretaceous high-pressure belt in Rhodope province [58,59]. Late orogenic Eocene to Early Miocene molassic-type (turbidites) basins, such as the Mesohellenic trough (Figures 1–4; [60–65]) and the Thrace basin (Figures 1–4; [7,30,66,67]), were developed locally on the top of the External and Internal Hellenides structural sequences. Finally, post-orogenic Neogene–Quaternary intramontagne and other terrestrial sedimentary basins cover, unconformably in many places, all the pre-Alpine and Alpine Hellenides' tectonostratigraphic domains (Figures 1–4; e.g., [68–73]).

2.1. External Hellenides

2.1.1. Paxos Zone

The Paxos zone forms the most external zone of the External Hellenides and continues to the north in the Albanides and Dinarides (Figures 1, 2 and 4). It is characterized by continuous, neritic carbonate sedimentation from the Mid-Upper Triassic to the Oligocene–Miocene without typical flysch deposition, which is exposed in all other External Hellenides zones. Thin strata of siliceous sediments and shales are locally interbedded with the Jurassic carbonate succession. Furthermore, evaporites form the older, lower-most litho-stratigraphic sequence in the zone [26,74–79].

2.1.2. Ionian Zone

The Ionian zone (Figures 1–4) is built up from a continuous sedimentary series from the Triassic to the Oligocene–Miocene. This is also recognized to the north in the Albanides and Dinarides orogenic belts. Until the Early Jurassic, the sedimentation was characterized by neritic calcareous deposits, terminating with the characteristic Pantokrator white limestone series of the Liassic age. In contrast, from the Middle Jurassic until the Eocene, the sedimentary conditions changed to pelagic with radiolarite and pelagic limestone deposition and finally ended with an Oligocene–Miocene flysch deposition. As in the Paxon zone, evaporites also form the older, lowermost litho-stratigraphic sequence in the Ionian zone [25,26,30].

Equivalent to the Ionian sediments seems to be the Plattenkalk unit in the Peloponnese and on Crete island, cropping out tectonically together with the Jurassic age's Tripali unit under the Phyllite-Quartzite unit and the Gavrovo zone (Figures 2, 4 and 6; [32–34,80–82]). The Plattenkalk, Tripali, and Phyllite-Quartzite units have been affected by the Oligocene–Miocene HP/LT metamorphic event of the External Hellenides, while the overlain Gavrovo zone remains unmetamorphosed here (Figures 2 and 6).

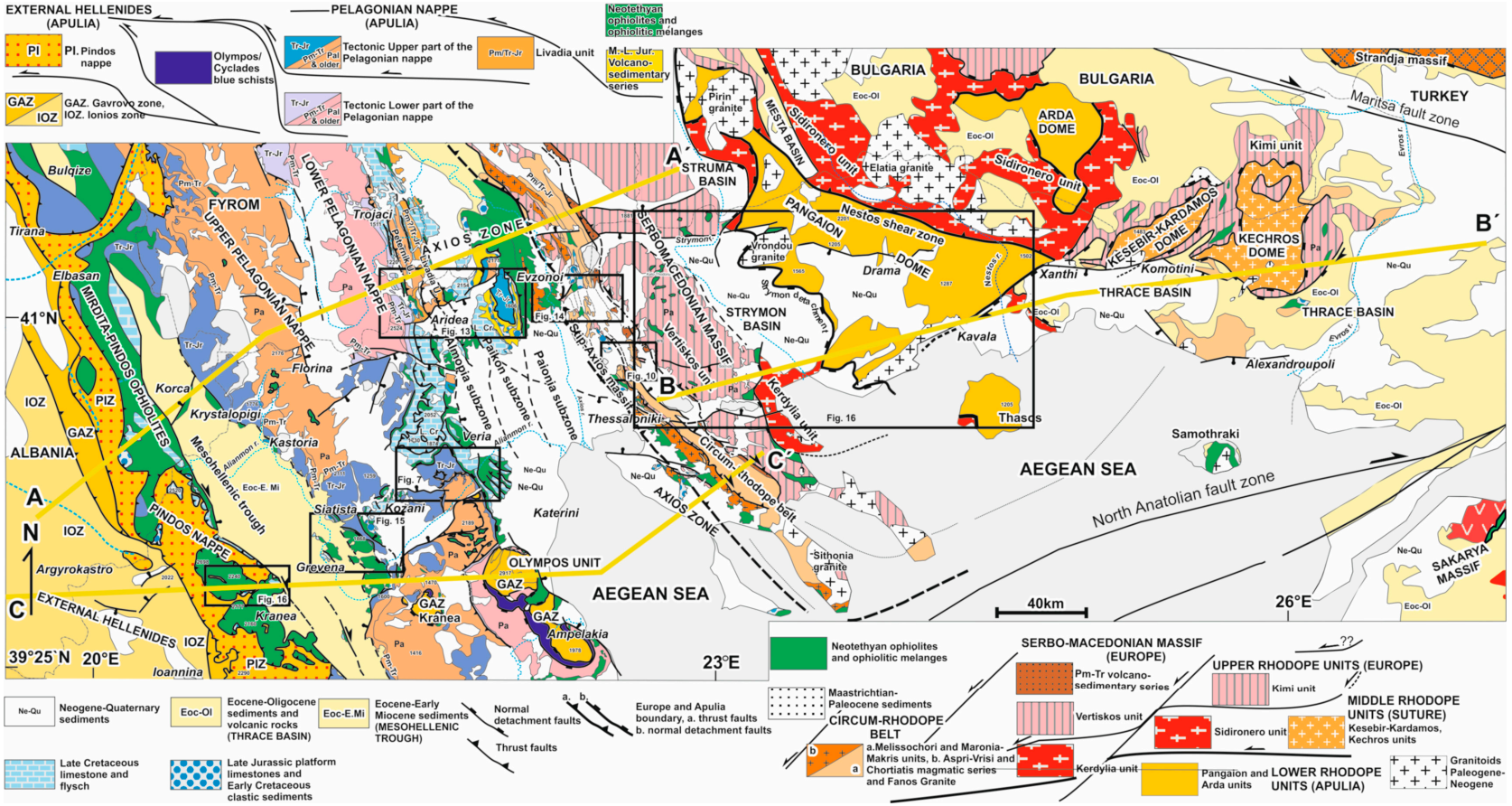

Figure 3. Geological map of Northern Greece compiled after [5–7,9–13,15–21,24–27,30,34,36,38–40,43,48,67,68]. Qu = Quaternary, Ne = Neogene, Mi = Miocene, Ol = Oligocene, Eoc = Eocene, Pal = Palecene, Cr = Cretaceous, Jr = Jurassic, Tr = Triassic, Pm = Perm, Pa = Paleozoic and older, L = Late, E = Early. A-A′, B-B′, and C-C′ are the cross-section lines of Figure 4.

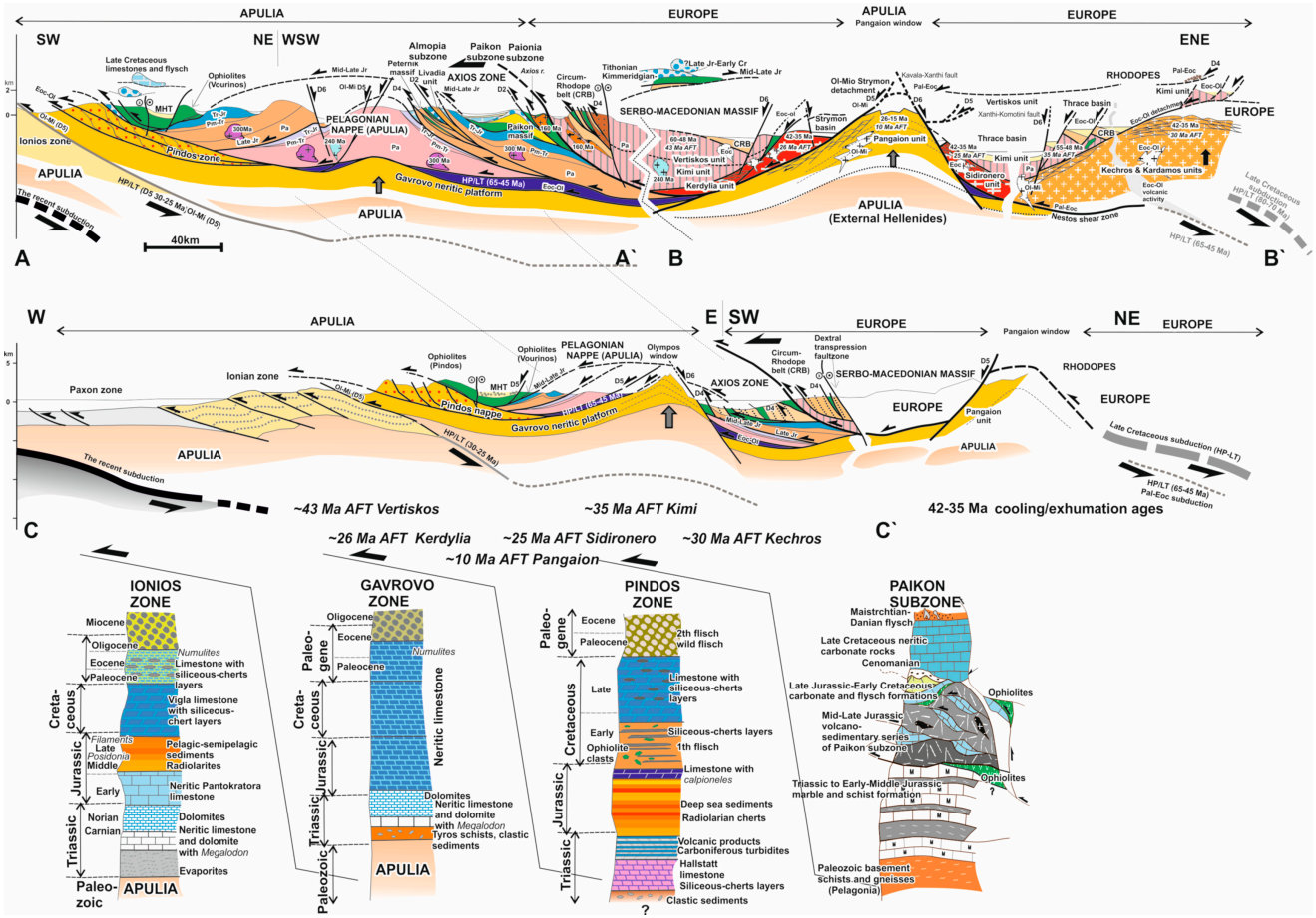

Figure 4. Representative geological cross-sections through northern Greece, showing the geometry of deformation and the structural architecture of the Hellenic orogenic belt as it was created by Alpine orogenic processes from the Jurassic to the recent era (the deformational events are described in detail in the chapter "Architecture of deformation and structural evolution"). The tectonic windows of Olympos-Ossa and the Rhodope Pangaion are shown. MHT = Mesohellenic trough. The stratigraphical columns of the External Hellenides are also shown. Legend and abbreviations as in Figure 3 (modified after [6,7,17,24,48,57,67]. 26–15 Ma = cooling/exhumation data, *43 Ma AFT* = apatite fission-track ages of the several Serbo-Macedonian/Rhodope tectonic nappes.

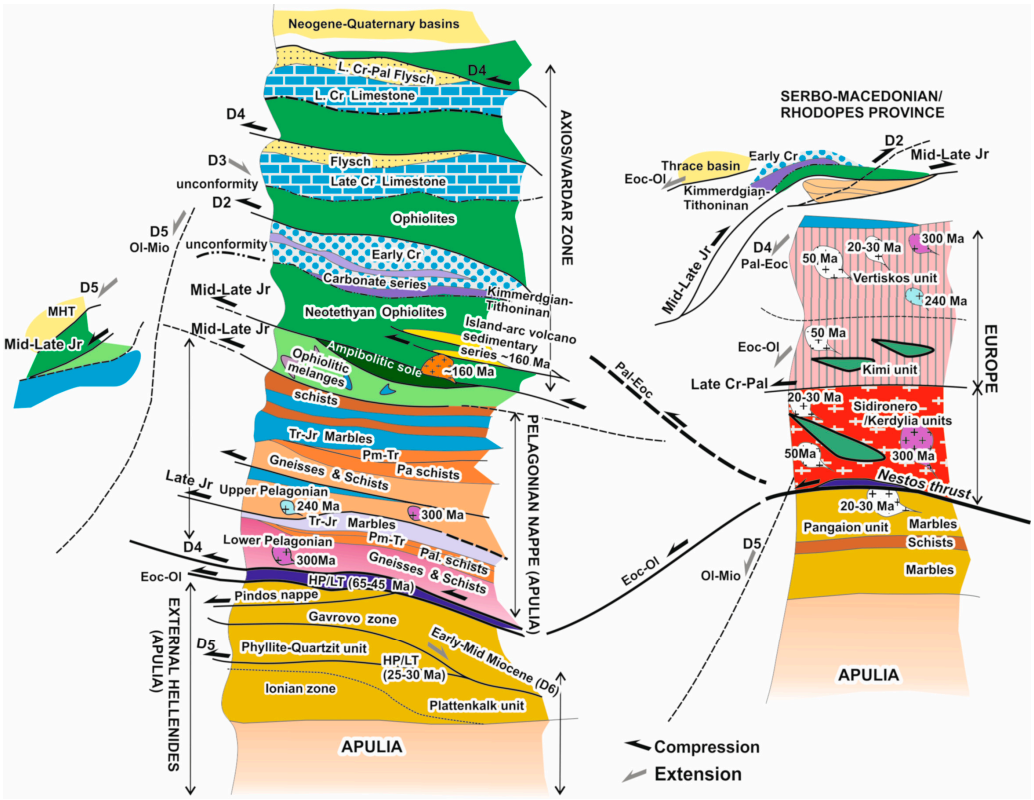

Figure 5. Schematically, the tectonostratigraphic column of the Hellenides. The several Alpine deformational events and their actions are shown (they are described in detail in the chapter "Architecture of deformation and structural evolution"). Abbreviations as in Figure 3.

The Plattenkalk unit is rich in metamorphic aragonite in the marble and Fe-Mg-carpholite in the intercalated thin metabauxite layers. Additionally, in the Phyllite-Quartzite unit, it has been recognized that glaucophane is also associated with Fe-Mg-carpholite. The Plattenkalk unit, together with the Tripali and Phyllite-Quartzite units, was uplifted and exhumed rapidly under Early–Middle Miocene extensional tectonics and isothermal decompression (Figure 6; [3–35,82–84]).

The Ionian zone was thrust over the Paxos zone towards the west during the Mid–Late Miocene (Figures 2 and 4).

2.1.3. Gavrovo Zone

The Gavrovo zone is characterized by continuous Triassic to Eocene neritic platform sedimentation on the Apulia continental passive shelf, terminated by the deposition of an Eocene–Oligocene flysch (Figures 1, 2, 4 and 5; [25,26,30,36,85]). It is also exhumed to the north in the Albanides and Dinarides. The western parts of the Gavrovo zone in the External Hellenides appear unmetamorphosed and intensively imbricated during the Oligocene–Miocene. However, its more eastern parts that crop out in the Internal Hellenides as tectonic windows or metamorphic core complexes (Olympos-Ossa, Rizomata, Almyropotamos-Attica and Cyclades provinces; Figures 2–4 and 7), beneath the Pelagonian nappe and the glaucophane-bearing Paleocene–Eocene high-pressure blueschist belt (Ampelakia and Cyclades units), show evidence of a Tertiary (Oligocene–Miocene) low- to high-grade metamorphism related to extension and exhumation. So, e.g., in Olympos-Ossa province, only low-grade metamorphism is recorded without any significant reheating (Figure 8a; [5,38,39,47,48,86,87]). In contrast, in the Almyropotamos-Attica and Cyclades provinces, significant reheating, high-temperature metamorphism, migmatization, and abundant granitoid intrusions occurred during the Oligocene–Miocene (Figure 8b; [45,88–95]).

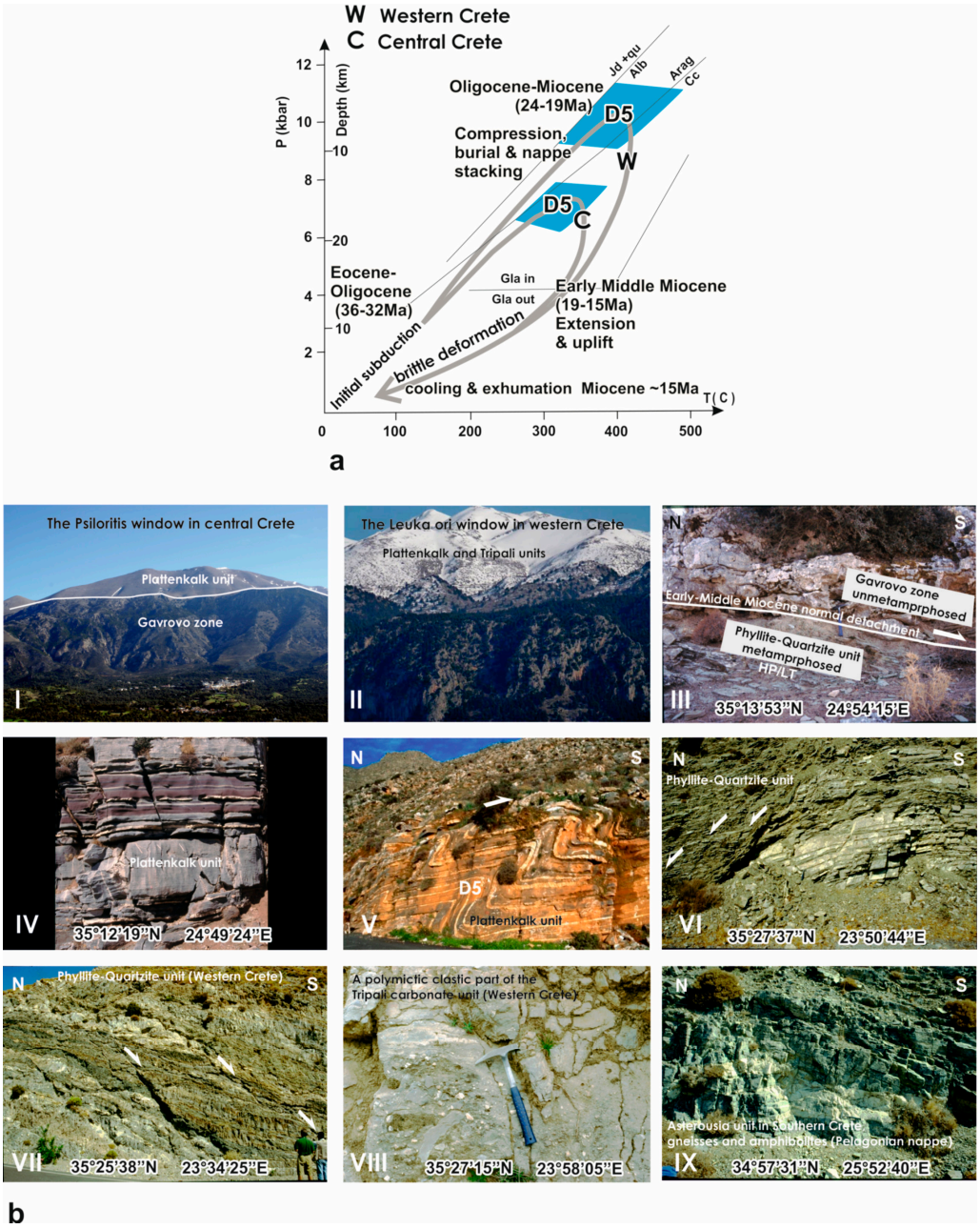

Figure 6. (**a**) P-T-t tectono-metamorphic path and exhumation history for the Oligocene–Miocene high-pressure belt (Plattenkalk, Tripali and Phyllite-Quartzite units) on Crete island [31–33,96,97]. (**b**) Field- and macroscale photos of the geological units and deformational structures on Crete island (**I**–**IX**). The sense of shear is shown by arrows and is related to the Early–Middle Miocene extension and exhumation of the Oligocene–Miocene HP/LT metamorphic belt of the External Hellenides (Peloponnese and Crete island).

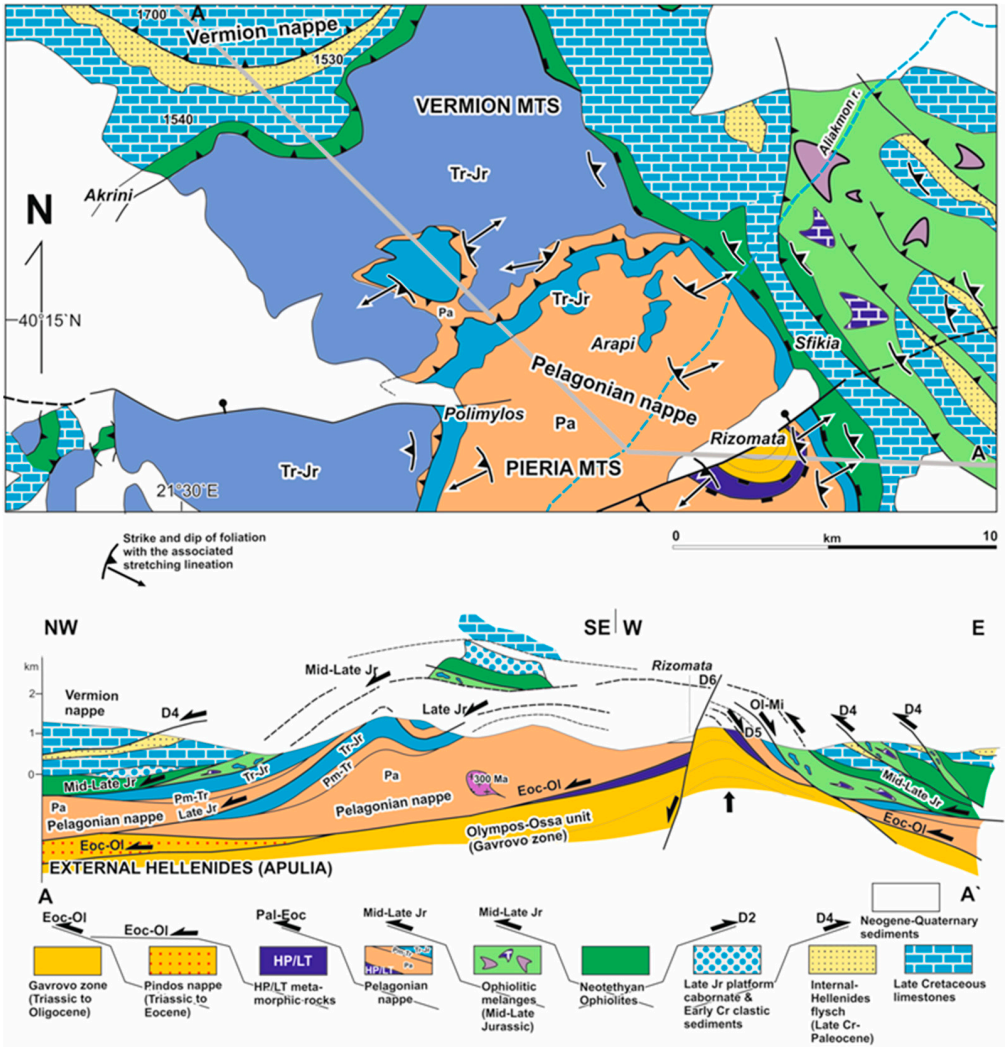

Figure 7. Geological–structural map and representative cross-section (A-A`) of the tectonic boundary between the Pelagonian nappe and the Axios/Vardar zone at the Vermion and Pieria Mts. The Rizomata window, equivalent to the Olympos-Ossa window, as well as the Late Jurassic tectonic duplication of the Pelagonian nappe and the Paleocene–Eocene Almopian tectonic sheets, are shown (based on [43,98,99]). Abbreviations as in Figure 3.

The pre-Alpine basement of the Gavrovo carbonate platform (the Apulian Plate) is exhumed as metamorphic core complexes in the Cyclades province beneath the Gavrovo carbonate series, the Cyclades blue schists unit, and the overlain remnants of the Pelagonian nappe with obducted Neotethyan ophiolites (Figures 2 and 4; [9,89,93,100–104]). It is possibly continued further to the east in western Turkey in the Menderes metamorphic core complex as its deeper structural level (Figure 2; [9,102]). Both the Cyclades and Menderes provinces show at least an equivalent tectonostratigraphic setting and Tertiary tectonic history. From the bottom to the top, the following are recognized: a pre-Alpine basement, covered by neritic limestones or marble in places, of Triassic to Eocene age (the Gavrovo carbonate platform), overthrust by the Paleocene–Eocene Ampelakia-Cyclades high-pressure belt, and topped tectonically by the Pelagonian nappe and the Lycian nappe in the Hellenides and the Menderes area, respectively. Triassic granitoid intrusions in both provinces are another common point among these. Oligocene–Miocene granitoid intrusions also occur in both the Menderes and Cyclades domains, but in different amounts. They are more common in the Cyclades massif (Figure 2; [9,10,15,45,89,95,103,105–113]). Furthermore, kinematic indicators show real similarities in both areas of the Cyclades and the Menderes. In the Cyclades, the Oligocene–Miocene extension direction evolves mainly

N- to NE-ward and is related to exhumation processes (Figure 9), as is also described for the Menderes region. Additionally, S- to SW-ward movements have also been described for both areas (Figure 9; [9,11,89,93,102,105–107,114]).

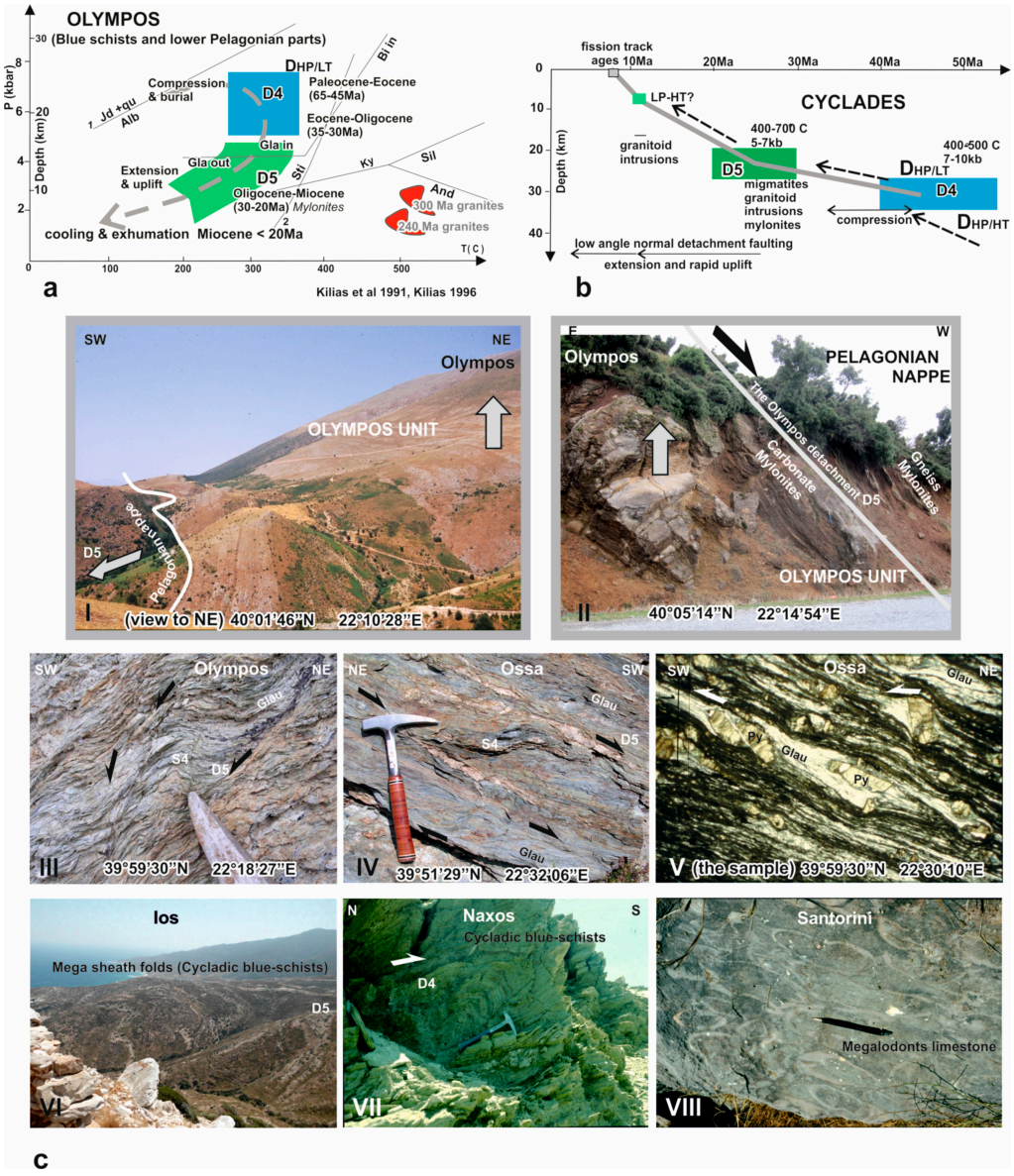

Figure 8. (**a**,**b**) P-T-t tectono-metamorphic paths and exhumation history of the Paleocene–Eocene high-pressure belt (blue schists), (**a**) in the Olympos-Ossa [45–48,86,88] and (**b**) Cyclades areas [44,46,88,91,115], respectively; (**c**) Field- and microscale photos of the geological units and deformational structures, (**I**–**V**) in the Olympos-Ossa and (**VI**–**VIII**) Cyclades provinces: (**I**,**II**) The Olympos normal detachment zone, along which the Pelagonian nappe pile detaches SW-wards with Late Jurassic obducted ophiolites and the overlain Late Jurassic–Cretaceous sedimentary series, resulting in the uplift and final exhumation of the high-pressure blue schists and the Olympos carbonate unit (Gavrovo zone); (**III**–**V**) Meso- and microscale features of deformation of the Ampelakia high-pressure belt. S-C fabrics and shear bands in the blueschists (**III**,**IV**), pyroxene σ-clasts in the intercalated metabasites of the blueschist unit, glaucophane growing in the pressure shadows of the pyroxenes during the high-pressure process (**V**), X-Z sections, the main sense of shear top-to-SW during the exhumation processes; (**VI**,**VII**). Fold structures in the Cycladic metamorphic belt; (**VIII**). Megalodonts bearing recrystallized limestones of the Triassic–Jurassic Emporio carbonate unit in Santorini island [107]).

Nevertheless, some lithological and structural differences should also be referred to here between the two regions, leaving some question marks about the correlation of the two areas and raising the need for further detailed research for the correct answer (for example, the absence of the Pelagonian nappe in Menderes province, where the Lycian nappes may be equivalent structural sequence to the Pelagonian nappe, taking the same tectonic position [9,10,103]).

Moreover, the Menderes basement forms a pan-African continental segment [102,105, 106,109,114]. One more difference is the obduction age of the ophiolites. In the Hellenides, these are of Mid–Late Jurassic age, while, in the Menderes province, they are of Late Cretaceous age [80,116,117]. Another difference is the larger amount of basement rocks in the Menderes massif than in the Cycladic massif (Figure 2; [45,90,103,105,106,109]).

Recent works by Dinter (1998) [118], Jahn-Awe et al. (2010) [17], and Froitzheim et al. (2014) [24] support the continuation of the Gavrovo carbonate platform as part of the Apulian's plate passive margin to the Rhodope metamorphic province, named the Pangaion metamorphic core complex. It is exhumed as a tectonic window below the metamorphic Serbo-Macedonian/Rhodope tectonic nappes or terranes of the Internal Hellenides (Figure 2).

The Gavrovo zone is thrust over the Ionian zone towards the west during the Oligocene–Miocene time (Figures 1, 2 and 4).

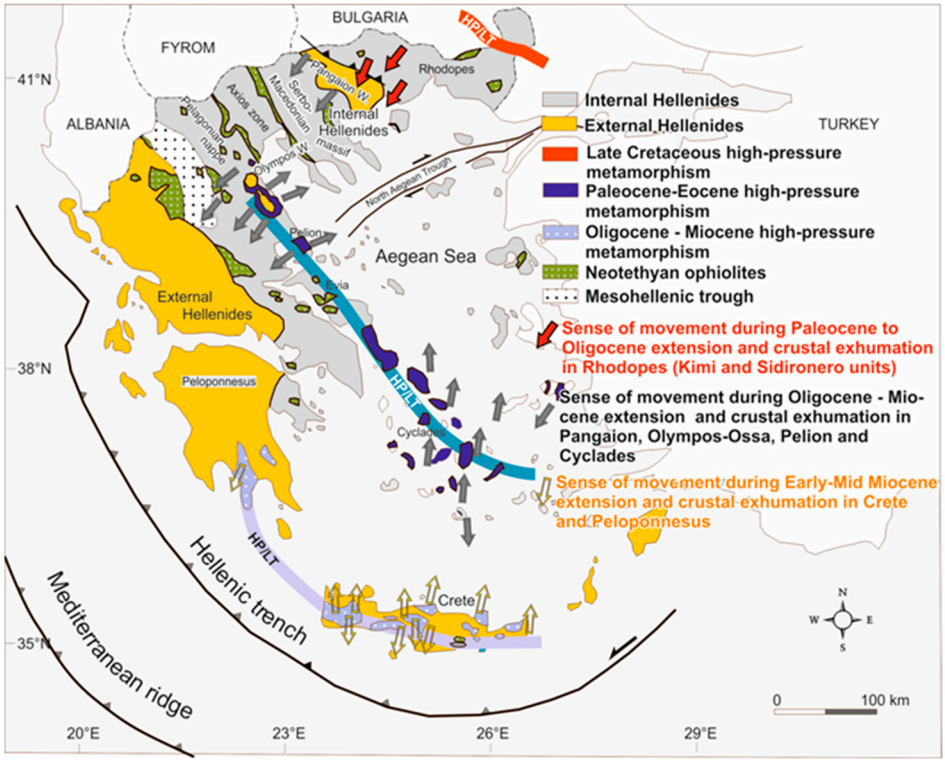

Figure 9. Geometry of the kinematics of ductile deformation (sense of shear) during the Tertiary extensional tectonics in the Hellenides that progressively migrated towards the SW (modified after [5]).

2.1.4. Pindos Zone

The Pindos zone continues to the north in the Albanides and Dinarides orogenic belts, while, to the south, it is recognized in small, residual tectonic nappes on Crete island, as well as on some Aegean islands east of Crete (Figures 1–3). The Pindos zone is characterized by deep-sea sediments (such as pelitic, siliceous, and pelagic carbonate deposits) of Triassic to late Late Cretaceous age, overlain by a Paleocene–Eocene flysch which shares in places the typical features of wild flysch. Nevertheless, the Pindos first depositional materials are clastic neritic sediments of Early–Middle Triassic age, with volcanoclastic products intercalated. An occurrence of Early Cretaceous flysch-type deposits (Pindos "first flysch")

between the deep-water Pindos strata remains under debate. These are composed of alternations of thin layers of red marls and radiolarian cherts, marly limestones, pelites, and green fine- to coarse-grained sandstones with ophiolitic materials as well as ophiolite pebbles [25,26,28–30].

The geotectonic–paleogeographic position of the Pindos zone is widely controversial. It is believed to have developed at the western Pelagonian margin, either as an ocean basin opening progressively due to the Permo–Triassic continental rifting of Pangea [3,14,19,25,117,119,120] or as a deep sea basin formed on a thinned continental crust [117]. Moreover, recent works by Jahn-Awe et al. (2010) [17], Papanikolaou (2013) [23], Froitzheim et al. (2014) [24], Petrik et al. (2016) [121] and Miladinova et al. (2018) [59] suggest the opening of a narrow ocean basin during the Late Cretaceous, named the Pindos-Cyclades ocean, which divided the Pelagonia from Apulia at this time. This small ocean, as part of the entire Pindos zone, was subducted NE-ward during the Paleocene–Eocene under the Pelagonian fragment and the Internal Hellenides nappe stack, where it metamorphosed under high- to ultra-high-pressure metamorphic conditions and then overthrust during the Eocene–Oligocene on the Apulian margin together with the Pelagonia [5,36,38,39,47,48,86,87].

In any case, the entire Pindos zone overthrusts W- to SW-ward the Gavrovo carbonate platform during the Eocene–Oligocene. It shows a similar structural position, with the Paleocene–Eocene blueschist belt, subducted firstly under the Pelagonia, and subsequently exhumed tectonically in the Olympos-Ossa and Cyclades provinces directly above the Gavrovo zone.

Therefore, the Pindos zone in the External Hellenides possibly represents the non-metamorphic part of the blueschist that has escaped subduction under the Pelagonian continental fragment and continues to the Paleocene–Eocene high pressure belt (Figures 1–4; [5,6,23,38,39,47,48,80,122–124]). In contrast, Stampfli et al. (2003) [125] regard this blueschist belt as of Pelagonian origin.

The Koziakas Unit in central Greece (Figures 2 and 3) is composed from the bottom to the top of pelagic carbonate sediments intercalated with radiolarian cherts and shales of Middle Triassic–Early Jurassic age, Jurassic thick-bedded oolithic limestones, and redeposited mass–flow sediments of Early Cretaceous age, as well as Early Cretaceous flysch-type sediments equivalent to the Beotian flysch and the Pindos "first flysch". On the Beotian flysch, the Triassic and Jurassic sequences of the Koziakas unit are overthrust W-SW-ward, forming additionally to the whole Koziakas unit an overturned W-ward-vergent mega-fold. Moreover, in the stratigraphic column of the Koziakas unit are also described shallow-water Late Cretaceous limestone and micro-breccia deposits (Thymiana limestones) and, finally, Paleocene–Eocene flysch. According to many authors, the Koziakas unit is a sedimentary series with continued sedimentation from the Triassic to the Eocene equivalent to the Pindos zone (Figures 2 and 3; [19,25,126–131]). Nevertheless, on the Triassic–Liassic deep-sea sedimentary series of the Koziakas unit are tectonically emplaced Middle–Late Jurassic ophiolitic mélanges and Neotethyan ophiolites. This raises some questions about the existence of continued sedimentation in the unit as well as its geotectonic position. Furthermore, according to other authors, the Koziakas unit has been regarded as an individual tectonostratigraphic unit of unknown origin, thrust during the Paleocene–Eocene on the Pindos unit from the east to the west [132], so that its geotectonic setting, as well as paleo-geographic position, remain under discussion.

2.2. Internal Hellenides

2.2.1. Pelagonian Zone or Nappe

The Pelagonian nappe or Pelagonian zone is composed from the top to the bottom of: **I.** a Triassic–Jurassic carbonate platform sequence; **II.** a volcano-sedimentary Permo–Triassic series characterized by bimodal magmatism; and **III.** a Paleozoic or older pre-Alpine crystalline basement, composed of gneisses, amphibolites, and schists, intruded by Carboniferous calc-alkaline (~300 Ma) and Triassic A-Type (~240 Ma) granitoid. Meso-

zoic or Cenozoic magmatic activity has not been recorded in the Pelagonian basement (Figures 3–5; [3,6,98,133–137]). The Pelagonian nappe was divided by [6], due to tectonic internal thrusting during the Late Jurassic, into a tectonic lower and a tectonic upper Pelagonian segment, both showing the same tectonostratigraphy column as described just above (Figures 3–5). Obducted Neo-Tethyan ophiolites, imbricated with mid–late Jurassic ophiolitic mélanges, occur in many places on the Triassic–Jurassic Pelagonian carbonate cover or secondary, directly on the pre-Alpine basement (Figures 1–4). The ophiolite obduction took place during the mid–late Jurassic, following intra-oceanic subduction/-s in the Neo-Tethyan ocean basin/-s [6,13,19,21,138–140]. The Pelagonian nappe, together with the obducted ophiolite belt, crops out mainly in continental Greece, overlying tectonically the Gavrovo zone and the Paleocene–Eocene Ampelakia-Cyclades high-pressure belt, which are exhumed as tectonic windows below the Pelagonia, as described above. The Pelagonian nappe is also recognized on top of the Cyclades metamorphic complex in small, far-traveled relics and on Crete island as the Asterousia nappe (Figures 2 and 6; [23,32,33,76,80,122,141]). Furthermore, clasts of Pelagonian nappe origins are also found in Early Miocene conglomerates deposited above detachment faults in the Cyclades province, showing that the Pelagonian nappe once covered a large part of the Aegean region and finally eroded or tectonically denudated [95,142–144]. The basement gneissic rocks and their Triassic–Jurassic carbonate cover of the Paikon subzone in the Axios/Vardar zone at the Tzena and Paikon Mts were regarded by [145] as a tectonic window of Pelagonian origin. Nevertheless, the Pelagonian nappe is also recognized to the north in the Dinarides, while its continuation to the east in Turkey remains under discussion today. As referred to above in the description of the Gavrovo zone, parts of the Lycian nappes in southwestern Turkey may form the relics of the Pelagonian nappe further to the east (Figure 1; [3,6,9,117]).

Furthermore, Late Jurassic, strongly eroded carbonate platform sediments; Early Cretaceous mass flows and flysch-like deposits; and transgressive Late Cretaceous shallow-water carbonate sedimentary series rest in places on top of the obducted Neo-Tethyan ophiolite realm or directly on the exhumed Pelagonian Triassic–Jurassic platform carbonate (Figures 5 and 10; [13,21,27,146–153]).

A detailed P-T-t-path for the complicated, polyphase Alpine tectono-metamorphic history of the Pelagonian basement rocks, which is discussed in detail in numerous works by Kilias et al. (1991, 2010, 2013) [6,7,48], Schermer et al. (1990) [47], Schermer (1993) [39], Most et al. (2001) [154], Mposkos et al. (2001) [155], Mposkos and Krohe (2004) [156], Katrivanos et al. (2013) [145], and Schenker et al. (2014, 2015) [43,99], is displayed in Figure 11a–c. This shows: **I.** High-pressure conditions during the Middle–Late Jurassic, associated with thrusting and crustal thickening, **II.** Amphibolite-to-greenschist facies retrogression during the Late Jurassic–Early Cretaceous and extensional crustal uplift, **III.** Late Early Cretaceous (Barremian–Aptian) greenschist facies prograde metamorphism related to compression and SW-ward thrusting, and **IV.** Late Cretaceous cooling/exhumation for the structurally upper Pelagonian parts and brittle compressional deformation and thrusting during the Paleocene–Eocene. This followed from the Oligocene–Miocene to the recent era by extension. In contrast, for the structurally lowermost Pelagonian parts, near their tectonic contact with the underlying Paleocene–Eocene blueschist belt or the External Hellenides (Gavrovo zone), ductile deformation under high-pressure conditions is followed by low-grade metamorphic retrogression under extension and strong mylonitization has been recorded during the Tertiary. Additionally, the cooling/exhumation path for the structurally lowermost Pelagonian parts is dated during the Oligocene–Miocene [38,39,47,48,86,157,158].

About the geotectonic position of the Pelagonian basement, it is regarded: **I.** either as the Mesozoic eastern passive margin of the Apulia continent, with a main wide ocean basin in the east, the so-called Neothethyan Meliata/Maliac-Axios/Vardar ocean basin [6,11,13,43,99,159,160] or **II.** as a microcontinent emerging in the middle of two separate ocean basins that were operating more or less contemporaneously during the Alpine orogeny; these were the Pindos ocean to the west and the Axios/Vardar ocean to the

east [6,11,13,43,99,159,160]. As accruing in these interpretations, the ophiolite rocks on both the western and eastern parts of the Pelagonian nappe should have originated either from one or two ocean sources, respectively. This leads to an ongoing discussion about the direction of the ophiolites' obduction onto the Pelagonian continent during the Middle–Late Jurassic: either only one main W- to SW-ward obduction direction (e.g., [1,6,11,13,20,37,139,160–162]), or both W- to SW-ward and E- to NE-ward obductions (e.g., [3,117]), or even only an E- to NE-ward obduction (e.g., [163,164]). Additionally, the last view sees only one main ocean basin, the Pindos basin, west of the Pelagonia.

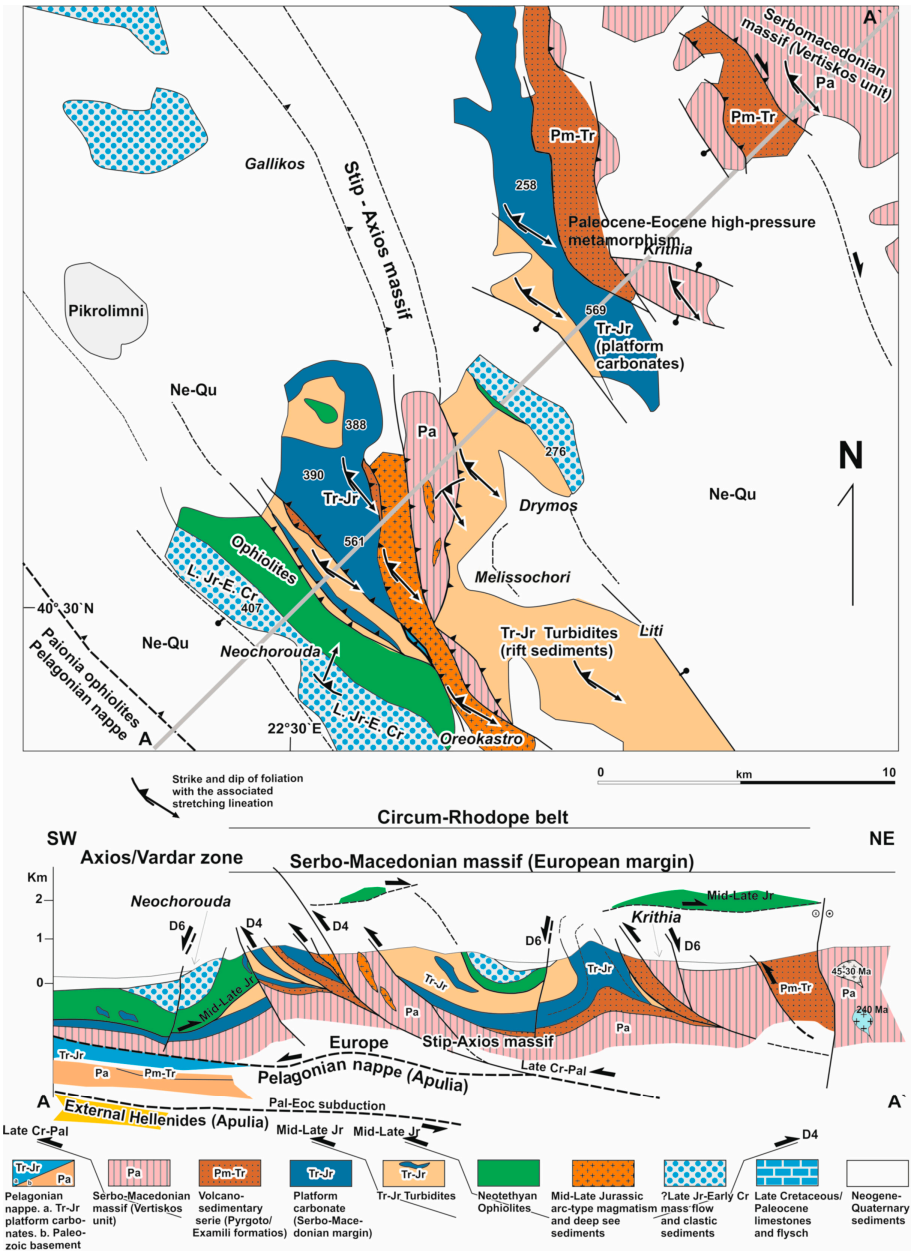

Figure 10. Geological–structural map and representative cross-section (A-A`) of the eastern tectonic boundary of the Axios/Vardar zone with the Serbo-Macedonian/Rhodope massif. The Pelagonian nappe is sandwiched between Europe (the Serbo-Macedonian/Rhodope nappe pile) and Apulia (the External Hellenides). Based on [123,124,152,153]. Abbreviations as in Figure 3.

The Sub-Pelagonian Zone is composed of a sequence of Triassic to Jurassic pelagic carbonate and siliceous sediments, which lie tectonically over the Mesozoic platform carbonate sediments of the Pelagonian nappe. Today, it is traced along the western Pelagonian

margin. The characteristic phase of the Sub-Pelagonian zone is the red, ammonite-bearing, pelagic sediments of the Hallstatt phase of the Late Triassic age (Figure 12). Ophiolites and ophiolitic mélanges overthrust the Sub-Pelagonian deep-water sediments (Figures 3 and 4). The latter emplacement took place during the Mid–Late Jurassic time, following the general geotectonic history of the Alpine orogeny in the Hellenides.

However, the Sub-Pelagonian zone remains an under-debated zone concerning its paleogeographic existence and geotectonic setting. One scenario wants the Sub-Pelagonian zone to be the Mesozoic continuation of the western Pelagonian continental margin to the continental slope and the deeper basin area towards the Pindos ocean basin (e.g., [3,19,117,165]). The opposing theory, with only one wide ocean basin to the east of the Pelagonian nappe (i.e., the Meliata/Maliac-Axios/Vardar ocean basin), explains the position of the Sub-Pelagonian zone along the western Pelagonian side as being of a tectonic nappe nature, having been thrust, together with the ophiolite belt, from the east to the west on the Pelagonian nappe [6,13,20,24,43,99,139]. In any case, the Sub-Pelagonian zone was affected by the Late Jurassic deformation and the subsequent, younger deformational events recognized in the Hellenides orogenic belt, placing the Sub-Pelagonian zone within the Internal Hellenides zones.

In addition, the Triassic–Eocene Parnassos carbonate unit develops in central Greece, (Figures 1 and 2), terminating in an Eocene–Oligocene flysch and known for rıch bauxite deposits. It is regarded as a platform carbonate sequence that was possibly deposited on the more western Pelagonian parts. In contrast, due to the absence of a clear stratigraphic gap in its tectonostratigraphic column, from the Triassic to the Eocene–Oligocene, the Parnassos unit is considered to be a part of the External Hellenides zones, forming a reef coralgal build-up belt near the Pelagonian western margin [129,166–169]. In any case, the geotectonic and paleogeographic setting of the Parnassos carbonate sequence remains under debate today.

The Parnassos unit, together with the Pelagonian nappes, overthrusts W-ward the External Hellenides Pindos zone during the Paleocene–Eocene. Its continuation is recognized further to the north in the “high karst” zone of Croatia and Bosnia-Herzegovina in the Dinarides, where important bauxite deposits are also appearing, as they are in the Parnassos unit in Greece (Figures 1 and 2; [129,167–170]).

2.2.2. Axios/Vardar Zone

The Axios/Vardar zone is another very structurally complicated Hellenides zone composed of units of both continental and oceanic origin. The whole zone forms a typical Tertiary thrust-and-fold belt, where ophiolites and Mid–Late Jurassic ophiolitic mélanges are intensively imbricated with Paleozoic continental basement rocks and low-grade to non-metamorphic Mesozoic sedimentary series, as well as Late Jurassic arc-type calc-alkaline granitoid cross-cutting in places as either basement slivers or ophiolites (e.g., Fanos granite, Figures 4, 13 and 14; [30,162,171,172]). The Axios/Vardar zone is traditionally subdivided into three (3) subzones. From the west to the east, they are the Almopia, Paikon and Paionia subzones Figures 3, 4, 13 and 14; [27,37]).

Several different interpretations have been proposed for the geotectonic position and structural evolution of the Axios/Vardar zone. Some authors believe that there were two ocean basins separated by the continental Paikon volcanic arc. West of the Paikon arc was the Almopia ocean basin, with a Triassic oceanic crust, while east of the Paikon arc, in a back-arc region, the Paionia ocean basin evolved during the Mid–Late Middle Jurassic, simultaneously with the subduction of the Almopia ocean beneath the Paikon continental arc [16,22,23,117,173–175]. The Middle–Late Middle Jurassic age of the Paionia oceanic crust was also documented by Danelian et al. (1994) [176] using the radiolarian ages of deep-sea sediments covering the Paionia oceanic crust. Furthermore, the same Middle–Late Middle Jurassic age for the Paionia oceanic crust was also studied by Zachariadis (2007) [177], who determined an isotopic age of 166 Ma for plagiogranite from Paionia ophiolites. Similar Middle Jurassic ages (Bajosian) for radiolarian assemblages in the cherts

stratigraphically on top of the Vourinos ophiolites at the western edge of the Pelagonian nappe (Figures 3, 14 and 15) have also been recorded by Chiari et al. (2003) [178].

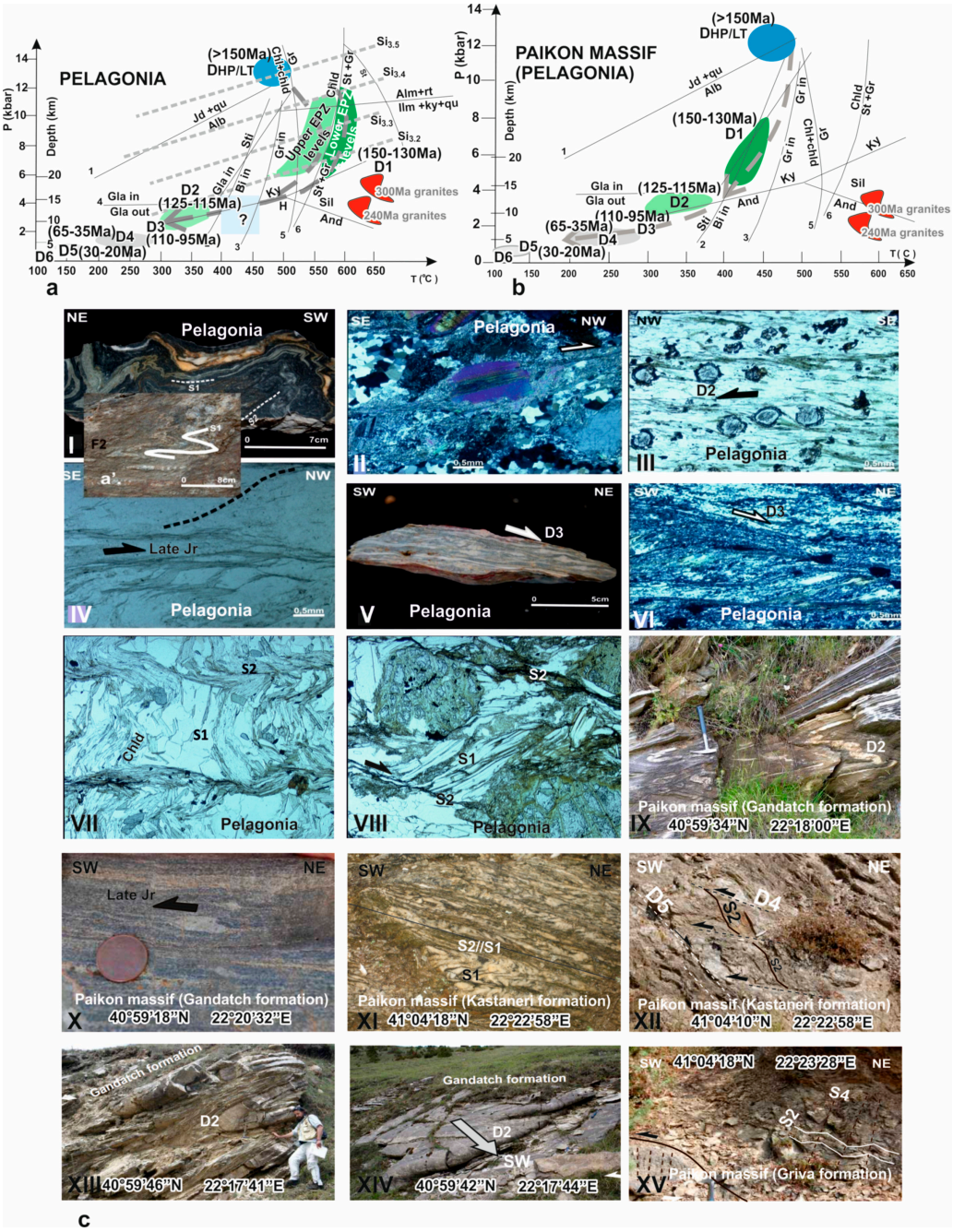

Figure 11. (**a**,**b**) P-T-t Alpine tectono-metamorphic paths and exhumation history (**a**) of the Pelagonian basement [6,154,179] and (**b**) Paikon basement [6,136,145]. Red color: granite intrusions in the Pelagonian basement. (**c**) Meso- and microscale features of the deformational events. (**I**) Main S1 foliation related to isoclinal recumbent folds. Asymmetric F2 folds overprint the previous isoclinal folds. S2 foliation is also shown. Garnet mica schist of the Upper Pelagonian segment, Peternik unit. (**II**) Recrystallization of sericite along the S2 planes around white mica porphyroclast. The asymmetry of the mica fish indicates a top-to-NW sense of shear during D2. XZ section. Garnet-bearing mica gneiss of the Upper Pelagonian segment, Peternik unit. (**III**) Garnet with characteristic zonation and

internal fabric (Si) rotated during D2. Chlorite aggregates (after garnet) and sericite growth in asymmetric pressure shadows and along the dominating S2 foliation planes. Garnet σ-clasts and the S-C fabric indicate a top-to-NW sense of shear. XZ section. Garnet mica schist (Lower Pelagonian segment). (**IV**) S-C fabric in mica gneiss from the tectonic contact between the lower and upper duplicated Pelagonian parts during the Late Jurassic. X-Z section. Sense of shear top-to-WNW. (**V**,**VI**) Augengneisses of the Pelagonian tectonic sheets in the Axios/Vardar zone (Livadia and Peternik units). Feldspar σ-clasts, S-C fabrics, and shear bands indicate a top-to-NE sense of shear (D3 event). XZ section. (**VII**) S1/S2 relationship. S1 is defined by white mica and chloritoid. Chloritoid rotates into S2. YZ section. Garnet–chloritoid mica schist (Lower Pelagonian segment). (**VIII**) Shear bands and the S-C fabric indicate a top-to-WNW sense of shear during D2. Intensive chloritization of D1 garnet σ-clasts took place during D2. X-Z section. Garnet mica schist (Lower Pelagonian segment). (**IX**) D1 and D2 fold realms on the Triassic–Jurassic carbonate sequence of the Paikon subzone (Gandatch marbles). Isoclinal, recumbent folds related to the D1 event are overprinted by the D2 event. The S2 foliation dominates. (**X**) Calcite σ-clast in the Triassic–Jurassic carbonate sequence of the Paikon basement (Gandatch marbles), indicating a top-to-SW sense of movement (D1). (**XI**) S1/S2 fabric in the Late Jurassic volcanosedimentary formation of the Paikon subzone (Kastaneri formation). The old S1 foliation is strongly reoriented along the S2 foliation, forming a cranulation cleavage fabric. Due to the strong translation along the S2-planes, the two foliations are usually developed parallel to one another, so that only one fabric element seems to be recognized on the geological formation, and this is the S2 foliation. Paikon subzone, Axios/Vardar zone. (**XII**) Brittle D4 thrust zone towards SW, cutting the main S2 foliation. Brittle also is the D5 semi-low angle normal fault zone cutting the D4 thrust zone and S2 foliation with a top-to-NE sense of shear. Late Jurassic volcanosedimentary formation of the Paikon subzone (Kastaneri formation). (**XIII**,**XIV**) B-axis scattering of D2-isoclinal folds due to their re-orientation subparallel to the X-axis of the strain ellipsoid. D2 stretching lineation plunging SW-ward. Triassic–Jurassic carbonate sequence of the Paikon basement (Gandatch marbles). (**XV**) Kink folds in the Late Jurassic–Early Cretaceous carbonate Griva formation of the Paikon subzone related to the Paleocene–Eocene compressional event (D4). Microscopic pictures (**III**,**IV**,**VII**,**VIII**) with one Nicol and (**II**,**VI**) with crossed Nicols (modified after [6,145]).

In another view, the Paionia ocean basin here is equivalent to the Axios/Vardar ocean basin, formed during the Mid–Late Middle Jurassic in a supra-subduction zone setting or back-arc region, behind an ensimatic island arc that resulted from Early–Middle Jurassic intra-oceanic subduction in the Neotethyan Meliata/Maliac ocean basin [11,20,138,177,180]. In this case, the Paikon subzone is interpreted as a tectonic window of Pelagonian origin, where the ophiolites of the Almopia's and Paionia's subzones, together with the ensimatic arc volcano-sedimentary products, were W-SW-ward obducted during the Mid–Late Jurassic (Callovian–Oxfordian) from a single ocean basin, the Neotethyan Axios/Vardar basin located east of the Pelagonian continental margin (Figures 3, 4, 13 and 14; [2,6,13,138,145,162,181]). On the other hand, ophiolites of the eastern–northeastern part of the single Axios/Vardar ocean basin were obducted simultaneously during the Mid–Late Jurassic on the European margin but with an N-NE-ward sense of movement (Figures 4, 10, 13 and 14; [24,41,182–185]). In this case, simultaneous SW-ward and NE-ward ophiolite obduction during the Mid–Late Jurassic on the continental margins of both the Pelagonia and Europe, respectively, was related to an arcuate type NW-ward convex intra-oceanic subduction zone of a more western–northwestern part of the Neotethyan, the Meliata/Maliac ocean realm [17,24].

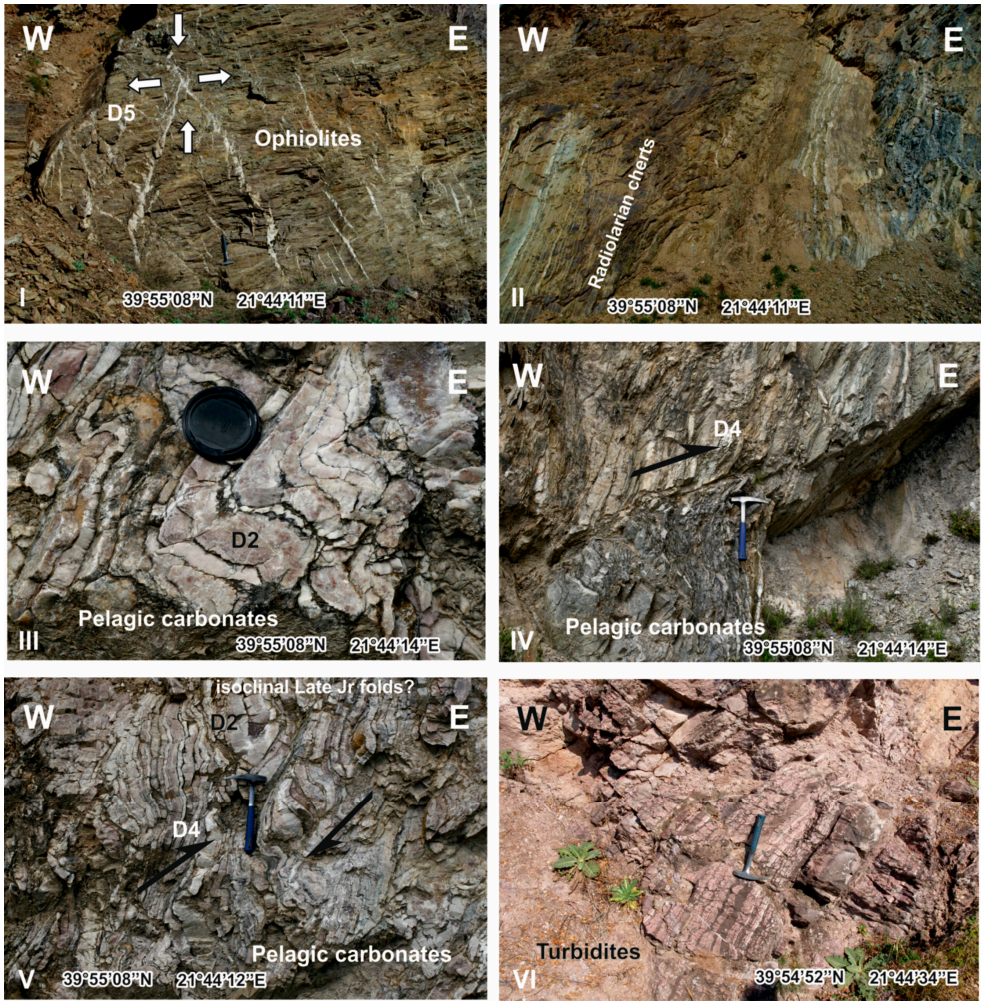

Figure 12. Field photographs of the ?Sub-Pelagonian zone at the western margin of the Pelagonian nappe (modified after [30]; Kilias et al., 2016): (**I**) Green schists and deep-water sediments of the Sub-Pelagonian zone with a conjugate set of tension gashes related to a vertical maximum σ1-axis and a subhorizontal σ3-axis, a dynamic that coincides with the Oligocene–Miocene extension (D5 event) and the carbonate Olympos-Ossa unit's exhumation under the downwardly detached blue schist unit and the Pelagonian nappe pile. (**II**–**V**) Multicoloured deep-water sediments composed of green schists, red- and green-coloured radiolarian cherts, pelagic red carbonates, and metapelite rocks, possibly of Jurassic age. These show low-grade metamorphism, but they are intensively deformed by compressional structures (e.g., isoclinal folds, reverse shear bands, and brittle thrust faults), as well as extensional structures (e.g., down-dip shear bands, S-C fabric, and semi-ductile normal fault zones). These deep-sea sediments, together with the ophiolite belt, overthrust the neritic Triassic–Jurassic carbonate rocks of the Pelagonian nappe during the Middle–Late Jurassic. The sense of movement during their initial emplacement is not clear here due to the intensive after-emplacement multi-phase deformation that affected these rocks. (**VI**) Red carbonate sediments lying under the previous multicoloured metasediments. These represent a deep-sea basin environment and show sedimentary brecciation as well as turbidity layering. Their contact with the underlying Paleozoic Pelagonian schists and Triassic–Jurassic Pelagonian platform carbonate cover is a Neogene–Quaternary normal fault zone. The age of this sequence remains under debate. It should most likely be of Jurassic age, equivalent to the previously described multicoloured deep-water sediments of the ?Sub-Pelagonian zone, having also overthrust the neritic Triassic–Jurassic Pelagonian platform carbonate cover during the Middle–Late Jurassic together with the Neotethyan ophiolites.

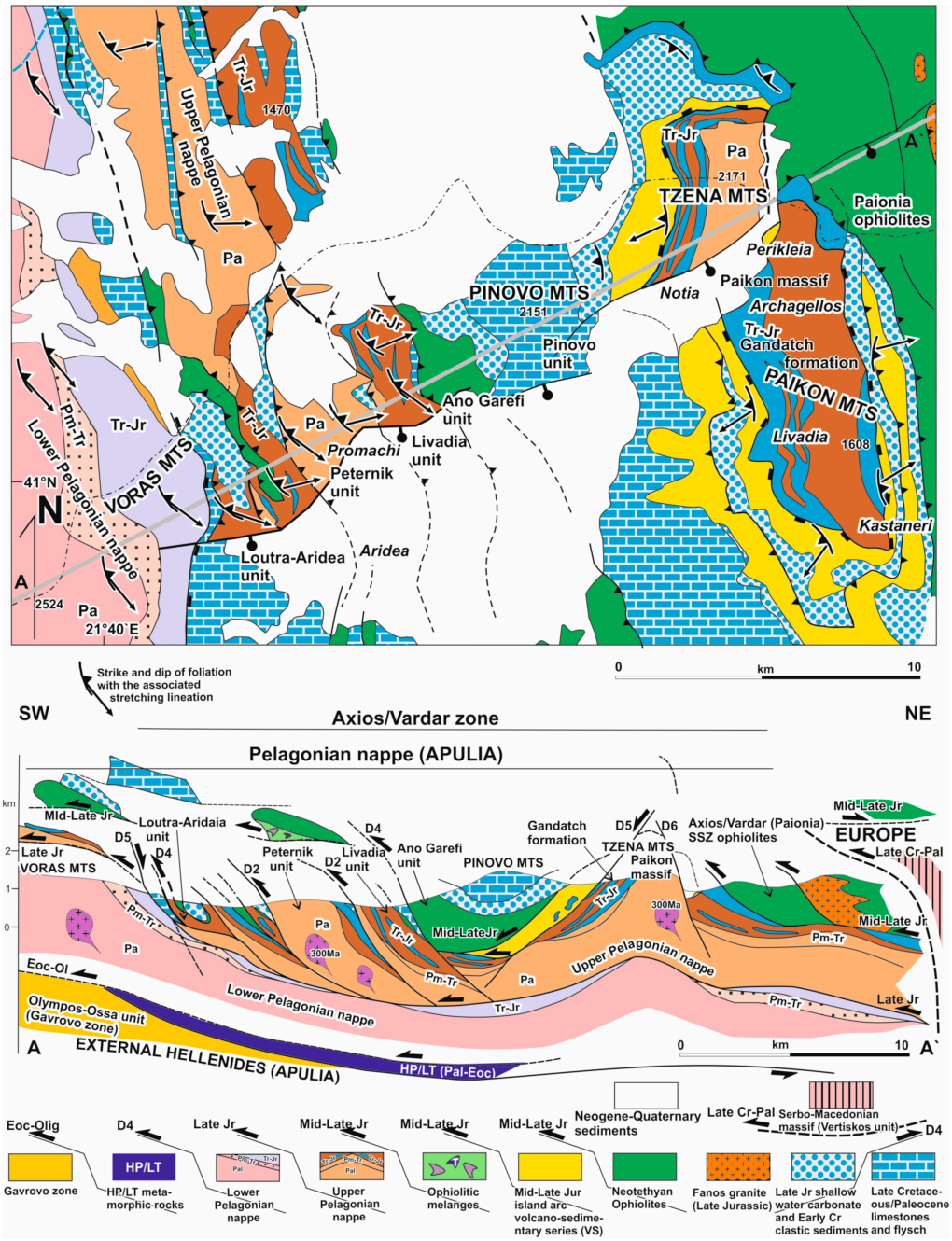

Figure 13. Geological–structural map and representative cross-section (A-A`) of the whole Axios/Vardar zone (including the Almopia, Paikon, and Paionia subzones) and its contact with the eastern Pelagonian margin at the Voras and Paikon/Tzena Mts. The Paikon basement and its Triassic–Jurassic carbonate cover are shown as a tectonic window of Pelagonian origin beneath the obducted Neotethyan Axios/Vardar ophiolites and the Mid–Late Jurassic island arc-type magmatic products (Volcanosedimentary series, VS). The Late Jurassic–Early Cretaceous and Late Cretaceous sedimentary sequences are also shown (based on [6,27,145,146,173,174]). Abbreviations as in Figure 3.

In a more recent scenario, the "maximum allocthony hypothesis" suggests that the Axios/Vardar zone is allochthonous, emplaced secondarily as a tectonic nappe in its present outcropping position, and the Axios/Vardar suture zone is located at depth along the NE boundary of the Rhodopes, forming the root zone of the most eastern nappe pile of the Internal Hellenides (e.g., [17,24,123,124,186]). Continent collision between Europe and Pelagonia, as a fragment of Apulia, intense imbrication, and nappe stacks

following the final closure and suturing of the Middle–Late Jurassic Axios/Vardar ocean basin occurred in the Paleogene (Paleocene–Eocene) after subduction during the Late Cretaceous of the remnants of the Axios/Vardar ocean realm beneath the European continental margin [17,19,21,24,59,117,121]. This Axios/Vardar suturing continues further to the north (called the Sava zone) and to the east, to the Ankara suture zone in Turkey (Figures 1 and 2; [11,21,24,117,187–189]).

Furthermore, slices of Paleozoic basement rocks, gneissics, and schists (e.g., Peternik and Livadia units), tectonically emplaced between the Axios/Vardar Mesozoic sequences, form the root parts of the Upper Pelagonian unit (KoWPZ), which overthrusts the Lower Pelagonian unit (EPZ). This was caused by internal Middle–Late Jurassic thrusting that cut the Pelagonia into two main segments, of which one was placed upon the other, with the upper being rooted in the Axios/Vardar zone (Figures 2, 3 and 13; [6,190]).

2.2.3. Cycladic Massif

The Cycladic massif is composed of a complicated, heterogeneous nappe stack system, including parts of the Internal and External Hellenides zones. In a general view, the Cycladic tectonostratigraphy can be given as follows, although it cannot be mapped entirely in a region due to the evolution of individual parts of the whole Cycladic massif in the small islands of the central Aegean sea (Cyclades islands), the Attica peninsula, and south Evia island (Figures 1 and 2: [45,80,88–95,102,114,115,191]). The deepest unit comprises a Variscan or older basement of schists and gneisses, as well as Carboniferous granitoid (~300 Ma) and abundant Oligocene–Miocene migmatites and granites. It constitutes the most deeply exhumed part of the Hellenides, belonging to the Apulian basement of the External Hellenides, possibly equivalent to the Menderes Massif, as discussed previously [9,102,191]. The Cycladic basement is overlain by a post-Variscan, Alpine sedimentary cover, containing marble, metapelites, and Early Triassic volcanic intercalations, which form the metamorphic continuation of the Apulian passive margin, equivalent to the Gavrovo carbonate platform sequence on the Hellenic mainland. The marble contains emery and metabauxites in some places, e.g., on Naxos island (Figures 4, 7 and 15; [9,191,192]). Tectonically, on top of the Alpine passive margin sequence rests the Paleocene–Eocene high-pressure belt of marble, metapelites, and metabasite intercalations, as in the Olympos-Ossa and Pelion areas, but, in the Cyclades, eclogites also occur. Highly attenuated, high-pressure-metamorphosed ophiolitic mélanges containing slivers of oceanic crust formed during ~80–70 Ma [193,194] are usually incorporated in this Paleocene–Eocene high-pressure belt. They are considered the NE-ward subducted parts of a small Pindos/Cyclades oceanic crust beneath the Pelagonian nappe [17,24,195]. Furthermore, all lithologies from the basement to the post-Variscan sedimentary cover show this Paleocene–Eocene high-pressure metamorphic overprint [45,46,49,91,115]). Additionally, intensive Oligocene–Miocene high-temperature/low-pressure (HT/LP) retrogressive metamorphism until migmatization and granitization is recognized elsewhere in the Cyclades massif, related to extension and crustal uplift [88,95]. The P-T-t tectonometamorphic path for the Cycladic massif is given in detail in Figure 8b.

On the Cycladic high-pressure belt, emplaced tectonically during the Paleocene–Eocene, is the Pelagonian nappe, with Mid–Late Jurassic obducted Neotethyan ophiolites. Today, due to the intensive Aegean Oligocene–Miocene extension, they are tectonically denudated and eroded, and only small rests are saved or as conglomerate clasts in the sediments of the Neogene basins [80,141,142].

The Cycladic high-pressure belt constitutes a typical metamorphic core complex exhumed during the Oligocene–Miocene extension in the Hellenides along normal detachment faults associated with mylonite formation and high-temperature metamorphism in the deeper tectonic levels [9,10,89–92,94,95,114,191,196,197]. Nevertheless, several studies argue that extension started no earlier than the Early Miocene [90,94,114,191,197].

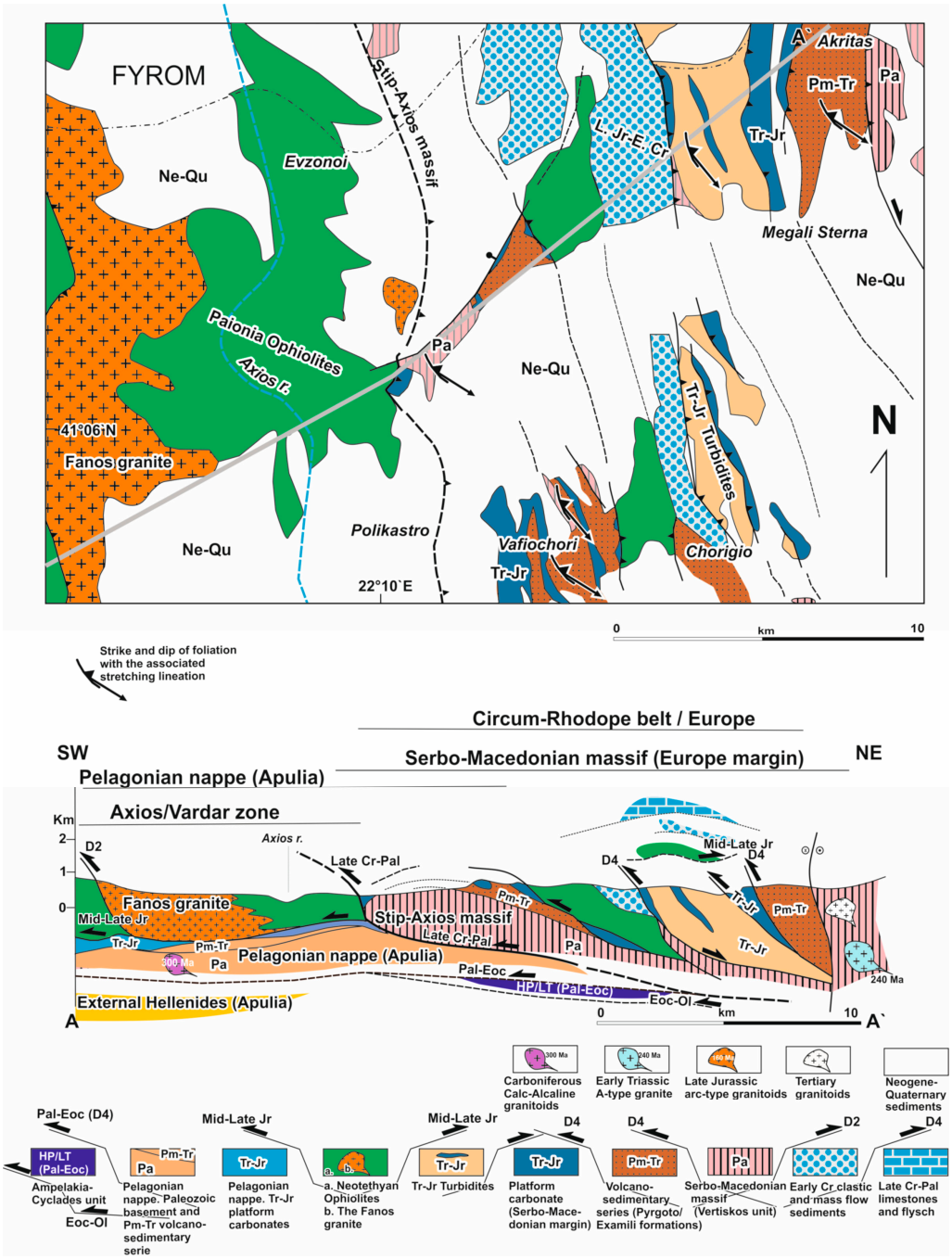

Figure 14. Geological–structural map and representative cross-section (A-A`) of the eastern Axios/Vardar zone (Paionia subzone) and the Circum-Rhodope belt, which is regarded as the sedimentary sequence initially deposited on the western margin of the Serbo-Macedonian massif (European margin). Fanos granite, connected with an ensimatic island arc, is shown overthrust together with the ophiolites on the eastern Pelagonian margin. The tectonic contact between Europe (Serbo-Macedonian) and Apulia (Pelagonia) is also shown (based on [123,124,162,186,198,199]). Abbreviations as in Figure 3.

2.2.4. Serbo-Macedonian and Rhodope Metamorphic Massifs

The Serbo-Macedonian and Rhodope metamorphic massifs are located in the northeastern Hellenides region and they continue with the same composition and structural architecture farther north, in Bulgaria and Serbia, and perhaps farther east in northwestern Turkey (Figures 1–4; [9,12,18]). They are composed of complex Alpine nappe stacks of

several metamorphic units or terranes of both continental and oceanic origin, with the Rhodopes constituting the core of the arc-type Hellenic orogenic belt (Figures 1 and 2). The Axios/Vardar zone and the Circum-Rhodope belt border the Serbo-Macedonian/Rhodope metamorphic province to the west, and the Maritza dextral strike-slip fault in Bulgaria forms its other boundary to the northeast (Figures 1–4).

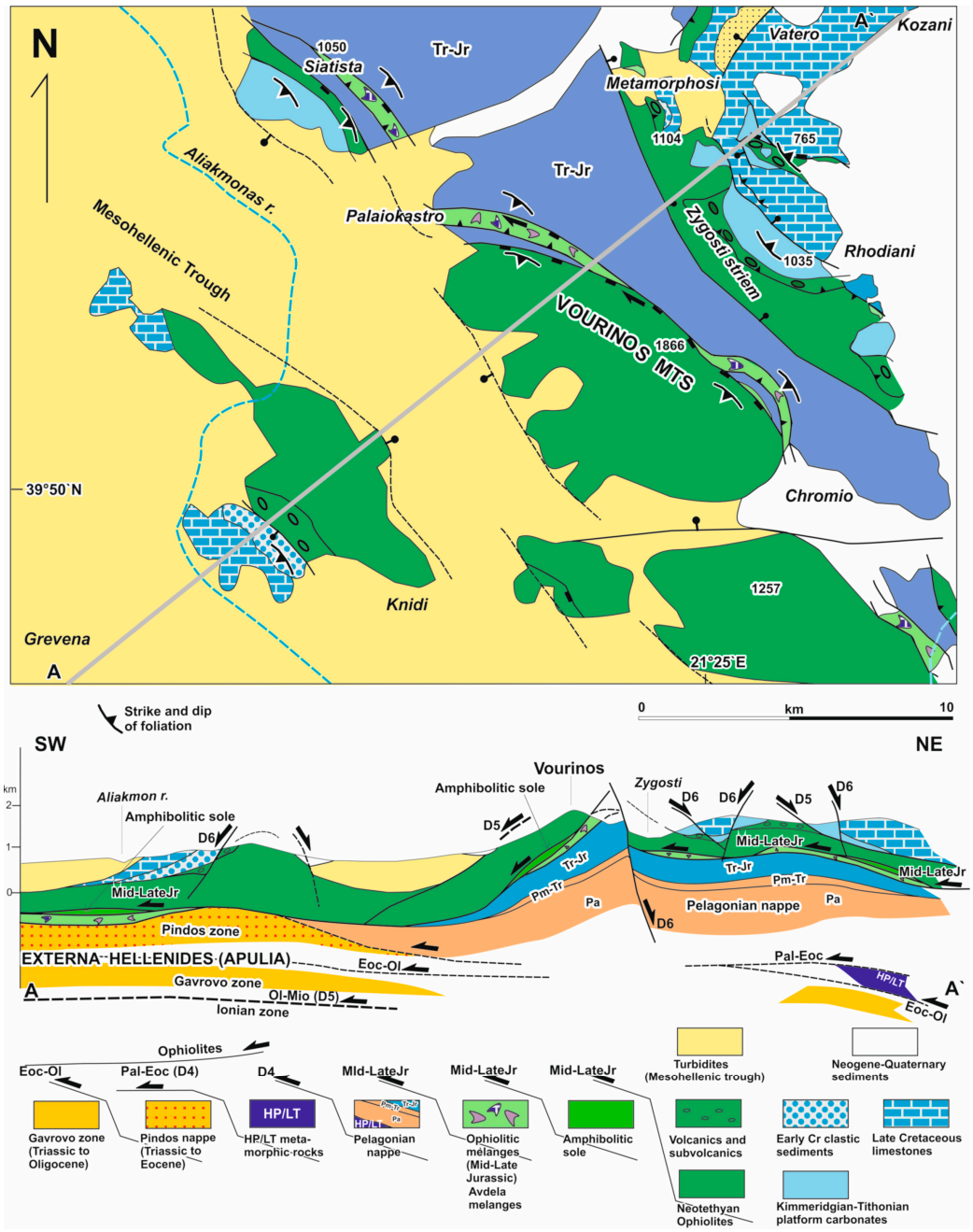

Figure 15. Geological–structural map and representative cross-section (A-A`) of the Vourinos ophiolites and the western Pelagonian margin, including the Zygosti stream ophiolite rocks and the Late Jurassic–Early Cretaceous and Late Cretaceous carbonate series, unconformably overlying either the Vourinos ophiolites or the Zygosti stream ophiolite rocks (based on [25,120,148]). Abbreviations as in Figure 3.

The various Serbo-Macedonian and Rhodope nappes were successively emplaced, one on top of the other, by intense compressional tectonics and thrusting from the Jurassic to the Tertiary. In any case, compressional tectonics and thrusting are related to multiple sub-

duction processes, high- to ultra-high-pressure metamorphism, and the final closure of the Meliata/Maliac-Axios/Vardar ocean basin, which developed, as was already mentioned, in the peculiar position between the Apulian Plate to the west and the European Plate to the east. Today, the tectonic contacts between the several nappes remain only in part as the original thrust faults related to the orogeny nappe stacks. They have usually been reworked to Tertiary, low-angle, normal detachment faults due to extensional tectonics, progressively following the several compressional stages and nappe stacking. This Tertiary extensional period was also accompanied by high-grade metamorphism, syn- to post-tectonic granitoid intrusions, and abundant migmatite formations (Figures 3 and 4; e.g., [25,120,148]).

The Serbo-Macedonian and Rhodope metamorphic nappe piles in the Greek part are made up of tectonically lower to tectonically higher nappes as follows: in the Rhodope province by the Pangaion, Sidironero, and Kimi units and in the Serbo-Macedonian province by the Kerdylia and Vertiskos units (Figures 3–5).

Rhodope Massif

I. Pangaion unit

The structurally lowermost Rhodope Pangaion unit consists of mica-schists, gneisses and marble intercalations, covered at the higher levels by a thick marble sequence (Figures 5 and 16). The age of the unit is under debate. In recent works, it has been described as a segment of Variscan or older continental crust covered by a thick marble sequence, of possible Mesozoic age [17,22–24,200–202]. Nevertheless, other authors suggest a Paleozoic age for the whole Pangaion unit, including the overlain thick marble sequence [203–207]. The Pangaion unit was intruded by Oligocene–Miocene granitoids, and during the Tertiary (Oligocene–Miocene) it underwent low-grade metamorphism under greenschist facies conditions and an extensional regime [118,200,208]. Nevertheless, some authors also describe a possible Paleocene–Eocene high-pressure metamorphic event for the lower Rhodope Pangaion unit (45.8 $\pm$ 5.8 Ma; [57,209]).

The Pangaion unit is bordered to the northeast by the Nestos shear zone (Figures 3, 4 and 16). This is interpreted as a ductile thrust zone along which the tectonically middle Rhodope Sidironero unit overthrusts the Pangaion unit during the Tertiary (Paleocene–Eocene; [17,24]), although some other authors date the Nestos thrust zone as of Cretaceous or Jurassic age (e.g., [18,22,23,210]). Furthermore, [202] interpreted the Nestos thrust zone as a suture zone between the lower Rhodope Pagaion unit and the middle Rhodope Sidironero unit of Jurassic–Cretaceous age.

In contrast, the southwestern border of the Pangaion unit is controlled by an Oligocene–Miocene normal detachment zone, along which the Serbo-Macedonian massif was detached SW-wards, resulting in the final exhumation of the Pangaion metamorphic core complex and the formation of the supra-detachment Neogene Strymon basin (Figures 3, 4 and 16; [7,118,200,211,212]).

The Pangaion unit has been variably interpreted until today as an Oligocene–Miocene metamorphic core complex belonging to the External Hellenides Apulian Plate [17,24,118,123,124,186] or as microcontinent, named the Drama or Thracia terrane [4,202], accreted to the European continent, either during the Early–Middle Jurassic following the closure of a Triassic age's ocean basin [22,23] or during the Cretaceous [18,202,210]. Furthermore, [213] interpret the Pangaion unit as a continental crust derived from the Pelagonian segment.

II. Sidironero unit

The Sidironero unit tectonically overlies the Pangaion unit and is composed of rocks of oceanic and continental origin. It is possible to distinguish amphibolites, ortho- and paragneisses, marbles, migmatites, and metaophiolites. The orthogneises are derived from Late Jurassic–Early Cretaceous arc-type granitoids as well as from Variscan granitoids that intrude the older Paleozoic Sidironero basement rocks [202,214,215]. The Late Jurassic–Early Cretaceous arc-type granitoid intrusions highlight the Sidironero unit as a Late Jurassic

subduction-related volcanic arc and the Pangaion unit as a microcontinent possibly underthrusting the Sidironero unit during the Late Jurassic, although this interpretation remains under discussion (e.g., [17,22–24,202,206,207]). Furthermore, Eocene–Oligocene adakitic and Oligocene–Miocene calc-alkaline granitoids also intrude the basement rocks during an extensional tectonic regime (Figures 3–5 and 16; [24,118,216–223]). Metaophiolites occuring in between the Sidironero continental rocks yielded a ca. 160 Ma age for their protolith. They have been interpreted as equivalent to the Axios/Vardar ophiolite belt, emplaced tectonically in the Sidironero unit during the Late Cretaceous–Paleocene following the closure of the Axios/Vardar oceanic basin [17,24].

In the Greek and southern Bulgaria Rhodope province, two dome-shape tectonic windows, the Kesebir-Kardamos and Kechros domes, exhumed along Tertiary normal detachment faults below the upper Rhodope Kimi unit and composed by Paleozoic gneissic and schists rocks intruded by Variscan and Triassic, as well as Tertiary, granitoids, have been grouped with the lowermost Pangaion metamorphic core complex (Figures 3 and 4; [17,18,40,202]). Nevertheless, taking into account that their composition and structural evolution are not exactly defined, some questions about their geotectonic setting as equivalent to the Pangaion metamorphic core complex are raised. Therefore, the Kesebir-Kardamos and Kechros domes are not characterized by the thick carbonate cover sequence dominating the Pangaion unit and they are affected by a higher- grade Tertiary metamorphism than the Pangaion unit associated with migmatization, which is not observed in the Pangaion unit [40,200,224–226]. Furthermore, they show a cooling/exhumation path during the Eocene–Oligocene extension (~42–35 Ma), which is the same as for the Sidironero unit (Figures 4 and 17a; [227]). The cooling/exhumation path for the Pangaion unit is related to Oligocene–Miocene extension (26–10 Ma, Figures 4 and 17a; [227,228]). On this basis, considering the structural positions of the Kesebir-Kardamos and Kechros domes, exactly below the Kimi unit, their geotectonic–paleogeographic regime as equivalent to the Pangaion unit is under dispute.

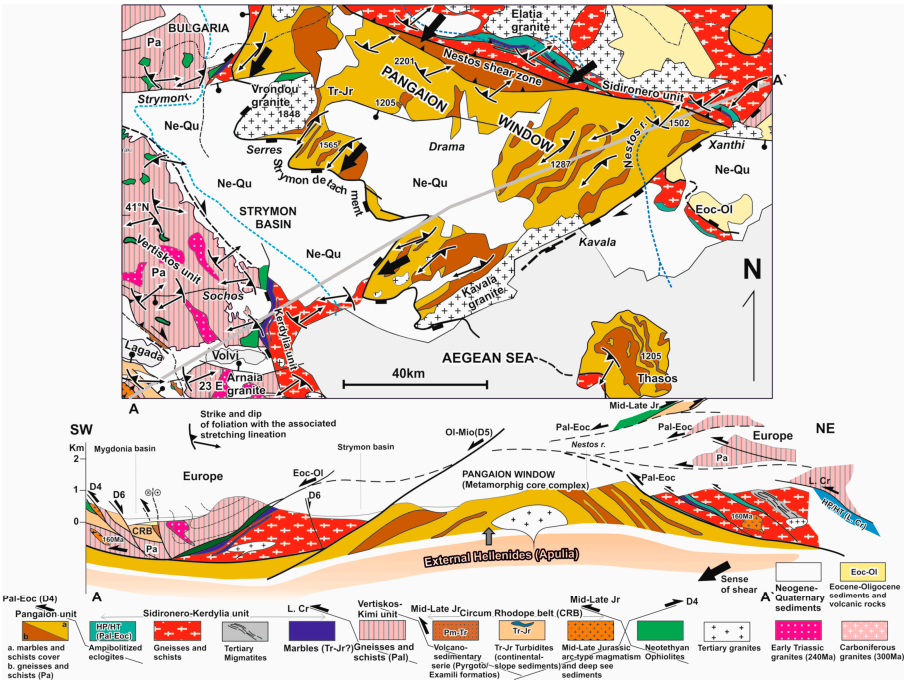

Figure 16. Geological–structural map and representative cross-section (A-A`) of the Pangaion metamorphic core complex and the Serbo-Macedonian/Rhodope nappe pile. The Paleocene–Eocene Nestos thrust zone [17,24] and the Oligocene–Miocene Strymon valley normal detachment fault zone [118,212], as well as the Miocene–Pliocene supradetachment Strymon basin, are shown [7,30]. Abbreviations as in Figure 3.

High-pressure eclogite facies metamorphic paragenesis remnants and ultra-high-pressure diamond-bearing rocks, including mainly basic Morb-type rock bodies, were described for the Sidironero unit. Isotopic analysis data for the high-pressure rocks have given various ages that have been partially interpreted differently by several authors. In any case, high-pressure metamorphic conditions are related to subduction, compression, and crustal thickening due to thrusting or crustal sinking due to overloading setting of the nappe stacks. The ages of the recognized high-to ultra-high-pressure metamorphic events are: ca. 200 Ma [54–56,121,202]; 150–140 Ma [53,226]; 92–70 Ma [58,59]; and 51–45 Ma [51,53,57,229]. The high-pressure metamorphic events were finally strongly reworked by an Eocene–Oligocene retrogressive high-temperature event in the amphibolite facies metamorphism, partly reaching migmatization conditions and granitoid genesis. This high-temperature metamorphic event was related to extension and crustal exhumation. Moreover, it is the dominant metamorphism in the Sidironero unit and strongly reworked all other older metamorphic events [51,53,118,200,208,216]. The pre-Paleocene–Eocene ages of the high- and ultra-high-pressure metamorphic events described for the Sidironero metamorphic rocks have also been detected in the tectonically overlying upper Rhodope Kimi. These high-pressure rocks were interpreted as parts of the Kimi unit that were imbricated between the Sidironero rocks due to younger, successively thrusting events [24,59].

Furthermore, a migmatization event at ca. 140 Ma for the Sidironero unit referred to by [226] remains without any clear explanation of its geotectonic framework. In any case, the two migmatization ages at the Early Cretaceous and Eocene indicate the multiphase evolution of the Alpine orogeny in the Rhodope massif.

III. Kimi unit

The Kimi unit represents the upper tectonic nappe of the Rhodope nappe stack. It is composed of various metamorphic rocks of continental origin (ortho- and paragneisses, amphibolites, thin marble layers, and gneiss-schists) and meta-ophiolites. The protolith ages of the orthogneisses are dated as Paleozoic (Ordovician and Silurian), while the meta-ophiolites yielded Early Paleozoic and Triassic protolith ages [41,215,230–233].

High- to ultra-high-pressure metamorphic rocks, including eclogites and diamond-bearing gneisses, were also recognized in the upper Rhodope Kimi unit. Geochronological isotopic data again yielded here a large dispersion of ages for the high- to ultra-high-pressure metamorphic rocks and different interpretations for their development. Their isotopic ages are described as follows: ca. 200 Ma, ca. 158 Ma, ca. 125 Ma, and 82–74 Ma [50,59,121,234–236]. The 200 Ma age [121,234] was related to the diamond occurrence in gneisses and meta-ophiolites. This event has been possibly related to the closure of the Paleotethys around 200 Ma ago (in the Early Jurassic) and thus represents the palaeogeographic location of the actual suture of the Paleotethyan ocean [24,56,121,234]. The high-pressure metamorphism that occurred during the Late Cretaceous (~80–85 Ma; [59,121,235,236]) is in very good concordance with the proposed Late Cretaceous subduction of the remnants of the Neotethyan Axios/Vardar Ocean below the European margin and the formation of a Late Cretaceous magmatic arc with arc-type granitoid inclusions in the European margin (Sredna-Gora massif; [59,215,237–239]). For the other high-pressure events referred to, there is still no clear evidence for their structural evolution or geotectonic regime.

The Late Cretaceous high-pressure metamorphic event, associated with compression and nappe stacking, was progressively reworked by a Paleocene–Eocene retrogressive high-temperature event in the amphibolite facies metamorphism, partly reaching migmatization and granitization conditions. High-grade temperature metamorphism was related to extension, tectonic denudation of the Rhodope nappe stack, and crustal exhumation [7,17,24,40,67,233,240].

Moreover, regarding the cooling/exhumation paths of the Kimi, Sidironero, and Pangaion Rhodope units, the whole Rodope nappe stack is characterized by a gradual cooling/exhumation history during extension. From the top to the bottom unit, the cooling/exhumation path for the upper Kimi unit was dated to the Paleocene–Eocene

(~60–48 Ma), for the middle Sidironero unit to the Eocene–Oligocene (~42–30 Ma), and, finally, for the lowermost Pangaion unit, to the Oligocene–Miocene (~26–10 Ma). This shows the progressive exhumation evolution of the Rhodope units from the top to the bottom (Figures 4 and 17a; [7,17,24,40,67,118,200,208,216,227,241]).

Finally, my view is in agreement with the interpretation that the upper Rhodope Kimi nappe represents the Mesozoic western continental margin of Europe, where the Neotethyan ophiolites were obducted NE-ward during the Mid–Late Jurassic arc–continent collision [24,41,123,124].

Serbo-Macedonian Massif

I. Kerdylia unit

As already mentioned, the Serbo-Macedonian massif is divided into the lower Kerdylia and the higher Vertiskos units, which form parts of a nappe stack (Figures 3–5). The Kerdylia unit is composed of Paleozoic ortho- and paragneisses and schists, as well as granitoid intrusions and a relatively thin marble cover of unknown age, constituting the highest lithostratigraphic sequence of the unit (Figure 16). Papanikolaou (2009, 2013) [22,23] records the marble cover as a possible Triassic sedimentary series, deposited on a passive continental margin. Migmatites also occur, with their age still under discussion, possibly ranging from the Paleozoic to the Tertiary [1,68,242,243]. The Kerdylia unit was tectonically placed secondarily on top of the western side of the Rhodope Pangaion unit along an Oligocene–Miocene normal detachment fault zone related to the final exhumation of the lowermost Rhodope Pangaion unit (Figures 3, 4 and 16; [118,122,200,208,211]. In contrast, previous works described this normal detachment fault zone as a thrust fault, along which the Kerdylia unit was tectonically placed on the Pangaion unit [203,204,244,245].

At the boundary between the Vertiskos and Kerdylia units, tectonically metamorphic mafic and ultramafic rocks of oceanic lithosphere origin crop out, named the Volvi ophiolite complex (Figures 3, 4 and 16; [246,247]). Recently, works dated the protolith of the Volvi ophiolite complex as of Mid–Late Jurassic age, originating in the Axios/Vardar ocean basin and emplaced in its current position during the Late Cretaceous–Paleocene, following Axios/Vardar ocean closure and subduction under the European margin [17,24]. Nevertheless, Papanikolaou (2009, 2013) [22,23] suggests an Early Jurassic emplacement of the Volvi ophiolite complex sandwiched between the upper Vertiskos and the lower Kerdylia units and originating in a Volvi-East Rhodope ocean basin. In this scenario, the Kerdylia unit is considered equivalent to the lowermost Pangaion Rhodope unit. A question arises here because the Volvi ophiolite complex protolith has been dated as of Mid–Late Jurassic age. It is impossible that it was emplaced during the Early Jurassic. Furthermore, [201,248] interpret this tectonic contact between the Kerdylia and Vertiskos units as a secondary reactivated normal detachment fault zone of the Eocene–Oligocene age, along which the overlain Vertiskos unit detached westwards, causing the exhumation of the lower Serbo-Macedonian Kerdylia unit (Figures 3, 4 and 16).

According to the most recent work (e.g., [17,24,249]), the Kerdylia unit is regarded as equivalent to the middle Rhodope Sidironero unit, with both forming a single tectonic nappe above the Rhodope's lowermost Pangaion unit, named the Middle Alochthon, while the Pangaion unit is named the Lower Allochthon. This is concluded from a recognition of their same structural settings and tectonostratigraphy, as well as of the same Eocene–Oligocene cooling/exhumation paths for both the Sidironero and Kerdylia units (Figures 3, 4 and 16; [17,18,24,118,208,227,249]). Moreover, the dating of granitoids of the Kerdylia unit reveals ages from the Late Jurassic and also of the Permo-Carboniferous [250,251], again the same as is recorded for the Sidironero unit [234]. Nevertheless, the exact ages of the high-pressure metamorphic rocks that were recognized in the Serbo-Macedonian Kerdylia unit remain under debate. A general Mesozoic age was proposed by [213].

II. Vertiskos unit

The Vertiskos unit mainly comprises amphibolites, schists, ortho- and paragneisses, and, in places, thin marble layers of a Paleozoic-age protolith [231,252]. Furthermore, abundant migmatite rocks also occur in the lithostratigraphic composition of the Vertiskos unit. Their age remains today under debate, ranging from the Paleozoic to the Tertiary [243,253,254]. A-type leucocratic granitoids (e.g., Arnea granite) intrusions of Early Triassic age (240–220 Ma) are recognized within the Paleozoic rock sequence. They were intruded upon during the continental rifting of the Pangea supercontinent (Figure 16; [136,137,251]. Moreover, Neotethyan ophiolite bodies are also tectonically intercalated as imbricated sheets within the Vertiskos basement gneissic and schist rocks (Figures 3 and 16; [4,42,243,255]). The ophiolites were initially obducted NE-wards during the Middle–Late Jurassic on the Serbo-Macedonian Vertiskos unit, which formed the European continental margin at the eastern part of the Neotethyan Meliata/Maliac-Axios/Vardar ocean [17,24,42,183,255].

In the Vertiskos unit, similar to the Rhodope Sidironero and Kimi units, high-pressure to ultra-high-pressure diamond-bearing parageneses have been recorded. Their age once again remains under debate. It ranges from Paleozoic to Mesozoic (e.g., [213,253,256]). Moreover, the amphibolite facies metamorphic conditions of the Late Jurassic–Early Cretaceous, possibly related to extension and crustal uplift, have been recognized for the Vertiskos unit. This was followed by retrograde greenschist facies Early Cretaceous (Barremian–Aptian) metamorphism related to compressional tectonics (Figure 17b; [240,247,257]). Remnants of Variscan age metamorphism are also recorded [231,243,257,258]. The cooling/exhumation path of the Vertiskos unit has been dated as Early Paleocene–Eocene, while AFT analyses give cooling ages of ~43 Ma (Figures 4 and 17b; [227,259]).

Structurally, the Vertiskos unit occupies the same tectonic level as the Rhodope Kimi unit, lying above the Kerdylia unit, and shares the same lithostratigraphic composition as the Kimi unit. Additionally, it records a similar tectono-metamorphic evolution as well as cooling/exhumation history to the Kimi unit. These ages are Early Paleocene–Eocene for the Vertiskos unit and Paleocene–Eocene for the Kimi unit. Furthermore, the AFT cooling ages for the Kimi unit reach about 35 Ma [227,241]. Therefore, both units could be regarded as parts of the same tectonic nappe, named the "Upper allochthon" according to the subdivision of [17,24,249], tectonically lying above the single Sidironero-Kerdylia nappe ("Middle allochthon"), and which tectonically overlaps the lowermost Pangaion unit ("Lower allochthon"). These nappe columns form the Serbo-Macedonian/Rhodope metamorphic nappe stack (Figures 3–5 and 16; [7,24,201,227]). Nevertheless, the somewhat older Early Paleocene–Eocene cooling/exhumation path of the Vertiskos unit, as well as the AFT cooling ages (~43 Ma), show that it was at least one level higher than the Kimi unit or possibly a higher tectonic nappe [18].

The Vertiskos unit is bordered to the west by the Axios/Vardar zone, as described earlier in detail, and by the Circum-Rhodope belt (CRB). The latter is an Alpine volcano-sedimentary sequence composed of Triassic–Jurassic pelagic and neritic sediments distal and proximal to the continental margin. These include platform carbonate sequences, shales, and flysch-type rocks, tectonically intercalated with Triassic bimodal-type volcanic products and acid-to-intermediate ensimatic-island-arc volcanic rocks formed progressively during an Early–Middle Jurassic intra-oceanic subduction progress in the Neotethyan ocean (Meliata/Maliac-Axios/Vardar ocean). Moreover, a NW–SE-striking tectonic slice of pre-Alpine gneisses and schists, possibly belonging to the Serbo-Macedonian Vertiskos unit, the so-called Stip-Axios massif, is also tectonically incorporated between the Mesozoic-Alpine geological formations of the Circum-Rhodope belt (Figures 2–4, 13 and 14; [68,138,198,199,242,260]). Equivalent units to the Circum-Rhodope belt are the Alexandroupolis-Maronia unit in northeastern Greece and the allochthonous Strandja and Mandrica units in Bulgaria (Figures 2 and 3; [17,24]. The Circum-Rhodope belt shows a blueschist facies metamorphism of probable Jurassic age, overprinted by a greenschist facies metamorphic event during the late Early Cretaceous [17,24].

Kockel et al. (1971, 1977) [68,242] and Kaufmann et al. (1976) [260] interpreted the Circum-Rhodope belt as the Alpine Triassic–Jurassic sedimentary cover of the continental margin of the Vertiskos unit (western European margin) towards the Axios/Vardar ocean basin. According to more recent work [17,24,182,183], the Circum-Rhodope belt and its equivalent units were initially tectonically placed over the Vertiskos margin, together with Neotethyan Axio/Vardar ophiolites with a main NE-ward emplacement direction during the Mid–Late Jurassic in the course of an arc–continent collision forming the uppermost tectonic nappe or the "Uppermost allochthon" of the Serbo-Macedonian/Rhodope nappe pile. Through a younger tectonic event during the Late Cretaceous–Paleogene, the initial Mid–Late Jurassic NE-wards stacking was reversed to SW-ward thrusting, causing intense imbrication of the CRB unit and the Vertiskos unit. Finally, along a NW–SE-striking dextral transpression fault zone of Oligocene–Miocene age, the Vertiskos Unit was emplaced on the CRB (Figure 3, Figure 4, Figure 10, Figures 13, 14 and 16; [6,7,198,240,261]).

3. Alpine Magmatic and Depositional Processes

For a better understanding and explanation of the Alpine structural–geodynamic evolution of the Hellenides, it is considered to be important, before the analysis of their structural architecture and kinematics of deformation, to provide here a summary, first **(I)** of the magmatic activity that affected the Hellenides from the Upper Paleozoic to the Neogene–Quaternary and second **(II)** of the sedimentary processes recorded in the Hellenides from the Permo–Triassic to the Neogene–Quartenary. Moreover, magmatic and sedimentary processes are very important for dating the several deformational events that have affected the Hellenides.

3.1. Hercynian to Neogene–Quaternary Magmatism

Initial, Upper Paleozoic (~300 Ma) calc-alkaline granitoid intrusions within the Paleozoic basement units of the Internal Hellenides, related to subduction processes and the Paleotethys closure, have been widely described by several authors (Figures 4, 5, 13 and 18; [3,135,136,171,172,262,263]. Early Triassic (~240 Ma) A-type granitoid intrusions and bimodal-type volcanic rocks, usually intercalated with clastic and shallow-water carbonate sediments, forming a Permo–Triassic volcano-sedimentary series in the Internal Hellenides, have been interpreted as magmatism related to the initial Permo–Triassic continental rifting of Pangea and the Neotethys ocean opening (Figures 3, 4, 16 and 18; [134,136,137,264]). Mid–Late Middle Jurassic arc-related volcanic products and magmatic activity with granitoid intrusions have been recorded in the Axios/Vardar zone and the Serbo-Macedonian/Rhodope metamorphic province. They intrude the ophiolites and the continental basement rocks and are related to Meliata/Maliac-Axios/Vardar intra-oceanic subduction processes and progressively evolved structural stages (Figures 3, 4 and 11; [24,41,138,145,162,171,172,265]). Late Cretaceous calc-alkaline arc-type magmatic activity is described for the European margin in the Strandja/Sredna-Gora massif due to the NE-ward subduction of the remnants of the Axios/Vardar oceanic lithosphere under Europe.

This Late Cretaceous magmatic activity migrated to the southwest, as shown by the later SW-ward granite intrusion ages, from 80 to 70–60 Ma, along the European margin. This magmatic activity was possibly related to a SW-ward rollback of the subduction zone [59,266–269].

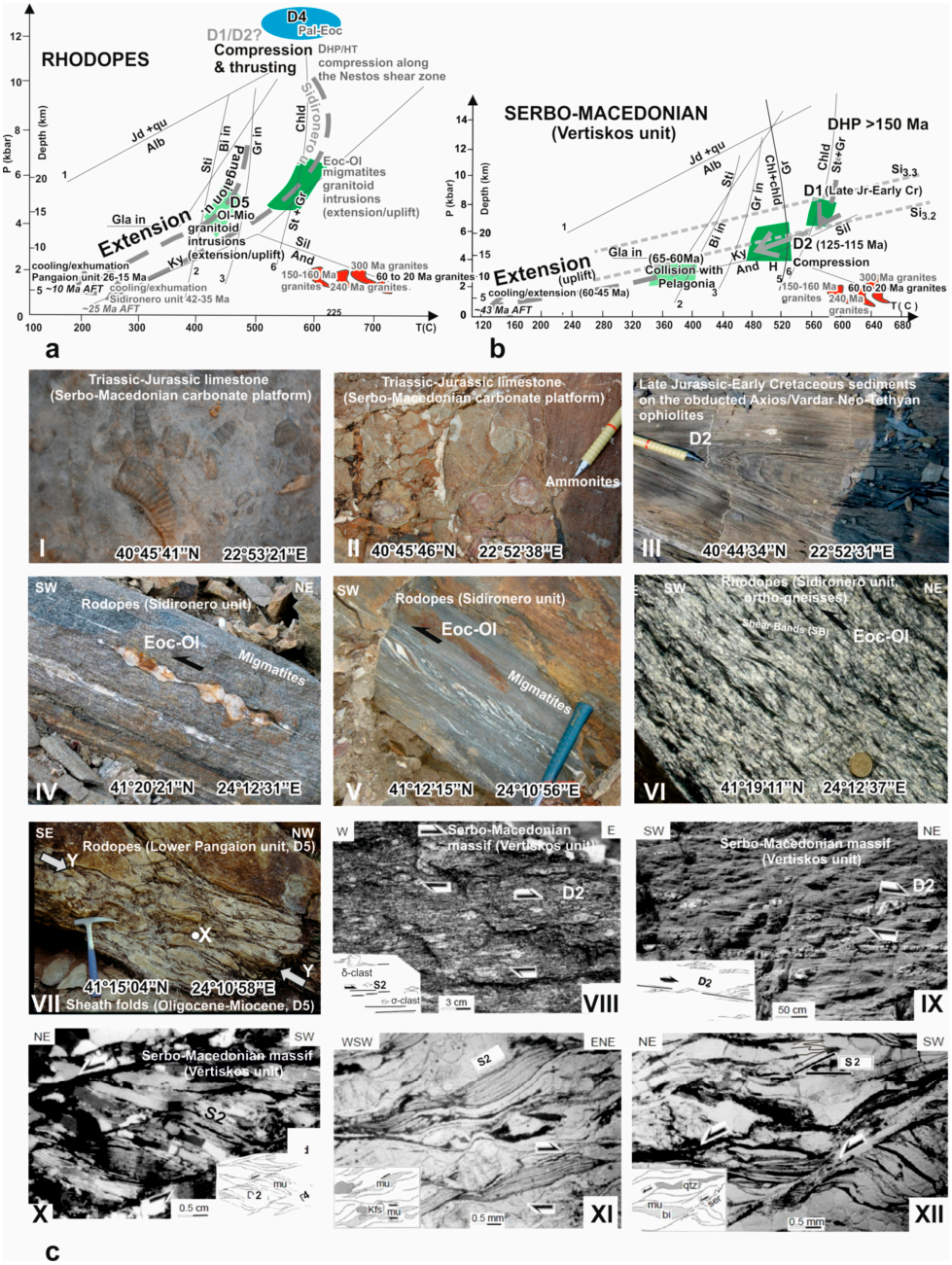

Figure 17. (**a**,**b**) P-T-t Alpine tectono-metamorphic paths and exhumation history of the (**a**) Rhodope Pangaion and Sidironero units [24,41,200,227] and (**b**) Serbo-Macedonian Vertiskos unit [172,227,240,247], *AFT* = apatite fission-track ages [227]. (**c**) Meso- and microscale compositional features and architecture of the deformational events within the Rhodope and Serbo-Macedonian massifs. Shear sense criteria along the X-Z sections [30,240]: (**I**,**II**) Fossiliferous Triassic–Jurassic carbonate cover of the Serbo-Macedonian continental margin (European margin). Gastropod (**I**) and ammonite (**II**) fossils are distinguished. (**III**) D2 isoclinal, recumbent fold of the ?Late Jurassic–Early Cretaceous sedimentary series on the top of Mid–Late Jurassic obducted ophiolites at the western European margin (Serbo-Macedonian massif). S2 foliation has developed parallel to the fold's axial plane (Axios/Vardar zone, Paionia subzone). (**IV**,**V**) Asymmetric boudins and σ-clasts of leucosoms in Paleocene–Eocene migmatites of the Sidironero unit (Rhodope massif). A top-to-SW sense of movement is clearly recognized. (**VI**) S-C-C` fabric of Paleocene–Eocene age in orthogneisses (possible

Carboniferous age for the Granite protolith) of the Rhodope Sidironero unit. The sense of shear is top-to-SW. (**VII**) Sheath folds, reoriented parallel to the dominant SW–NE-trending stretching lineation (X-axis of the strain ellipsoid) in the Pangaion unit's marbles. (**VIII**) σ- and δ-type feldspar clasts within the augen gneiss of the Serbo-Macedonian Vertiskos unit at Kerkini Mt. The sense of shear is top-to-east (D2 event; Barremian–Aptian). (**IX**) Pervasive shear bands and asymmetric quartzitic boudins in schist-gneisses of the Serbo-Macedonian Vertiskos unit. The sense of shear is top-to-NE. (**X**–**XII**) Shear bands, σ-feldspar clasts and mica "fish" from mica-gneisses of the Serbo-Macedonian Vertiskos unit. The sense of shear is clearly top-to-ENE/NE, related to the Paleocene–Eocene D4 event and the exhumation of the Vertiskos unit. The mica notes S2 foliation but is also reoriented along the D4 shear bands. Microscopic pictures: (**X**–**XII**) with one Nicol (detailed description of the deformational events in the chapter "Architecture of deformation and structural evolution").

Additionally, Paleocene to Miocene magmatic activity and Tertiary migmatization have been mainly recognized in the Serbo-Macedonian/Rhodope and Cyclades metamorphic provinces, related to extensional regime and/or mantel delamination processes (Figures 3, 4, 16 and 19; e.g., [7,17,89,95,216,220,222,223,270]). Finally, Neogene to Quaternary volcanic products are recorded in the broader Internal Hellenides zones until the active Hellenic volcanic arc, showing, from the older to the younger products, S-SW-ward propagation (Figures 2 and 20; [271–276].

3.2. Sedimentary Processes

Here are briefly described the main Alpine sedimentary processes of the Hellenides, from the Permo–Triassic to the Neogene–Quaternary. From the older formations to the younger ones, they are (**I**) The Permo–Triassic volcano-sedimentary sequence with Triassic–Jurassic neritic and pelagic sediments proximal and distal to the continental margins (Internal Hellenides), (**II**) Mid–Late Jurassic ophiolitic mélanges, (**III**) Late Jurassic neritic carbonate sediments, (**IV**) ?late Late Jurassic–Early Cretaceous turbidites and mass-flow deposits, (**V**) Late Cretaceous shallow-water carbonates and the Paleocene flysch of the Internal Hellenides, and (**VI**) Paleocene–Eocene to Oligocene–Miocene flysch sediments of the External Hellenides and their Mesozoic sedimentary series as well as the Eocene to Early Miocene turbiditic deposits of the Meso-Hellenic trough and the Thrace basin. Finally, the younger, post-orogenic Hellenides sedimentary series of Neogene–Quaternary age should also be mentioned.

3.2.1. Triassic–Jurassic Sediments

The Triassic–Jurassic sediments of the Internal Hellenides were deposited on the passive continental margins of the Apulian Plate (including Pelagonia) and the European Plate (including the Vertiskos-Kimi unit) in the west and east of the Meliata/Maliac-Axios/Vardar ocean basin, respectively, during its opening. These sediments were deposited under an extensional tectonic regime before the onset of the Alpine deformational history, containing successive nappe stack processes and, subsequently, extensional events associated with tectonic nappe denudation and crustal uplift [3,6,19,21,134,199,277]. The sedimentary sequences follow a passive continental margin's typical proximal and distal sedimentation evolution [140,277]. From the continent to the ocean, these are neritic platform carbonate sediments, in some places dolomitic; pelagic sediments of the Hallstatt facies; flyshoid sediments of the continental slope of the Meliata facies; and deep-sea sediments of the ocean (shales, radiolarites and clay sediments).

From among the described Triassic–Jurassic sedimentary sequences, the outer shelf sequences are still poorly known, because they were strongly reworked during the evolution of the subsequent Jurassic and later tectonic history. Today, they are detected only in the form of resedimented pebbles or blocks in melange sequences due to their active participation in the imbrication regime during Jurassic obduction and the far-travelling advance of Neo-Tethyan ophiolites on the continental margins [13,30,139,140,277–279].

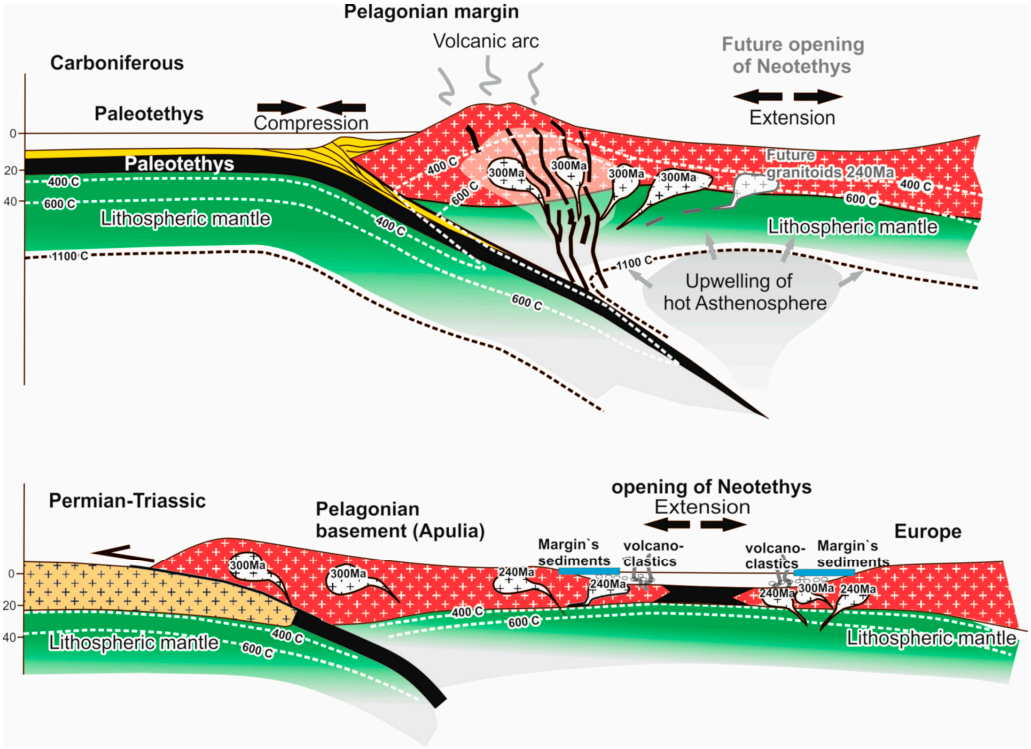

Figure 18. Schematic crustal-scale transects showing the geotectonic setting of Hercynian granitoid intrusions (~300 Ma) into the Pelagonian continental margin and Permo–Triassic magmatic activity (240 Ma: A-type granitoid intrusions and bimodal volcanism) during the initial stages of the Neotethys opening (modified after [136]). Triassic–Jurassic sedimentation processes take place at both the Pelagonian (Apulia) and Serbo-Macedonian (Europe) passive continental margins. Sedimentation was broken down by Middle–Late Jurassic Neotethyan ophiolite obduction [6,17,24,145,240].

The neritic Triassic–Jurassic sediments rest on top of a Late Permo-Early Triassic volcano-sedimentary series composed of the intercalation of clastic sediments, thin carbonate layers, and bimodal volcanic products. The Permo–Triassic series evolved, as already mentioned, during the initial breaking of the Pangea supercontinent and the onset of the opening of the Neotethyan ocean [3,134,264].

3.2.2. Mid–Late Jurassic Ophiolitic Mélanges

These Mid–Late Jurassic ophiolitic mélange successions, reaching in places several hundred metres thick, are characterized by folds and thrust fault deformation as well as intensive shearing (Figures 21 and 22; [20,21,278,280]). They form "block-in-matrix" complexes with a complicated compositional structure composed of up to kilometre-sized exotic blocks (Olistholiths) of Triassic–Jurassic pelagic and shallow-water carbonate sediments, radiolarites, basalts, serpentinites, pillowed and massive lavas, and gabbroic rocks, as well as amphibolites from the amphibolite metamorphic sole, which are interbedded between radiolarites, radiolarian cherts, shales, and siliceous shales, dated from the Bathonian to Oxfordian ages. Furthermore, redeposited fine-grained carbonates and quartzose turbidites are intercalated in places within Mid–Late Jurassic deep-water successions composed of radiolarites, shales, and volcanoclastics. Medium to coarsely basic-intermediate sills intrude in places in these lithostratigraphic, polymictic tectono-sedimentary sequences (Figure 22; [13,140,278–281].

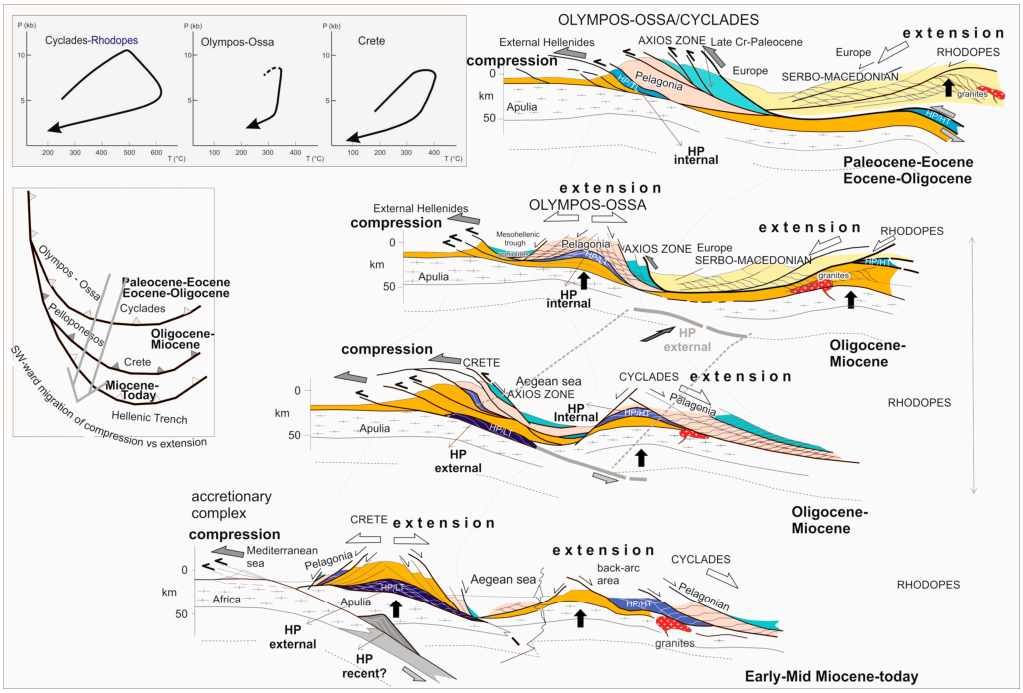

Figure 19. The Tertiary until today: SW-ward migration of dynamic peer compression vs. extension, responsible for the configuration of the Hellenic orogen and its structural architecture, is illustrated (HP = high pressure). The associated Tertiary P-T metamorphic paths of several high-pressure belts in several regions of the Hellenides are also shown [5,240]).

Two very well structurally maintained and representative Mid–Late Jurassic ophiolitic mélange sequences are the Avdella and Vourinos mélanges in the Pindos and Vourinos mountainous regions, respectively [119,269,280,282]. In Orthrys Mountain, as well as in the Axios/Vardar zone at both its western and eastern marginal parts, similar ophiolitic mélange formations are also described [21,27,37,42,184,283,284]. They are sandwiched, on the one hand, between the External Hellenides Pindos flysch at the bottom and the detached ophiolite belt at the top, and, on the other hand, between the Pelagonian (Vourinos Mountain) or Serbo-Macedonian Triassic–Jurassic carbonate platform cover at the bottom and the obducted ophiolites at the top (Figures 4, 11, 21 and 22). The internal deformation of the mélange formations shows a main sense of movement ranging from the top to the NW to the SW for the successions on top of the Pelagonian nappe at the west of the Axios/Vardar marginal edge and the top to the NE for the successions on top of the Serbo-Macedonian margin at the east of the Axios/Vardar marginal edge, respectively. The sense of movement is recognized by shear sense indicators such as σ- and δ-clasts, shear bands, asymmetric boudins, and thrust vergence (Figure 22). It is interpreted as the kinematics related to the initial ophiolite and mélange nappe thrusting and their final emplacement on the Pelagonian and Serbo-Macedonian continental margins during the Mid–Late Jurassic [6,13,30,42,123,124,140,151,182,183,186,277]. Their emplacement on the Pindos flysch, together with the overlain ophiolites, clearly westwardly directed, belongs to the younger Tertiary tectonics of the Hellenides, related either to compressional or extensional tectonics [19,278,280,285–287]. During these Tertiary tectonics, the ophiolite nappes, together with the underlain ophiolitic mélanges, were simply detached on the External Hellendes Pindos flysch without any important effect or reworking on the older Jurassic inherited thrusting nappe structures (Figures 3, 4 and 21; [123,124,129,186,285,286]).

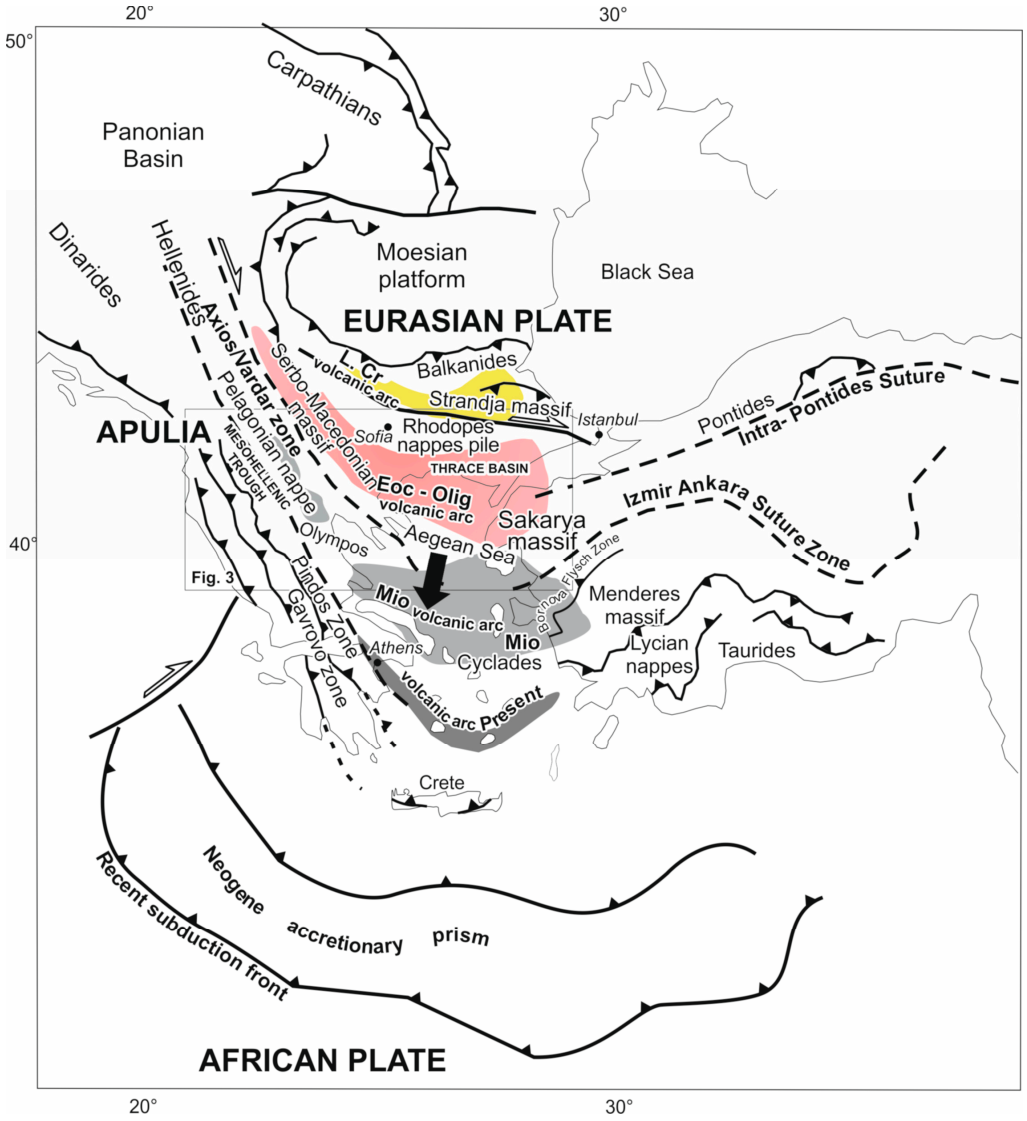

Figure 20. The SSW-ward migration of the Late Cretaceous to present-day arc-type magmatic activity in the Hellenic arc is shown. The main tectonic units of southeastern Europe and the eastern Mediterranean region are also indicated. Abbreviations are as in Figure 3.

These Mid–Late Jurassic ophiolitic mélanges were interpreted as a synorogenic, tectono-sedimentary sequence, deposited in progressively formed Mid–Late Jurassic basins at the front of the advanced ophiolite thrust sheets, following Early–Middle Jurassic intra-oceanic subduction and partial destruction of the Neotethyan ocean floor (Meliata-Axios/Vardar ocean; [6,13,123,124,140,151,186,277]). Amphibolite metamorphic sole, always of 180–170 Ma age [160,288,289], tectonically incorporated between all ophiolite belts, shows clearly this late Early–Middle Jurassic intra-oceanic subduction event only in a single ocean basin, and this is the Neotethyan Meliata/Maliac-Axios/Vardar ocean between the Apulian and European plates (e.g., [11,13,17,24,277]).

Ophiolitic mélanges of similar composition and Mid–Late Jurassic age are also described by several authors in the northern continuation of the Hellenides ophiolites in the Albanian Mirdita ophiolite belt, as well as the Dinarides and eastern Alpen area (e.g., [13,19,140,163,277]. These mélange formations were interpreted as radiolarite-ophiolitic wild flysch [13] and these correspond to similar sequences known from the eastern Alpen region (Hallstatt mélanges; [290]).

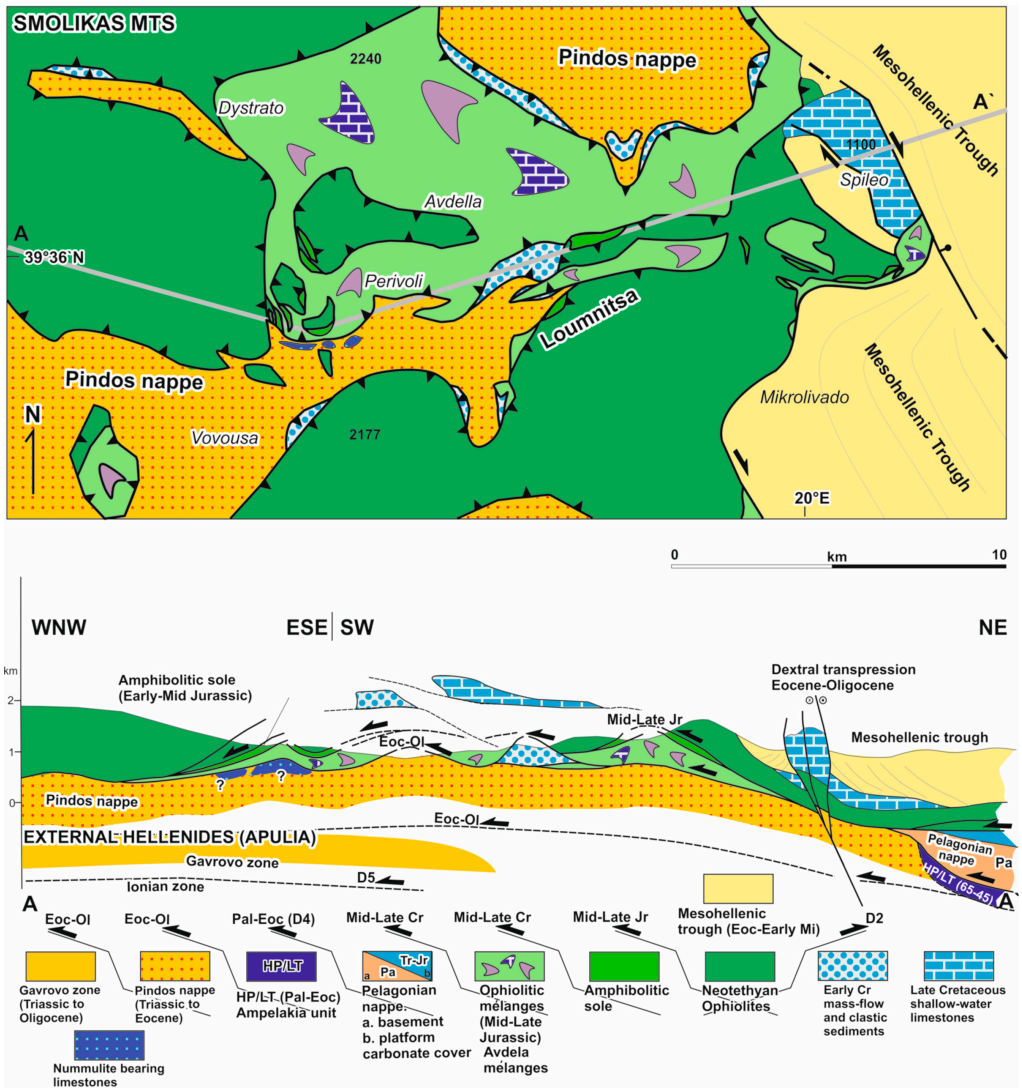

Figure 21. Geological–structural map and representative cross-section of the Pindos ophiolites and the tectonically underlying Middle–Late Jurassic Avdella ophiolitic mélange, which are tectonically emplaced on the Paleocene–Eocene Pindos flysch. Outcrops of the sedimentary formations of the western molassic Mesohellenic trough and its tectonic boundary with the basement rocks (ophiolites, Late Cretaceous limestone, and Pindos flysch) are also shown (based on [64,65,278,280]). Abbreviations as in Figure 3.

3.2.3. The Late Jurassic Sedimentary Series

These sedimentary series comprise shallow-water fossil-rich platform limestones of the Kimmeridgian–Tithonian age, unconformably deposited on the ophiolites directly after their emplacement on the Pelagonian and Serbo-Macedonian continental margins (Figures 3, 4, 5, 15 and 23VIII,IX; [13,19,21,150,151,279]). Furthermore, oolithic limestone layers constitute, in some places (e.g., the Koziakas unit), a common compositional component of the lithostratigraphic succession. This Late Jurassic shallow-water carbonate formation today remains only as several small rests on its basis (Figure 23VIII), because its greater mass is eroded, in some places totally eroded. Its age and existence are proven by the dating of its eroded compositional material contained as carbonate clasts and blocks in mass-flow and clastic formations, which have been dated to the ?late Late Jurassic–Early Cretaceous age and are described below [6,140,150–153,277,279].

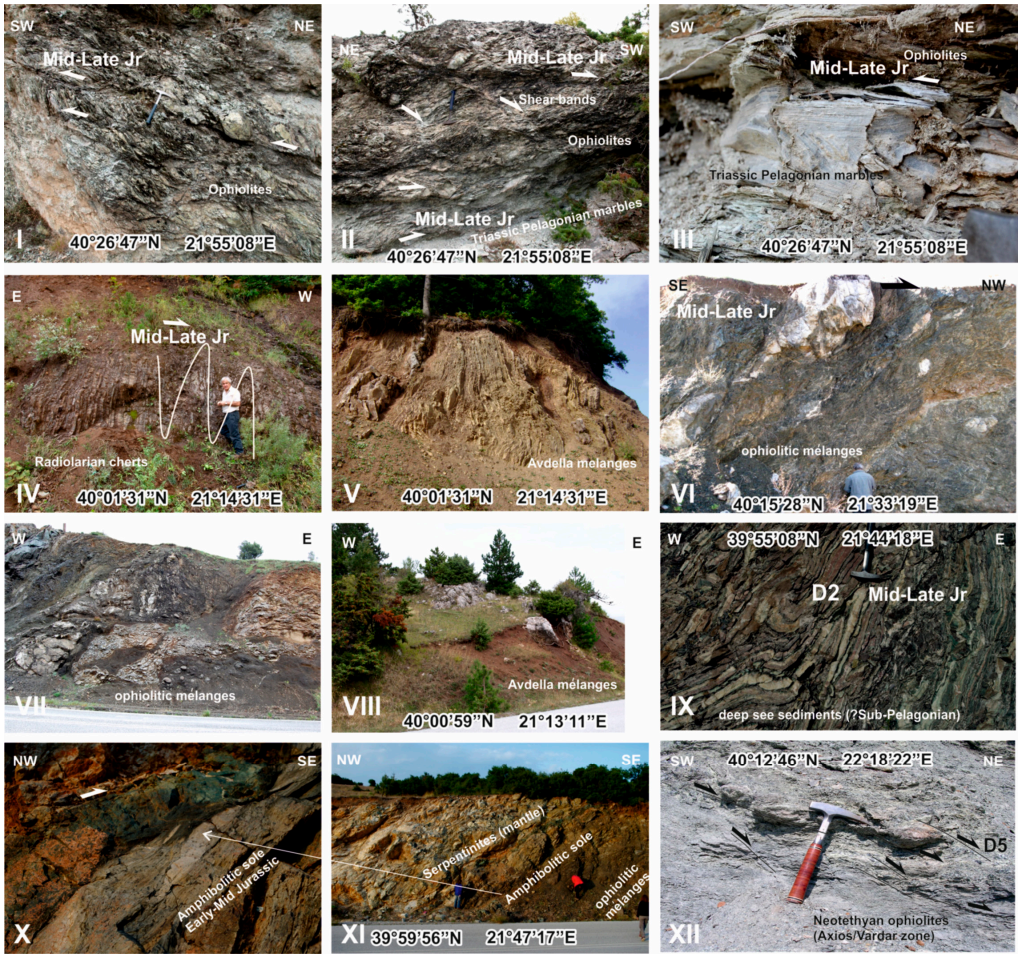

Figure 22. (**I**–**XII**) Field photos of structural and compositional features of the ophiolite belt and ophiolitic mélanges, as well as the deep sedimentary sequences of the ?Sub-Pelagonian zone that underlie the ophiolites and ophiolitic mélanges (modified after [30]). The sense of shear is indicated by arrows and the respective tectonic events are shown in each photo. The Early–Middle Jurassic amphibolite metamorphic sole, formed during the Early–Middle Jurassic Neotethyan intra-oceanic subduction between the overriding hot lithospheric mantle (the serpentinites) and the ophiolitic mélanges, is also shown (**X**,**XI**). The (**I**–**III**,**XII**) photos refer to the ophiolites of the Axios/Vardar zone along the eastern Pelagonian margin and the (**IV**–**VII**,**VIII**,**IX)** photos refer to the Pindos ophiolite belt and ophilolitic mélanges, as well as the ?Sup-Pelagonian pelagic sediments along the western Pelagonian margin. Abbreviations as in Figure 3.

3.2.4. ?Late Late Jurassic–Early Cretaceous Mass Flow and Clastic Sedimentary Series

These sedimentary series also rest unconformably, mainly directly on top of the ophiolitic belts. (Figures 3–5, 10, 11 and 23). These sediments form very complicated reef slope rock units but are very important for the explanation of the structural–geotectonic evolution of the Internal Hellenides. They form polymictic mass-flow deposits containing a large number of carbonate components from the formerly described and intensively eroded Late Jurassic shallow-water carbonate platform, as well as from the underlain ophiolites and basement rocks (e.g., Pelagonian or Serbo-Macedonian Triassic–Jurassic carbonate platforms). Radiolaritic and flyschoid clasts also occur as components in the mass flow. As components of the eroded Late Jurassic carbonate platform, resedimented bioclasts of reefal limestones, shells, stromatoporoids, corals, brachiopods, foraminifera, crinoids, and sponges dominate. Some fragments are coated and encrusted (Figures 23 and 24; [151,153]).

Figure 23. Field photos of the Late Jurassic and ?Late Jurassic–Early Cretaceous carbonate sequences on the top of the Late Jurassic obducted ophiolites on the Pelagonian and Serbo-Macedonian continental margins: (**I**) Deposition of the ?Late Jurassic–Early Cretaceous carbonate neritic and clastic sediments over the Axios/Vardar Paionia ophiolite belt at the Serbo-Macedonian margin. (**II**,**III**) Carbonate clasts and the thin carbonate layer at the base of the ?Late Jurassic–Early Cretaceous sedimentary sequence, rich in fossils representative of a Late Jurassic fauna collection. Axios/Vardar zone, Paionia Subzone, Serbo-Macedonian margin. (**IV**–**VII**) Early Cretaceous clastic and carbonate semi-pelagic sediments on top of the Vourinos ophiolite complex at the western Pelagonian flank. Clastic sediments with small belemnite fragments (**IV**) and calpionellides bearing turbidity layers (**V**) are distinguished. Furthermore, the Early Cretaceous compressional D2 event related to subisoclinal, asymmetrical folds is shown (**VI**,**VII**). (**VIII**,**IX**) Contact between the Late Jurassic shallow-water limestones and Zygosti ophiolites, which form the W-ward continuation of the Axios/Vardar ophiolites. (**VIII**) Fauna from the rich fossiliferous neritic Late Jurassic limestone at the Zygosti stream, covering the obducted ophiolite belt on the Pelagonian continent (**IX**) (based on [30,152,153]).

Calpionellids bearing semi-pelagic limestone, which are dated as Early Berriasian [156,291], followed by calcareous–siliciclastic turbidites of Late Berriasian age [292], overlay the mass-flow sequence (Figure 23). The whole succession of mass flow deposits with Calpionellid limestone was dated as Early Cretaceous (Berriasian-Valanginian; [13,150–153,279]). A late Late Jurassic (late Tithonian) age remains questionable. Moreover, in some places the stratigraphic succession through shallow-water carbonate rocks and flysch-like deposits continues until the Barremian–Aptian [13,21,140,146,279,293].

Where these Late Jurassic and Early Cretaceous sedimentary formations are mapped on top of the obducted ophiolites in several localities of the Alpine orogenic belt from the eastern Alps, Dinarides Albanides, to the Hellenides (Figures 1, 3, 4, 10 and 15; e.g., the western and eastern boundaries of the Pelagonian nappe, Axios/Vardar zone, and Serbo-Macedonian province), they show an identical stratigraphical succession, with similar sedimentary features and component compositions, and were dated with about the same stratigraphic ages: **I.** Late Jurassic (Kimmeridgian–Tithonian) for the first intensively eroded shallow-water carbonate platform formation and **II.** ?late Late Jurassic–Early Cretaceous for the second. Additionally, these strongly eroded Late Jurassic (Kimmeridgian–Tithonian) shallow-water limestones, on top of the obducted ophiolitic belts, clearly define the upper

limit of the ophiolites' emplacement as Callovian–Oxfordian everywhere in the Alpine orogenic belt in Europe (Alps, Dinarides, Albanides and Hellenides). Moreover, the ophiolite belts in the Hellenides, whether they are displayed at the western or eastern Pelagonian parts, or even at the Serbo-Macedonian margin, should have the same emplacement ages (Figures 2–4; [13,21,140,152,153,279]).

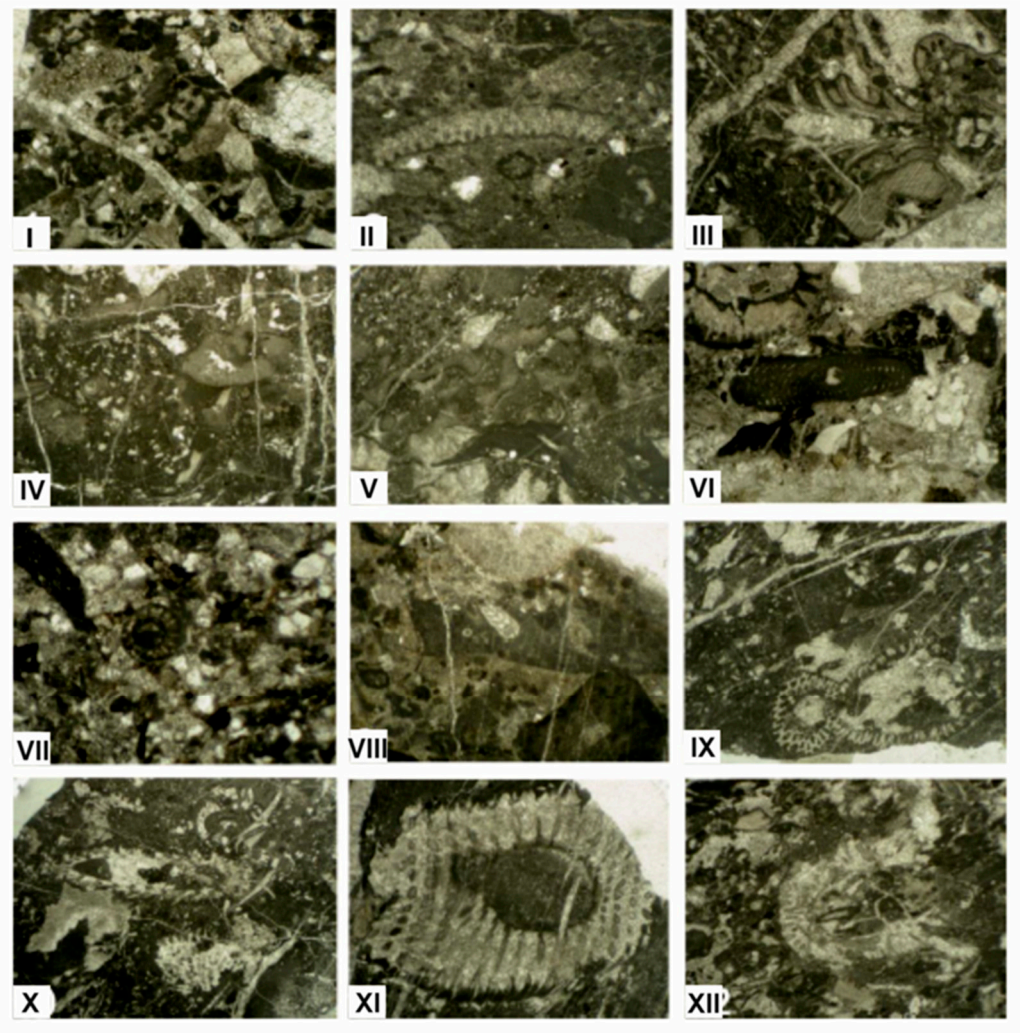

Figure 24. Components of ?Late Jurassic–Early Cretaceous polymictic mass flows and clastic sedimentary sequences. (**I**) Rudstone with different clasts and *Labyrinthina mirabilis* Weynschenk (width: 0.5 cm). (**II**) A fragment of *Griphoporella jurassica* (Endo) (width: 0.25 cm). (**III**) *Neoteutloporella socialis* (Praturlon) (width: 0.5 cm). (**IV**) Boundstone with *Thaumatoporella* sp (width: 0.5 cm). (**V**) Boundstone with *Perturbatacrusta leini* Schlagintweit and Gawlick (above) and *Labes atramentosa* Eliasova (below) (width: 0.5 cm). Components from the ?Late Jurassic–Early Cretaceous turbiditic sequence of sandstones with intercalated coarse-grained mass flows. (**VI**) *Anchispirocyclina lusitanica* (Egger) (width: 0.5 cm). (**VII**) Grainstone with different clasts and *Salpingoporella pygmaea* (Gümbel) (width: 0.5 cm). Components from the polymictic conglomerate in the ?Late Jurassic–Early Cretaceous sedimentary sequence. (**VIII**) Metamorphosed shallow-water clasts of, most probably, Middle Triassic age containing foraminifera (width: 0.5 cm). Microfossils from the shallow-water ?Late Jurassic–Early Cretaeous sedimentary sequence. (**IX**) *Griphoporella cretacea* (Dragastan) (width: 0.5 cm). (**X**) Boundstone with *Suppiluliumaella* aff. *methana* Dragastan and Richter and debris of *Selliporella neocomiensis* (Radoicic) (width: 0.5 cm). (**XI**) *Linoporella* aff. *capriotica* (Oppenheim) (width: 0.25 cm). (**XII**) *Furcoporella? vasilijesimici* Radoicic (width: 0.25 cm). Refs. [152,153].

3.2.5. Late Cretaceous Shallow-Water Carbonate Formation

This formation was deposited unconformably upon all pre-Late Cretaceous geological units and structures of the Internal Hellenides. The deposition began during the Cenomanian. The formation is met transgressively above the Mid–Late Jurassic obducted ophiolite belts, the Triassic–Jurassic Pelagonian carbonate cover, the Late Jurassic neritic limestone, and the Early Cretaceous mass flow deposits (Figures 3–5 and 11). The formation is composed mainly of neritic carbonate deposits terminated with a late Late Cretaceous–Paleocene flysch sedimentation, known as the flysch of the Internal Hellenides.

A detailed, representative stratigraphic column of the formation, from the bottom to the top, is given in the following. The base of the Late Cretaceous succession forms a few metres of thick conglomerates. These are dominated by clasts of marble, ophiolite, and schist, in some places with a matrix of reworked ophiolitic material or thin layers of terrigenous ophiolitic fine-grained material and shales. The succession is continued with a thin dolomitic layer passing upwards into intercalations of thin- to medium-bedded bioclastic, neritic limestones, mudstones, terrigenous sandstones, and redeposited limestones. In places, debris flow material rich in limestone clasts is also observed between the limestone layers. In the uppermost part, semi-pelagic limestones dominate and the rocks show a deepening of the basin until the final deposition of Maastrictian–Danian turbiditic deposits. The overall thickness of the Late Cretaceous carbonate succession ranges accordingly, from a few metres to ~2km [21,27,164,173,174,294].

3.2.6. The External Hellenides Flysch Series and the Turbiditic Deposits of the Meso-Hellenic trough and the Thrace Basin: Post-Orogenic Neogene–Quaternary Sediments

The External Hellenides are characterized by Paleocene to Miocene synorogenic flysch sedimentation. Its age was progressively dated as younger W-ward, simultaneous with its W-ward migration. From the east to the west the following can be distinguished: **I.** The Pindos Paleocene–Eocene flysch; **II.** The Gavrovo Eocene–Oligocene flysch; and **III.** The Ionian Oligocene–Miocene flysch. The flysch sediments generally seal progressively the sedimentary history of the External Hellenides zone, which is characterized by continuous neritic and pelagic sedimentation from the Early Mesozoic to the Tertiary (details described in Chapter 2.1). The flysch sediments developed during the final collision of the Apulian-origin Pelagonian continental fragment with the Apulian Plate, closely related to intensive compressional and W-SW-directed folds and thrust fault tectonics (Figures 1–4; [25,26,139,280]).

Furthermore, very important for the geological history of the Hellenides are the mollasic-type turbiditic syn- to late orogenic, Paleocene to Middle–Late Miocene sedimentary deposits of the Meso-Hellenic trough, defined as a polyhistor strike-slip and piggyback basin behind the Tertiary External Hellenides thrust belt. Finally, the Eocene–Oligocene turbidites' intercalations with the volcanic products of the supra-detachment Thrace basin in the Rhodope province should also be referred to here (Figures 1–4; [7,25,61–65,67]).

Post-orogenic Neogene–Quaternary sedimentary series deposited in intramontagne and other terrestrial sedimentary basins cover, unconformably in many places, all the pre-Alpine and Alpine Hellenides' tectonostratigraphic domains. These basins are usually bounded by high-angle normal faults (Figures 1–4; e.g., [68–73,295]).

4. Architecture and Kinematics of Deformation and Related Metamorphic Conditions

From the Early–Middle Jurassic to the present, the Hellenides have been affected by complicated multiphase stages of deformation and metamorphism during the Alpine orogeny. Deformation started with Early–Middle Jurassic intra-oceanic subduction followed by Middle–Late Jurassic ophiolite obduction. The later, younger deformational and metamorphic history, from the Late Jurassic to the present, is divided into six main (D1 to D6) deformational events. (Figures 4, 5, 25 and 26). The whole Alpine deformational, metamorphic and magmatic history of the Hellenides is described in detail below. In some places in the Paleozoic basement rocks of the Internal Hellenides an older deformational

event of Ercynian age is also recognized, but strongly overprinted by the younger Alpine deformation [6,7,30,98,145,241,296].

In a general view, during the Alpine orogeny in the Hellenides, compression, nappe stacking, and crustal thickening alternated successively over time with extension and orogenic collapse, which led to the exhumation of deep crustal levels, crustal thinning, and the formation of tectonic windows and/or metamorphic core complexes. The exhumation structural processes were accordingly evolving from ductile to brittle deformation conditions. Furthermore, a S-SW-ward migration of dynamic peer compression vs. extension is recognized during the Tertiary Alpine orogenic stages in the Hellenides. Extension and crustal uplift follow compression and nappe stacking or act simultaneously in different sections of the Hellenic orogen (Figures 4, 19 and 20; [9,10,32,33,48,89,90,96,97,139,158,240,297]).

4.1. Late Jurassic–Early Cretaceous Deformational Event (D1) and Associated Pre-Late Jurassic Alpine Structural Processes (~180 to 130 Ma)

The D1 event is recognised in the Internal Hellenides, including the Pelagonian nappe, the Sup-Pelagonian zone (as defined), the Axios/Vardar zone, the Circum-Rhodope belt, and the Serbo-Macedonian massif [3,6,37,145,154,182–184,240,247].

The D1 event is dated to the Late Jurassic–early Early Cretaceous age (150–130 Ma; [154,179]) and is characterized by a penetrative syn-metamorphic foliation (S1) associated with residual forms of recumbent isoclinals, as well as sheath folds (F1), which deform a pre-existing foliation (S0). The F1-fold axes develop parallel to the mineral stretching lineation (L1), which usually trends NE–SW, but in some places a NW–SE trend is also recognized, for example, in the lower Pelagonian segment in Voras Mountain and the Circum-Rhodope belt, as well as in Paleozoic basement slices incorporated in the Axios/Vardar zone (Figure 11b,c and Figure 26; [6,154]). No clear kinematic indicators of the D1 event have been preserved, because the D1 structures have been strongly overprinted by the subsequent tectonics. However, in a few places where the D1 kinematics are recognized, a main sense of movement the top to the SW or the top to the NE may be reconstructed. An NW-ward sense of movement is also recorded, e.g., in the lower Pelagonian segment in northern Greece (Figure 26; [6,41,42,145,182–184,240]). Furthermore, an important bulk coaxial component of the D1 deformation is also recognized [6,145,240]. The syn-D1 mineral parageneses, also identified in the L1-stretching lineation, show metamorphic conditions from greenschist to amphibolite facies from the structurally higher to the structurally deeper crustal levels, respectively (Figure 11a–c, Figures 17b and 25; [6,145,247]).

High-pressure metamorphism in the Internal Hellenides, predating the D1 event, has been suspected in several works only from residuals of high-pressure metamorphic assemblages, without any clear syn-metamorphic structural evidence due to strong overprinting by younger tectonics [6,52,54,145,154,179,298,299]. High-pressure metamorphism is normally related to compression and subduction processes, but, in our case, high-pressure metamorphism has been interpreted as the result of tectonic overpressure and continental crustal sinking due to overloading and nappe stacking in an arc–continent collision setting and to ophiolite obduction on the Pelagonian and Serbo-Macedonian/Rhodope continental margins, respectively [6,21,145]. Pre-D1 high-pressure metamorphic assemblages have been dated to the early Late Jurassic age (>150 Ma, Figure 11a,b, Figures 17b and 25; [6,154,179,298,299]).

Here must also be mentioned the very important formation of the metamorphic sole of the Early–Middle Jurassic age, developed during Early–Middle intra-oceanic subduction in the Neothyan ocean realm (180–170 Ma, Figure 22; [160,288,289]). This event, in any case, predates Middle–Late Jurassic ophiolite obduction, high-pressure metamorphism, and the D1 event, but is closely related to their evolution (Figures 3 and 4; [6,17,24,123,124,151,182–184,186]). Amphibolite metamorphic sole predates, to the same ages, the obduction of the ophiolite belt both on the Pelagonian and on the Serbo-Macedonian margins, indicating at least its simultaneous evolution at a similar origin, which was Early–Middle Jurassic intra-oceanic subduction in the Neotethyan

Meliata/Maliac-Axios/Vardar ocean basin (Figure 22; [6,13,24,123,124,186,298]). Intra-oceanic subduction is associated with Middle–Late Middle Jurassic island arc magmatism, now represented mainly as slices in the rock sequences of the Circum-Rhodope belt and the Axios/Vardar zone (Figures 3–5, 10 and 14; [138,145,162,198,199]). Furthermore, the previously described Middle–Late Jurassic ophiolitic mélanges were deposited and intensively imbricated in basins at the front of the advanced ophiolites during their inneroceanic thrusting and subsequently obduction on the Pelagonian and Serbo-Macedonian continental margins. The upper limit of ophiolite obduction, as previously mentioned, is defined as in the Callovian–Oxfordian age, much earlier than previously assumed (Figures 15 and 23VIII,IX; [13,19,21,150,151,278–280,286,300]).

Tectonic events	Mineral paragenesis	Metamorphism	Age	References
DHP	quartz, blue Na amphibole, phengite, chlorite, rutil, lawsonite	High pressure-Low temperature conditions (blue schist facies)	(>150 Ma) Mid-Late Jurassic K/Ar, Ar/Ar, Rb/Sr isotopic dating	[6,154,179,299]
D1	**Upper Pelagonian levels & Paikon basement** quartz, white mica, biotite, aktinolite, epidote, chlorite, plagioclase	Greenschist to amphibolite facies	(150-130 Ma) Late Jurassic-Early Cretaceous K/Ar, Ar/Ar, Rb/Sr isotopic dating	[6,154,179]
	Lower Pelagonian levels quartz, garnet, white mica, biotite, K-feldspar chloritoid, plagioclase, ilmenite, sphene kyanite, epidote, staurolite, green amphibole	Amphibolite facies.		
D2	quartz, plagioclase, (albite/oligoclase), sericite, chlorite, actinolite, sphene .	Greenschist facies	(125-115) late Early Cretaceous K/Ar, Ar/Ar, Rb/Sr isotopic dating	[6,30,145, 154,179]
D3	Discrete, narrow mylonite shear zones with dynamic recrystallisation of quartz and sericitisation of white mica. Feldspar clasts brocken, showing subgrain formation are embedded in a dynamically recrystallized quartz and sericite matrix	Low grade greenschist facies	110-95 Ma late Early to early Late Cretaceous	[6,30,145, 154,179]
D4	**Upper structural levels of the Pelagonian basement & Paikon basement (Northern Greece)** Dynamic recrystallisation of quartz and sericite or chlorite growth along the D4 thrust faults	Semiductile conditions	(65-30Ma) Early Paleocene-Early Oligocene K/Ar, Ar/Ar, Rb/Sr isotopic dating	[6,30,47,87, 145,154,179]
	Deepest structural levels of the Pelagonian basement (Olympos-Ossa, Rizomata, Pelion areas) quartz, glaucophane, lawsonite, chlorite, albite	High pressure-Low temperature conditions (blue schist facies)	(65-40Ma) Early Paleocene-Eocene	
D5	**Upper structural levels of the Pelagonian basement & Paikon basement (Northern Greece)** Dynamic recrystallisation of quartz and sericite or chlorite growth along the D5 normal detachment faults	Semiductile conditions	(30-20 Ma) K/Ar, Ar/Ar, Rb/Sr isotopic dating	[6,30,47,87, 145,154,179]
	Deepest structural levels of the Pelagonian basement (Olympos-Ossa, Rizomata, Pelion areas) quartz, chlorite, sericite, stilpnomelan, albite, mylonites formation	Low grade greenschist facies	Oligocene-Miocene	
D6	———	Brittle conditions	Neogene-Quaternary	[301,302]

Figure 25. The metamorphic conditions of the Pelagonian and Paikon basements [6,30,47,87,145,154, 179,299,301,302].

Taking into account **I.** the previously described intensively eroded Late Jurassic platform carbonate sediment (Kimmeridgian–Tithonian) on top of the obducted ophiolites; **II.** the subsequent Early Cretaceous resedimented mass-flow sedimentary series, containing components of the eroded Late Jurassic sediments; and **III.** the P-T-t metamorphic path during the Middle–Late Jurassic to Early Cretaceous for the Pelagonian and Serbo-Macedonian basements (Figure 11a,b and Figure 17b), an uplifting process was proposed during the D1 Late Jurassic–Early Cretaceous event for the Pelagonian and Serbo-Macedonian continental margins, respectively [6,123,124,130,131,137]. Uplift took place after the Mid–Late Jurassic Neotethyan Axios/Vardar ophiolite obduction (Callovian–Oxfordian) and the

high-pressure metamorphic event and was associated with extension and exhumation of the Pelagonian and Serbo-Macedonian marginal parts [6,131]. This crustal uplift and exhumation could be attributed to buoyancy forces due to the lighter, formerly submerged continental crust of the obducted ophiolites overloading or, additionally, slab break-off from the subducted lithosphere [41,180]. Furthermore, isoclinal, recumbent folds described during the D1 event have also been described during synorogenic crustal extension and uplift in the Betic Cordilleras (Spain) by Orozco et al. (1980) [303], Orozco and Alonso Chaves (2011) [304], as well as in the Alps (Austroalpin domain) by Froitzheim (1992) [305] and Froitzheim et al. (2012) [306].

4.2. Late Early Cretaceous Deformational Event (D2; ~125–115 Ma)

D1- and the pre-D1-related older structures are strongly overprinted by a younger, contractional, D2 syn-metamorphic deformation, recognized everywhere in the Internal Hellenides zones. The D2 event has strongly affected all pre–late Early Cretaceous (Albian) geological units. These include the Paleozoic basement rocks with their Triassic–Jurassic sedimentary cover and the obducted ophiolite belt, as well as the Early Cretaceous mass flows and turbiditic sedimentary series. Additionally, the D2 contractional structures are sealed by Late Cretaceous neritic carbonate deposits (Figures 13–15). These clearly indicate a late Early Cretaceous age for the D2 event (Figures 3, 4, 11a,b, 13 and 14; [6,43,99,145,296]). Furthermore, isotopic dating analyses show similar late Early Cretaceous age deformation in the Pelagonia and Axios/Vardar zones (Figure 11a,b; Barremian–Aptian, 125–115 Ma; [154,179]).

D2 is characterized by the evolution of thrust faults and the development of micro- to macro-scale asymmetric, recumbent to overturned, tight to isoclinal folds (F2). These refold both the S1 foliation and the isoclinal F1 folds. A new S2 foliation was developed parallel to the F2 folds' axial planes, forming, in places, a well-recognized crenulation cleavage with the S1 foliation. Usually, due to the intensive rotation of S1 along the S2, the S1 is parallelized to the S2 foliation. As a result, the two foliations coincide and only one foliation is observed (Figure 11c,I,III,VII,XI and Figure 26). The F1 and F2 fold axes have developed mostly parallel to each other, while, in some places, the F2 folds show a scattering of their trend from NW–SE to NE–SW. This scattering of the F2 folds' trend is attributed to a progressive rotation towards the stretching direction and the X-strain axis developed during the D2 deformation. The stretching lineation trend is mainly NE–SW, but, in some cases, an NW–SE trend is also observed, as is concluded from the development of syn-D2 metamorphic mineral parageneses on the S2 foliation planes. The sense of shear during D2 is according to the stretching lineation trend and the shear sense indicators, mainly the top to the SW in the Pelagonia and Axios/Vardar zone and the top to the NE in the Serbo-Macedonian province. Additionally, an NW-ward sense of movement is also observed, mainly in the lower Pelagonian segment and the Axios/Vardar zone. This geometry of the D2 deformation is considered to be the result of a transpressional tectonic regime (Figures 3 and 26; [6,17,24,43,99,157,182,183]). M2-metamorphic mineral parageneses show metamorphic conditions in the greenschist facies (Figures 11a–c and 25; [6,145,154]). Recent works by [43,99] mention late Early Cretaceous ages of ca. 117 Ma for migmatites in the deeper Pelagonian levels.

4.3. Late Early Cretaceous–Late Cretaceous Deformational Event (D3; ~110–80 Ma)

The late Early Cretaceous–Late Cretaceous event is mainly recognized in the Internal Hellenides; in the Pelagonian nappe and its metamorphic basement sheets in the Axios/Vardar zone (e.g., Peternik, Paikon, etc., basement rocks); and in the Serbo-Macedonian and Rhodope massifs.

In the Pelagonian nappe and the Axios/Vardar zone basement sheets, the western edge of the Axios/Vardar ocean, D3 is related to extension and has been dated to the late Early to early Late Cretaceous age (110–95 Ma, Figure 11a–c; [6,30,154,179]) The D3 extensional structures form discrete, mylonitic shear bands with a well-developed S3-mylonitic foliation dipping mainly towards the NE. The associated L3-stretching lineation

also plunges to the NE. The D3 shear bands are usually characterized by the dynamic recrystallization of quartz and the growth of chlorite and sericite minerals. The sense of shear during D3 was mainly identified down-dip towards the NE, although in a few cases an opposite, again down-dip, SW sense of shear was also observed, related to the SW-ward dipping of the S3 foliation and the SW-ward plunge direction of the L3 stretching lineation (Figure 11c,V,VI and Figure 26; [6,154,179]).

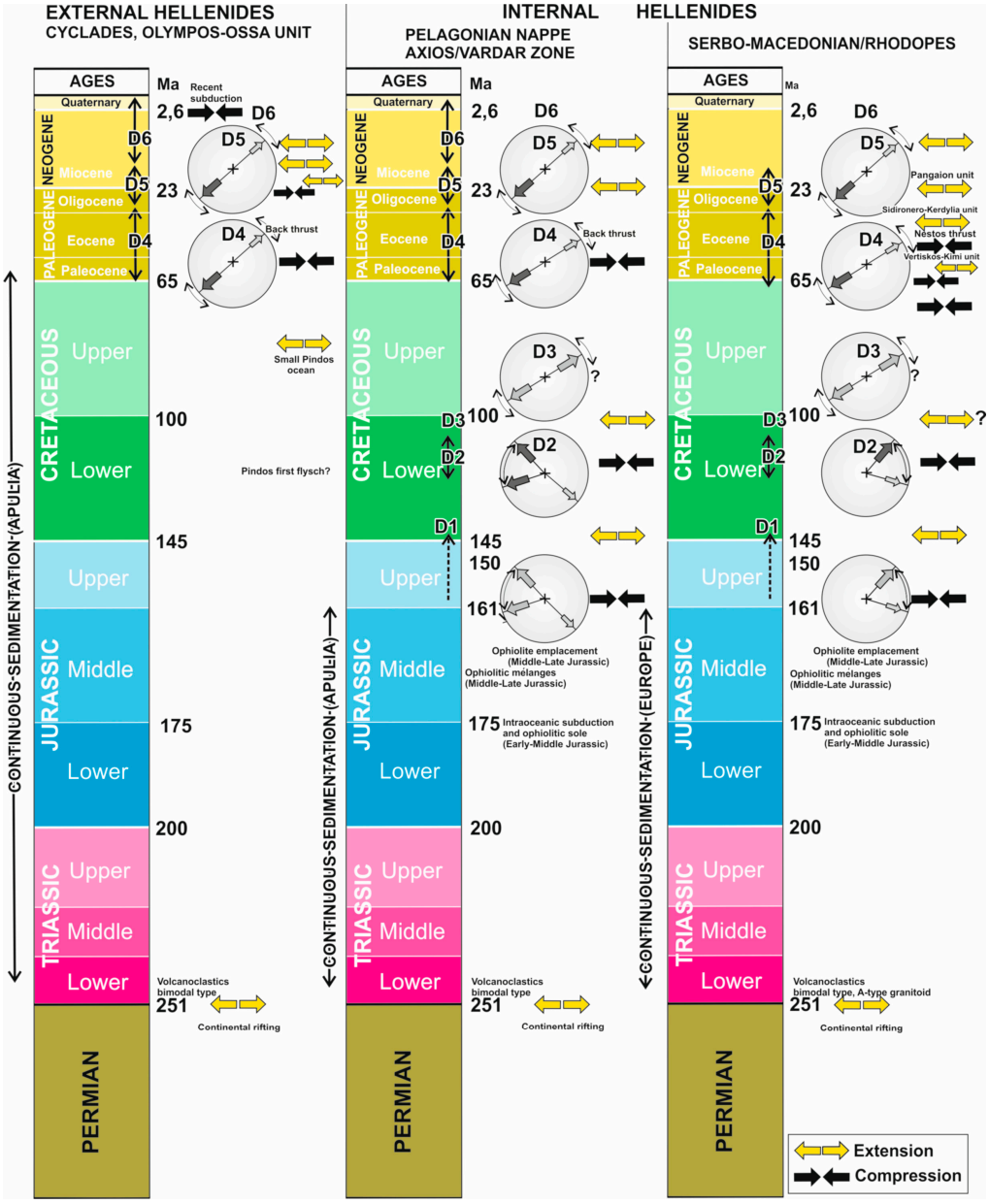

Figure 26. In comparison, the main deformational events recorded in the External and Internal Hellenides from the Early Triassic to the present. Shortening alternated successively with extension. Compressional events are related to nappe stacking, crustal thickening and high-pressure metamorphism, while extensional ones are related to tectonic denudation, low- to high-temperature metamorphism, isostatic rebound, crustal thinning, and exhumation of deep crustal levels (see also Figures 27 and 28). The main senses of movement for each event, as deduced by shear sense indicators and kinematic analysis, are shown in the Schmidt diagrams with arrows (lower hemisphere equal-area projections) (based on [6,30,145]).

In contrast to the described D3 extensional structural setting in the Pelagonian and Axios/Vardar basement rocks, in the Serbo-Macedonian/Rhodope province, Late Cretaceous contraction is revealed by eclogite occurrences at ca. 80–85 Ma between the Rhodope units and, specifically, between the middle Rhodope Sidironero and the upper Rhodope Kimi units (Figure 27). Eclogites are related to ongoing NE-ward subduction processes of the Axios/Vardar oceanic lithosphere remnants under the European continental margin, including the Serbo-Macedonian/Rhodope single Vertiskos-Kimi unit and the Strandja/Sredna-Gora massif in Bulgaria. The subduction processes are also inferred from Late Cretaceous calc-alkaline volcanic-arc magmatism along the southwestern European continental margin (Figures 2 and 20; [24,59,121,183,266,268]). Therefore, according to the described D3 structural setting, Late Cretaceous contraction at the easternmost area of the Internal Hellenides in the Serbo-Macedonian/Rhodope province (European margin) takes place about simultaneously with late Early Cretaceous–early Late Cretaceous extension in the Pelagonia (Apulian margin).

4.4. Early Paleocene to Early Oligocene Deformational Event (D4; ~65–30 Ma)

The D4 event is also characterized by a very complicated evolutionary history. It is related to ductile up to brittle deformational conditions in the different Hellenides orogenic parts, causing either intense folding, imbrication, or nappe stacking during compressional setting or nappe denudation, orogenic collapse, and crustal exhumation during extension (Figures 3 and 4). The D4 structures are well recognized in the Pindos zone of the External Hellenides, as well as in the Pelagonian nappe pile, the Axios/Vardar zone, and the Sebo-Macedonian/Rhodope metamorphic province of the Internal Hellenides (Figure 11c).

Ductile and brittle deformation during D4 takes place simultaneously at the various structural levels of the Hellenic orogenic belt. This means that ductile deformation in the Serbo-Macedonian/Rhodope metamorphic province and the lower structural levels of the Pelagonian nappe, including the Paleocene–Eocene Ampelakia-Cyclades high-pressure belt, takes place at the same time as brittle deformation at the upper structural levels of the Pelagonian nappe pile, the Axios/Vardar zone, and the structural province of the external parts of the Pindos zone (Figures 27 and 28). This brittle deformation is characterized by intense crustal imbrication and thrust faults, as well as asymmetrical kink-folds (Figure 29). Additionally, the related ductile D4 structures are contractional in the middle Rhodope Sidironero unit, the Pelagonian nappe and the Ampelakia-Cyclades high-pressure belt, related to asymmetrical, tight to isoclinal folds and syn-metamorphic S4 schistosity. Today, they remain residual or destroyed due to the younger tectonics.

Furthermore, during the Paleocene–Eocene, the collision between Europe and Apulian's Pelagonian segment takes place, following the final closure of the Axios/Vardar ocean [17,24,182]. Progressively, during this contractional stage of D4 tectonics, the middle Serbo-Macedonian/Rhodope Sidironero-Kerdylia unit overthrusts the lowermost Rhodope Pangaion unit. About simultaneously, during the Eocene–Oligocene, the Pelagonian nappe and the Paleocene–Eocene Ampelakia-Cyclades high-pressure belt overthrust the Olympos-Ossa carbonate unit of the External Hellenides. In contrast, the D4 ductile structures are extensional in the uppermost structural nappes of the Serbo-Macedonian/Rhodope metamorphic province; i.e., the Vertiskos-Kimi unit and these structures are ductile shear zones, verging mainly down-dip and SW-ward and in some places also verging down-dip NE-ward. Remnants of asymmetrical and isoclinal or sheath folds are also sporadically recognized (Figures 3 and 4; [6,7,17,18,24,27,30,37–39,47,123,124,145,156,187,210,228,296]).

The D4 deformation, whether ductile or brittle, took place during the Paleocene to Eocene–Oligocene, as concluded from numerous isotopic dating ages and lithostratigraphic–structural relationships (Figures 25, 27 and 28); [3,6,7,24,27,30,37–39,87,154,173,174].

Tectonic events	Mineral paragenesis	Metamorphism	Age	References
D4	**Olympos-Ossa blue schists** quarz, glaucophane, lawsonite, albite,chlorite phengit, epidote, titanite, apatite,	**(1)** HP/LT conditions Glaucophane-lawsonite facies	(65-40 Ma) Paleocene-Eocene K/Ar, Ar/Ar, Rb/Sr isotopic dating	[38,47,48,86,87]
	Cyclades blue schists glaucophane, omphacite, jadeite, clinozoisite, garnet, phengite	**(1)** HP/HT conditions Glaucophan to eclogite facies	(65-40 Ma) Paleocene-Eocene K/Ar, Ar/Ar, Rb/Sr isotopic dating	[44,46,49, 91,115]
D5	**Olympos-Ossa blue schists** quartz, albite, white mica, chlorite, stilpnomelane	**(2)** Low grade metamorphism greenschist-facies	(30-20 Ma) Oligocene-Miocene K/Ar, Ar/Ar, Rb/Sr isotopic dating	[38,47,48,86,87]
	Cyclades blue schists quartz, green amphibole, garnet, biotite, staurolite, epidote	**(2)** high-greenschist to amphibolite facies migmatites, granitoid intrusions	(30-20 Ma) Oligocene-Miocene K/Ar, Ar/Ar, Rb/Sr isotopic dating	[45,88,89,95]
D6	————————	Brittle conditions	Neogene-Quaternary	[32,33,301,302]

Figure 27. The metamorphic conditions of the Olympos-Ossa and Cyclades HP belts.

The residual ductile compressional D4 structures in the lowermost Pelagonian parts, the internal high-pressure belt in Ampelakia-Cyclades, and the Rhodope Sidironero-Kerdylia unit are all associated with high-pressure metamorphic conditions (Figures 4 and 8a–c). In contrast, the ductile D4 extensional step took place under greenschist to amphibolite facies metamorphic conditions and partly migmatization, as well as granitoid intrusions associated with the exhumation of the upper Serbo-Macedonian/Rhodope Vertiskos-Kimi unit (Figures 4, 16 and 17b,c; [7,39,40,45,47,216,227,240,241]).

A main SW-ward sense of movement is recognized for all ductile or brittle D4 structures, whether they are related to contraction or extension. In some cases, a NE-ward back-direction sense of movement during the D4 event is also identified in the broader area of the Internal Hellenides, the same whether the structures are related to contractional or extensional settings (Figures 17c, 26 and 29; [6,7,18,27,37,40,145,173,174,240,307]).

4.5. Oligocene–Miocene Deformational Event (D5; ~30Ma–20 Ma)

In the Internal Hellenides, D5 structures are generally related to extensional tectonics and the exhumation processes of deep structural units, either in the form of tectonic windows or metamorphic core complexes. They are recognized in the Olympos-Ossa, Rizomata, and Paikon windows, as well as in the Pangaion and Cyclades metamorphic complexes (Figures 3, 4, 7, 8c and 16; [7,18,30,39,86,145,200,201,212,241,248,296]).

The D5 structures have been dated as of Oligocene–Miocene age (Figure 11a,b; e.g., [6,7,145,154]) and in the Internal Hellenides are characterized by normal detachment faults and mylonitic rock formation in the structurally lower crustal levels. Brittle to semi-ductile deformation is recorded at structurally higher crustal levels (e.g., the upper part of the Pelagonian nappe in northern Greece, including the Paikon window) and ductile deformation related to greenschist to amphibolite facies metamorphism and migmatization and granite intrusions at the lower levels (e.g., the Olympos-Ossa and Rizomata windows, the Cyclades, and the Rhodope Pangaion metamorphic core complexes). Here should be mentioned the Eocene–Oligocene period, when the middle Rhodope Sidironero unit was progressively exhumed during extension associated with high-temperature metamorphism, migmatization processes, and granitoid intrusions (Figures 4 and 17a,c; [7,17,24,40,67,216,240,241,307,308]). The cooling/exhumation path for the Sidironero unit, as it was previously referred to, was dated at 42-30 Ma, the same as the lower Serbo-Macedonian Kerdylia unit (Figures 4, 17a,b, 27 and 28; [227]). This Eocene–Oligocene extensional stage in the Rhodope province was further extended to the D5 Oligocene–Miocene extension.

The D5 stretching lineation on the S5 schistosity plane plunges, in general, SW- or NE-ward. Additionally, the sense of shear during the D5 event in the Internal Hellenides is mainly towards the SW (e.g., the Pelagonian nappe and Serbo-Macedonian/Rhodope nappe pile). An opposite sense of movement toward the NE has also been observed in a few places (e.g., Olympos-Ossa window), indicating a bivergent orogenic crustal deformation during D5 (Figures 3, 4 and 26; [5,6,86,145,157,158,212,240,297]). In the Cyclades massif, D5 tectonics is recorded in a mainly NNE-ward sense of movement related to extensional tectonics, high-temperature metamorphism, and the final exhumation of the Cyclades metamorphic complex. Nevertheless, an SSW-ward sense of shear is also described for the Cycladic massif during the D5 extensional setting (Figure 19; [89,107,309]).

Unlike in the D5 structural setting in the Internal Hellenides, a fold and thrust belt, in the form of a thin-skinned type of tectonics, was developed in the External Hellenides during the Oligocene–Miocene, clearly related to compression and crustal stacking. Here, metamorphic processes are not observred. A main SW-ward sense of movement is also recognized in the thrust faults' geometry and the folds' vergence. The thrust and fold structures strike mainly NW–SE (Figures 3, 4, 24 and 29). Back-thrusting from the top to the NE is often observed in places. During the Oligocene–Miocene, the Gavrovo zone, together with the overthrust during the Eocene–Oligocene external Pindos nappe, was thrust towards the SW over the Ionian zone, following the general Tertiary SW-ward orogenic migration of compression. Furthermore, the Pindos zone, possibly due to an out-of-sequence thrust fault, was thrust, in places, further to the west on the Ionian zone during the Early Miocene, completely covering the Gavrovo zone and its contact with the Ionian zone [25,28,29].

Additionally, HP/LT metamorphism of the Oligocene–Miocene age and compressional tectonics, causing nappe stacking and crustal thickening, are recognized farther south in the External Hellenides, in the Peloponnese and on Crete island. (Figures 6 and 19; [31–33,36,83,84]). Here, parts of the Ionian zone, together with the Phyllite-Quartzite unit of unknown origin, were subducted during the Oligocene–Miocene below the Gavrovo zone and metamorphosed in HP/LT conditions. Therefore, compression and extension again take place simultaneously in different geotectonic places in the Hellenides during the Oligocene–Miocene. HP/LT metamorphism and nappe stacking were progressively followed by Early–Middle Miocene ductile extensional tectonics, nappe collapse, and exhumation of high-pressure rock units in the form of a series of tectonic windows (e.g., the Taygetos-Mani, Lefka Ori, Psiloritis, Dikti-Lathisi, and Agios Nikolaos windows) under an isothermal decompression P-T-t-path (Figure 30). The sense of shear during extension and crustal exhumation was recorded from the top to the NNE and SSW (Figures 6 and 18; [32–34,83,96,97,310–312]). At the same time, compression migrated south of the Crete island along the Hellenic active subduction zone, where the African plate is subducted under the Hellenides (Figure 19).

Tectonic events	Mineral paragenesis	Metamorphism	Age	References
DHP	**Serbo-Macedonian massif (Vertiskos unit)** quartz, blue Na amphibole, phengite, chlorite, rutil, garnet, omphacite, graphitized diamonds?	High- to ultrahigh-pressure metamorphism eclogite facies conditions	? (>150 Ma) Mid-Late Jurassic Ar/Ar, Rb/Sr isotopic dating	[213,253,254]
	Rhodope massif (Sidironero unit) ———?———	?	?	
D1	**Serbo-Macedonian massif (Vertiskos unit)** quartz, white mica, biottite, garnet, disthen, staurolite, green amphibole, epidote,titanite	Amphibolite facies	(150-130 Ma) Late jurassic-Early Cretaceous K/Ar,Ar/Ar, Rb/Sr isotopic dating	[24,247,257]
	Rhodope massif (Sidironero unit) ———?———	?	?	
D2	**Serbo-Macedonian massif (Vertiskos unit)** quartz, white mica, garnet, recristalliza-tion of finegrain green amphibole and biotite	Greenschist facies	(125-115 Ma} mid Early Cretaceous K/Ar,Ar/Ar, Rb/Sr isotopic dating	[240,247]
	Rhodope massif (Sidironero unit) ———?———	?	?	
D3	**Serbo-Macedonian massif (Vertiskos unit)** ———?———	?	?	
	Rhodope massif (between Sidironero and Kimi units) quartz, omphacite, garnet, amphibole, epidote (subducted oceanic lithosphere)	Eclogite facies conditions	(80-85 Ma) Lu-Hf chronometry	[24,59]
D4	**Serbo-Macedonian massif (Vertiskos unit)** chloritisation of staurolite and disthen, quartz, actinolite, chlorite	Low greenschist facies	(65-60 Ma) Paleocene-Eocene K/Ar,Ar/Ar, Rb/Sr isotopic dating	[24,240,247]
	Rhodiope massif (Sidironero unit) quartz, omphacite, garnet, epidote, amphibole, kyanite	Eclogite facies conditions	(60-45 Ma) Paleocene-Eocene Ar/Ar, Rb/Sr,U-Pb-SHRIMP isotopic dating	[17,24,229, 235,236]
	Rhodiope massif (Sidironero unit) quartz, green amphibole, garnet, biotite, staurolite, epidote	Amphibolite facies migmatites, granitoid intrusions	(45-30 Ma) Eocene-Oligocene Ar/Ar, Rb/Sr,U-Pb-SHRIMP isotopic dating	[24,229,235,236]
D5	**Serbo-Macedonian massif (Vertiskos unit)** ———?———	Brittle conditions		[18,227,247]
	Rhodiope massif (Pangaion unit) quartz, green biotite, chlotite, calcite, actinolite, sericite, epidote, albite	Gruenschiefer facies granitoid intrusions, mylonites	(30-20 Ma) Oligocene-Miocene K/Ar, Ar/Ar, Rb/Sr,U/Pb isotopic dating	[24,118,200, 208,240]
D6	———————	Brittle conditions	Neogene-Quaternary	[32,33,301,302]

Figure 28. Metamorphic conditions of the Serbomacedonian/Rhodope massif. Question mark shows that there is no existing data about an event.

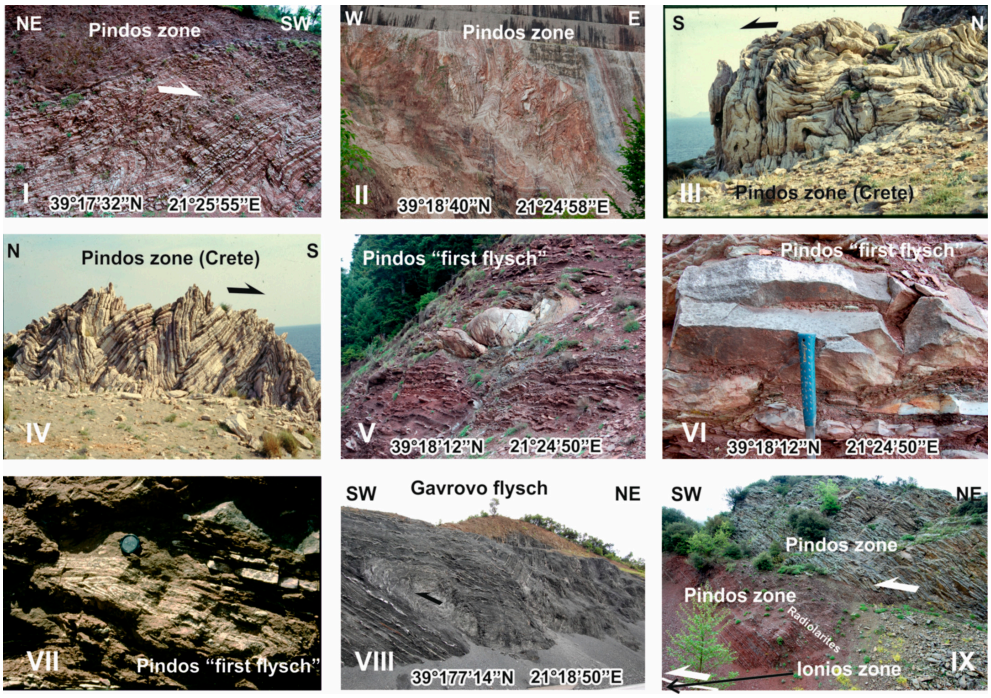

Figure 29. Field photos of stratigraphical sequences and tectonic structures of the External Hellenides zones: (**I**–**IV**) the typical S/SW-ward asymmetrical, tight folds of the Pindos series in red Jurassic radiolarian cherts (Pindos Mt., (**I**)), in intensively folded pelagic Cretaceous limestones with siliceous chert layers (Pindos Mt., (**II**)), in pelagic Triassic limestones with siliceous chert layers (south Crete island (**III,IV**)), (**V**–**VII**), intensively multi-folded Early Cretaceous Pindos "first flysch", (**VIII**) a SW-ward Eocene–Oligocene thrust fault in the Gavrovo flysch (Pindos Mt), and (**IX**) an Oligocene–Miocene out-of-sequence SW-ward thrust fault in the Pindos zone (Pindos Mt). The Triassic Pindos limestones overthrust the Jurassic Pindos radiolarian cherts, which overthrust secondarily the Ionian zone during the Oligocene–Miocene, possibly due to an out-of-sequence mega-thrust fault zone; see also Figures 3 and 4 (modified after [30]).

Tectonic events	Mineral paragenesis	Metamorphism	Age	References
D5	**Plattenkalk unit** metamorphic aragonite in the marbles, Fe-Mg-carpholite in the intercalated metabauxite layers	**(1)** HP/LT conditions Glaucophane-lawsonite facies	(24-19 Ma) Late Oligocene-Early Miocene Ar/Ar, Rb/Sr isotopic dating	[31-35,83,84, 296,297]
	calcite, serizite	**(2)** Very low grade metamorphism greenschist-facies	(19-15 Ma) Early-Mid Miocene	
	Phyllite-Quarzit unit quartz, glaucophane, Fe-mg-carpholite, chloritoide, phengite, epodote	**(1)** Low-grade high-pressure Glaucophane-lawsonite facies	(24-19 Ma) Late Oligocene-Early Miocene K/Ar, Ar/Ar, Rb/Sr isotopic dating	
	dynamic recrystallization of quartz, chlorite, actinolite, green biotite, epidote, albite, calcite, white mica	**(2)** Very low grade metamorphism greenschist-facies	(19-15 Ma) Early-Mid Miocene K/Ar, Ar/Ar, Rb/Sr isotopic dating zirkon, apatite fission tracks analyses	
D6	———	Brittle conditions	Neogene-Quaternary	[32,33,301,302]

Figure 30. Metamorphic conditions of the HP/LT belt of the External Hellenides (Crete and the Peloponnese).

4.6. Neogene–Quarternary Deformational Event (D6; ~20 Ma to Recent)

The D6 event is mainly related to extension in all the Hellenides' areas and took place under brittle conditions. The D6 structures overprint all the previously described structures and represent the final deformational stages of the orogen. At these stages, the compression and orogenic evolution migrated further SW-ward, now into the arcuate-form active Hellenic subduction zone south of Crete island, related to the active Hellenic volcanic arc in the central Aegean sea (Figures 19 and 20; [23,191,313]).

The D6 structures are characterized by high-angle, both dip-slip and oblique-slip, normal faults, as well as strike-slip faults, while some of them are related to the development of the Neogene–Quaternary basins in the Hellenides [70,295,301,302,314–316]. Many of the D6 faults produced significant tectonostratigraphic gaps, juxtaposing higher tectonic nappes against lower ones (Figures 4 and 13; [6,145,296]). Furthermore, some of the D6 faults are still active and are often associated with strong earthquakes [302,317–319].

5. Geotectonic Reconstruction of the Hellenides and Discussion

In this chapter, according to the described structural architecture, the kinematics of deformation and the main magmatic and sedimentary processes in the several Hellenides domains is attempted to be reconstructed for the Alpine geotectonic evolution of the Hellenic orogenic belt (Table 1). Additionally, this chapter discusses the several views that dominate in the modern international literature about the Hellenides' geological history. However, it should be emphasized that although much scientific research has been published about the structural and geotectonic evolution of the Hellenides, many questions remain open. In this case, our proposal about the geotectonic evolution of the Hellenides, although based on all available geological and structural data, remains speculative in some respects.

Initially, the described ultra-high-pressure metamorphic rocks with diamond-bearing paragenesis of a formation age of ca. 200 Ma [56,234] were possibly formed in the S-SW-ward dipping Paleotethys subduction zone and trace the old suture of the Paleotethys ocean [320–324]. Subsdequently, during the Alpine orogeny, these ultra-high-pressure rocks were tectonically incorporated into the upper and middle Serbo-Macedonian/Rhodope Vertiskos-Kimi and Kerdylia-Sidironero units, respectively [17,24].

Continental rifting of the Pangea supercontinent and the opening of the Neotethys ocean basin (Meliata/Maliac ocean) started during the Permo–Triassic, possibly related to the closure of the Paleotethys further to the north (Figure 18; [13,20,136,149,163,279,321–323]). Continental rifting is associated with bimodal volcanic activity and neritic–clastic sediment deposition along the newly formed passive continental margins of Apulia and Europe, at both edges of the newly established Neotethyan ocean. The northeastern continental margin belongs to Apulia, including the Pelagonian continental domain, and the southwestern continental margin belongs to the European continent, including the Vertiskos-Kimi unit of the Serbo-Macedonian/Rhodope massif. Furthermore, A-type leucocratic granitoids intruded into the Paleozoic Apulian and European basement rocks during the rifting. Carbonate neritic platforms to pelagic sediments and turbidites (e.g., the Dachstein, Hallstatt, and Meliata facies) were progressively deposited, from the Early Triassic to the Early–Middle Jurassic, along the continental margins of the European and Apulian plates (Figures 18 and 31; [3,13,20,98,134,136,149,150,163,262,263,277,279]).

During the Early–Middle Jurassic, parts of the Triassic Meliata/Maliac Neotethys ocean, subducted towards the SE in an intra-oceanic subduction regime (Figure 27a), progressed in an arcuate NW-ward convex subduction zone [11–13,24,43,99,162]. This geometry could be caused by a northwest-directed retreat of the subduction zone due to the roll-back of the subducting slab [11,12,24,183]. Due to this, intra-oceanic subduction developed progressively during the Middle–Late Jurassic, in a supra-subduction position in the backarc area behind an ensimatic island arc, the Axios/Vardar ocean, part of which should also be accepted as the Paionia ocean basin (Figure 31a; [11,12,16,20,24,145,162,177]). In the next stage, during the late Middle–Late Jurassic, the vorearc lithosphere, the is-

land arc formation together with the Axios/Vardar ocean lithosphere, and the ophiolitic mélanges (e.g., the Avdella mélange), formed in deepwater basins at the front of the overriding, advanced upper oceanic lithosphere, were obducted towards the west onto the Apulian–Pelagonian continental margin and towards the east onto the upper Serbo-Macedonian/Rhodope Vertiskos-Kimi unit, consisting a part of the European continental margin (Figure 31a,b; [6,13,17,20,24,43,99,183]). The simultaneous, opposite geometries of emplacement kinematics on both the western and eastern sides of the Meliata-Axios/Vardar ocean basin, in Apulia and Europe, respectively, were interpreted by the progressively evolved strong curvature of this Early–Middle Jurassic intra-oceanic subduction zone (Figure 27a,b; [17,24]).

Table 1. Summary of the Alpine structural evolution of the Hellenides.

1. **Permo–Triassic:** continental rifting; bimodal volcanism and A-type granite intrusion; start of the opening of the Neotethys ocean
2. **Triassic–Jurassic:** passive margins; extension and sedimentation
3. **Early–Middle Jurassic:** intra-oceanic subduction; amphibolite metamorphic sole; island arc magmatism during the Middle Jurassic; Middle–late Middle Jurassic development of the Axios/Vardar ocean in a supra-subduction zone
4. **Middle–Late Jurassic:** W-SW- and E-NE-ward ophiolite obduction and imbrication regime; high-pressure metamorphism in the two continental margins, Apulian and European, at the western and eastern edges of the Neotethian ocean, respectively; deposition of ophiolitic tectono-sedimentary melanges in basins at the front of the advanced ophiolitic belts
5. **Late Jurassic:** deposition of neritic platform carbonate on top of the obducted ophiolites
6. **Late Jurassic–Early Cretaceous:** greenschist to amphibolite facies metamorphism, possibly during extension and crustal uplift (D1); deposition during the Early Cretaceous of neritic and mass flow clastic sediments from the eroded Late Jurassic platform carbonates
7. **Late Early Cretaceous (Barremian–Aptian):** compression; mainly W- and E-ward imbrication and folding; syn-tectonic greenschist facies metamorphism (D2)
8. **Late Early Cretaceous–Late Cretaceous to Paleocene:** compression stops; extension in the late Early Cretaceous–Late Cretaceous (D3); possible formation of a small ocean basin west of the Pelagonia, the Pindos-Cyclades ocean basin; Late Cretaceous carbonate transgression terminating with the Paleocene Internal Hellenides flysch; subduction of the Axios/Vardar ocean remnants under the European margin and Late Cretaceous high-pressure metamorphism and compression; middle unified Serbo-Macedonian/Rhodope Sidironero-Kerdylia unit underthrust below the Vertiskos-Kimi unit
9. **Paleocene to Early Oligocene (D4):** compression; a mainly W-SW-ward sense of movement; final closure of the Axios/Vardar ocean and collision of Europe with Apulia/Pelagonia during the Paleocene–Eocene; imbrication of nappe stacks; strong imbrication of the Axios/Vardar units; HP metamorphism of the Internal Hellenides high-pressure belt (Ampelakia and Cyclades units) during the Paleocene–Eocene during subduction processes under the Pelagonia; progressively, emplacement of the Pelagonian and Sidironero-Kerdylia nappes together with the HP metamorphic belt on the External Hellenides during the Eocene–Oligocene; synorogenic extension in the Serbo-Macedonian/Rhodope metamorphic province associated with high-temperature metamorphism, migmatisation, granitoid intrusions, and progressively crustal exhumation, initially of the Vertiskos-Kimi unit (Paleocene–Eocene) and then of the Kerdylia/Sidironero unit (Eocene–Oligocene)
10. **Oligocene–Miocene (D5):** HP/LT metamorphism in the External Hellenides belt associated with compression and nappe stacking in the External Hellenides, Crete island, and the Peloponnese; syn-orogenic extension associated with low-grade metamorphism in the Olympos-Ossa area and high- to medium-grade metamorphism, migmatization, and granitoid intrusions in the Cyclades and Serbo-Macedonian/Rhodope metamorphic provinces; crustal exhumation of the Olympos-Ossa and Rhodope Pangaion units
11. **Neogene–Quaternary:** compression along the active Hellenic subduction zone, south of Crete island; ductile extension and exhumation of the Peloponnese and Cretan tectonic windows; brittle extension and intramontagne basin formation in the mainland (D6); recent neo-tectonic activity

Formations of the amphibolite sole of 170–180 Ma of age (Figures 23 and 31a; [160,288,289]) and Middle–Late Jurassic island-arc intermediate to silicic volcanic products, tectonically incorporated between the obducted ophiolitic belts, are related to the development of this intra-oceanic subduction framework and the formation of an ensimatic island arc (e.g., the volcanic and volcanoclastic products outcropping today in the Axios/Vardar zone and the magmatic Chortiatis series (Figures 4, 13, 14, 21, 22 and 31a,b; [6,17,24,138,145,164,180]). Additionally, Late Jurassic granite intrusions in the Axios/Vardar ophiolites are interpreted as products of the magmatic activity that took place during the progression of Meliata/Maliac intra-oceanic subduction and the formation of the Axios/Vardar ocean (e.g., I-type Fanos granite, Figures 3, 13, 14 and 31; [162]).

The Late Jurassic calc-alkaline granites today found as orthogneisses and mylonit-gneisses in the middle Rhodope Sidironero unit [202] and in the Stip-Axios massif [171,172] should also be related to the progressive stages of the supra-subduction Axios/Vardar ocean's development. They represent, possibly, the plutonic infrastructure of the arc volcanic products (Figures 3, 4 and 31a,b; [24,183]).

The Late Jurassic high-pressure metamorphism (>150 Ma), predating the D1 Late Jurassic–Early Cretaceous syn-metamorphic deformation, is ascribed to the Middle–Late Jurassic nappe stacking deformational stage. The Triassic–Jurassic sedimentary sequences of the Apulia–Pelagonia and Europe–Vertiskos/Kimi passive continental margins, together with the obducted arc-formations and ophiolitic belt, were detached outward and, due to their weight, the basement rocks of both margins were buried deeply, where they metamorphosed in high-pressure conditions (Figure 31b,c; [6,19,24,145]).

During D1 progression, the high-pressure metamorphic basement rocks came up to shallower crustal levels and were strongly deformed simultaneously with extension and greenschist to amphibolite facies metamorphism, well exposed in the Pelagonian nappe as well as in the Serbo-Macedonian massif (Figures 11a,b, 17b and 31b,c; [6,13,130,131,145,152–154,179,247,277,279]). Furthermore, the accumulated and strongly eroded Late Jurassic (Kimmeridgian–Tithonian) shallow-water sedimentary platform carbonates on the top of the obducted ophiolites, clearly determining the upper limit of the ophiolite emplacement in the Oxfordian–Kimmeridgian, either emplaced on the eastern and western margins of the Pelagonian nappe or the Serbo-Macedonian Vertiskos unit, indicate a simultaneous emplacement of ophiolites on both the Apulia (Pelagonian) and European (Serbo-Macedonian) continental margins (Figures 29c and 31c; [13,146,149,151–153,198,199,277,279,325]). According to this evidence, and also taking into account our structural works [6,145,162] as well as a lot of recent studies concerning the geodynamic evolution of the Hellenides [16,17,20,24,43,99], it can be inferred that all ophiolite nappes originated from a single source, the Neotethyan Meliata/Maliac-Axios/Vardar ocean basin. Consequently, the ophiolite nappes should be considered far-traveled nappes on the two different continental parts of Apulia (Pelagonian) and Europe (Serbo-Macedonian), (Figure 31b,c).

During the late Early Cretaceous (D2, Barremian–Aptian; ~125–115 Ma), ongoing plate convergence and the possible pull of the subducted oceanic lithospheric slab led further to outward W-SW-vergent imbrication and folding of the whole Pelagonian nappe pile, including the previously obducted ophiolites, the Late Jurassic neritic platform carbonates, the Early Cretaceous mass flow sedimentary formations, and the Paleozoic basement rocks. D2 was generally related to a greenschist facies metamorphism Figures 4, 11a–c and 31d; [6,43,99,145,152,153]). In contrast, an E- to NE-ward sense of movement and imbrication has been identified for the eastern side of the Axios/Vardar ocean at the same time, as can be explained by the proposed evolution of an arcuate Jurassic subduction zone in the Neotethyan Meliata/Maliac-Axios/Vardar ocean realm (Figures 4, 17b and 31d; [17,24,183]). Anatectic melts in the Pelagonian basement during the late Early Cretaceous (~117 Ma) have also been recorded by [43,99], indicating a high-grade temperature flow in places during D2. The Beotian flysch of the Early Cretaceous age [129], as well as some ophiolite mélange occurrences that were deposited at that time, should represent the sedimentary infill of the foreland basins formed at the front of the D2 thrust sheets. The Early Cretaceous high-

pressure metamorphism (~120 Ma) referred to by Wawrzenitz and Mposkos (1997) [50] and Kirchenbaur et al. (2012) [57] for the upper Rhodope Kimi unit could be explained as a consequence of the D2 compression and crustal thickening.

Crustal thickening due to the D2 event was followed at the Apulian/Pelagonian site by late Early Cretaceous–Late Cretaceous extension. During the Late Cretaceous–Paleocene, the transgressive shallow water carbonate series takes place, lying discordantly over all the previously described pre-Late Cretaceous sedimentary formations and structures (Figures 4, 13, 15 and 32a; [6,145]). This extensional regime may have led to the continental breakup of Apulia. The break-up of Apulia was associated with the formation of a small ocean basin in the Late Cretaceous named the Pindos-Cyclades ocean, which separated the Pelagonian fragment from Apulia (Figure 32a; [22–24,59,121]). This new oceanic crust is supported by the dating of the protolith of ophiolites at ~80 Ma in the Cyclades area and on Crete island [23,193,194].

In contrast, in the European margin, compression and W-SW-ward thrust vergence developed during the Late Cretaceous. This compressional tectonic was related to the subduction of the Axios/Vardar ocean remnants under the European margin, including the Serbo-Macedonian/Rhodope Vertiskos-Kimi unit. Late Cretaceous subduction processes are indicated here by the existence of a Late Cretaceous magmatic arc along the European margin above the subduction zone (i.e., the Strandja/Sredna-Gora massif in Bulgaria, Figures 2, 20 and 32a,b; [23,24,239,268]). Furthermore, the Late Cretaceous high-to-ultra-hig-pressure rocks (eclogites age 70–80 Ma), recognized as imbricated slices, between the Rhodope nappes, strongly support this Late Cretaceous subduction process [59,121]. During the late Late Cretaceous–Paleocene structural stage, the oceanic lithosphere of the subducted Axios/Vardar ocean, including Late Jurassic to Early Cretaceous calc-alkaline arc-related granitoids and segments of European continental origin, following the subducting ocean slab, was detached E-NE-ward and accreted to the active European continental margin (Kimi unit), forming the Serbo-Macedonian/Rhodope middle Sidironero-Kerdylia unit (Figures 4 and 32b).

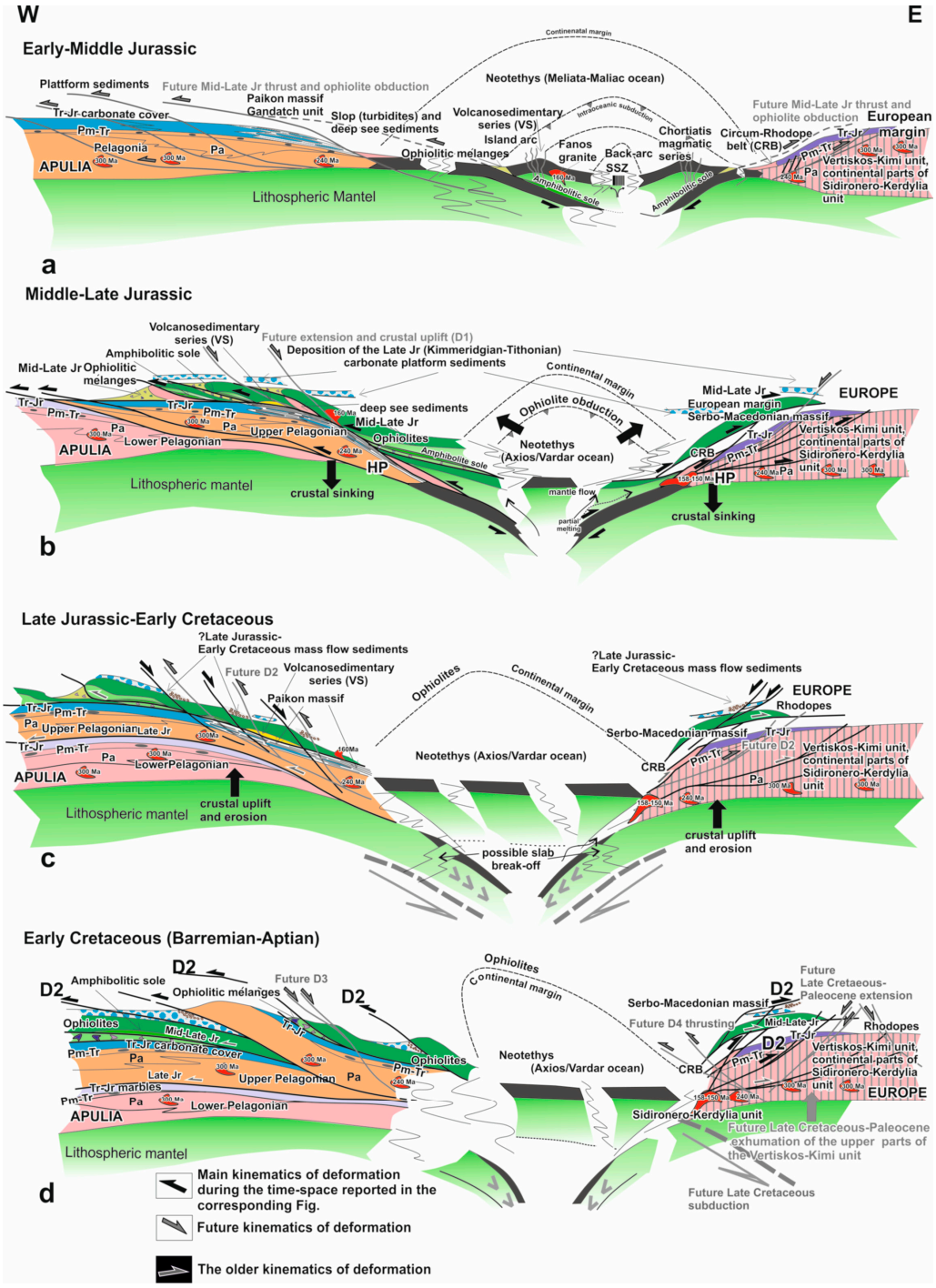

Figure 31. Schematic crustal-scale transects showing the structural evolution of the Hellenides during the Alpine orogeny from the Early–Middle Jurassic until the late Early Cretaceous (modified after [6,17,24,123,124,186]). This has been preceded by the Permo–Triassic Pangea continental rifting and the progressive Neotethyan Meliata/Maliac ocean opening, as shown in Figure 18; granite age is 240 Ma. (**a**) Early–Middle Jurassic: intra-oceanic subduction in an arcuate, northwestward convex subduction zone, associated with the formation of amphibolite metamorphic sole and ophiolitic mélanges at the front of the advanced, overriding oceanic lithosphere, as well as island arc magmatism. A new oceanic lithosphere was progressively formed (the Axios/Vardar ocean) by back-arc spreading

in the supra-subduction zone (SSZ). (**b**) Middle–Late Jurassic (Oxfordian–Kimmerdgian): arc–continent collision, ophiolite obduction, ophiolitic mélange formations at the front of the advanced ophiolites, high-pressure metamorphism, a W-ward and E-ward sense of movement, and crustal imbrication at the western (Pelagonian/Apulia) and eastern (Serbo-Macedonian/Europe) marginal parts of the Neotethyan realm, respectively. Subsequently, deposition of the Late Jurassic neritic sedimentary sequence on the obducted ophiolite realm. (**c**) Late Jurassic–Early Cretaceous: retrogression under greenschist to amphibolite facies metamorphic conditions during the Late Jurassic–Early Cretaceous and possible progressive uplifting of both continental margins (D1). Deposition of the Late Jurassic–Early Cretaceous mass-flow deposits during extension and crustal uplift. (**d**) Early Cretaceous (D2, Barremian–Aptian); W-ward and E-ward crustal imbrication and nappe stacking at both the Pelagonian and Serbo-Macedonian continental margins, respectively. Syn-tectonic greenschist facies metamorphism. The future Late Cretaceous subduction zone along which the remnants of the Neotethyan Axios/Vardar ocean will be subducted under Europe is shown by a dotted, grey line. Abbreviations as in Figure 3.

During the Paleocene–Eocene to Early Oligocene, the D4 compressional event followwed. This is related to the final stages of the Late Cretaceous subduction processes of the Axios/Vardar ocean under Europe and the subsequent development of the SW-ward vergent thrust and fold belt in the Apulian and Axios/Vardar structural units without any important metamorphic events, at least in their tectonically higher parts. In contrast, in the Serbo-Macedonian/Rhodope province, extension, crustal uplift and exhumation processes took place simultaneously with compression and nappe stacking under ductile conditions (Figures 4, 7, 13, 14 and 32b; [6,27,37,296]). During the Paleocene–Eocene, the entire Axios/Vardar ocean lithosphere was buried under the European margin and the Axios/Vardar ocean closed. As a consequence, the European Plate, together with fragments of the Axios/Vardar zone units, the late Late Cretaceous high-pressure metamorphosed rocks, and the Sidironero-Kerdylia unit, collided with the Apulian Pelagonian fragment, sliding SW-ward along segments of the Axios/Vardar oceanic remnants (Figures 4 and 32b; [17,24]). Due to the collision, the European Vertiskos-Kimi unit overthrust the Triassic–Jurassic volcano-sedimentary Circum-Rhodope belt. During the D4 event, as compression and nappe stacking were advancing towards the west over time time, at the Serbo-Macedanian/Rhodope nappe pile, compression and related high-pressure metamorphism were progressively replaced by extension, nappe collapse (mainly towards the SW), and gradual exhumation of the higher to the deeper crustal nappes (e.g., initially, with the Vertiskos-Kimi unit). The extension was now related to high-grade temperature metamorphism and migmatite creation, as well as new adakitic magmatic activity dated to the Paleocene–Eocene age (e.g., Elatia granite; Figures 4, 16, 17a,c and 28b; [51,57,216,217,222,223,228]). This high-temperature metamorphism and the magmatic activity were possibly triggered by the break-off of a deep-seated slab, maybe from the downgoing Pelagonian margin, either by delamination or convective thinning of the previously over-thickened Rhodope lithosphere, resulting in upwelling of asthenospheric material and flow heating (Figure 32b; [57,212,223]).

Paleocene–Eocene extension, nappe tectonic denudation, and crustal exhumation in the Serbo-Macedonian/Rhodope nappe pile take place at about the same time as compression, nappe stacking, and subduction of the Cyclades/Pindos small ocean or parts of the Pindos deep sea basin under the Pelagonian fragment. The same subduction event in the Olympos-Ossa area further to the north is described as an A-type subduction (Figures 4, 7, 19 and 32a,b; [24,47,86,93,157]). Simultaneously, further to the west, in the External Hellenides, the external parts of the Pindos zone were strongly SW-ward imbricated and folded. Thin-skinned tectonics characterized this compressional tectonic of the External Hellenides, building up the structurally complicated Pindos nappe (Figures 4, 29 and 31b). The Internal Hellenides Paleocene–Eocene Ampelakia-Cyclades high-pressure belt was formed during this subduction process (Figures 2, 7 and 32a,b; [47,48,86,93]). Refs. [17,24,118] suggest the continuation of this Paleocene–Eocene high-pressure belt to the Rhodope Sidironero unit, additionally interpreting the lowermost Rhodope Pangaion unit as an

exhumed part of the External Hellenides, equivalent to the Olympos-Ossa carbonate platform, which covers the Apulian basement. Paleocene–Eocene age (ca. 50–42 Ma) high- to ultra-high-pressure rocks were recognized imbricated in the Sidironero unit [51,53,57] and in the Nestos ductile thrust zone, along which the Sidironero unit overthrusts the Pangaion unit [17,24,121,226]. The same tectonostratigraphy is also found in a southwestern–southern direction in the Olympos-Cyclades nappe stack, where the Paleocene–Eocene Ampelakia-Cyclades high-pressure belt with the Pelagonian fragment overthrusts the External Hellenides Olympos-Ossa and Cyclades units [39,47,48,86]. As a result, the Ampelakia/Olympos-Cyclades thrust zone should be the same, with the Nestos shear zone continuing under the Pelagonian and Serbo-Macedonian/Rhodope nappe stacks, as was also proposed by [17,24,118]. In this scenario, it should be considered that the lower Rhodope Pangaion unit is really equivalent to the Olympos-Ossa unit and the Apulian Plate continues below the Serbo-Macedonian/Rhodope nappe stack (Figure 32).

Further Eocene–Oligocene nappe stacking and crustal thickening to the west, in the External Hellenides, are associated with the final emplacement of Ampelakia-Cyclades high-pressure rocks and the Pelagonian nappe stack on the External Hellenides Gavrovo carbonate platform. Compression again took place with simultaneous extension at the structurally internal higher Hellenides nappes and then exhumation of the Sidironero-Kerdylia unit (Figures 4, 17a, 26 and 32b; [17,24,40,146,240,241,297]). At the same time, new magmatic activity took place in the whole Serbo-Macedonia/Rhodope province (e.g., Vrondou and Xanthi granites, volcanic rocks in between the turbidites deposits of the Thrace basin, etc.; Figures 3, 4 and 16; [7,118,208,212,216,217,222,223,326]). Eocene syn-extensional high-temperature metamorphism and migmatization processes in the middle Serbo-Macedonia/Rhodope Sidironero-Kerdylia unit are ascribed to mantel delamination processes (Figure 17a,c and Figure 32; [17,24,51,222,223,240]). The higher-grade metamorphosed Rhodope units during the Tertiary, compared with the Pelagonian Apulian fragment, associated with migmatization processes, granitoid intrusions, and deep crustal exhumation, could be well explained due to their deeper tectonic position to the east in the Hellenides geotectonic frame.

Here should also be mentioned that the Kesebir/Kardamos and Kechros domes in the Rhodope province, which have been placed on many geological maps as equivalent to the lower Rhodope Pangaion unit, do not show clear structural and compositional relationships with the Pangaion unit. They do not contain the same thick carbonate sequence as the Pangaion unit; they are overlain directly by the upper Rhodope Kimi unit, equivalent to the Serbo-Macedonian Vertiskos unit, and their most important difference to the Pangaion unit is that their cooling/exhumation path was dated at the Eocene–Oligocene (~40–30 Ma; 225), which is the same cooling/exhumation age given for the middle Rhodope Sidironero unit [17,24,40,227]. Moreover, apatite fission-track analyses (AFT) for the Sidironero unit and the Kesebir/Kardamos and Kechros domes gave about the same ages, ~26 Ma and ~30 Ma, respectively. Apatite fission-track ages for the Rhodope lower Pangaion dome range between 15 and 10 Ma, which is younger than the Kesebir/Kardamos and Kechros domes (Figure 4; [227]). Furthermore, in the tectonic contact between the upper Rhodope Kimi unit and these two domes are, tectonically, Late Cretaceous high-pressure rocks—a tectonic contact that has been described as the tectonic contact between the upper Kimi and middle Sidironero Rhodope units. Regarding the described structural and compositional features of both metamorphic domes, the Kesebir/Kardamos and Kechros domes fit better as equivalents to the Sidironero-Kerdylia unit, as illustrated on our maps and cross-sections (Figures 3 and 4).

During the Oligocene–Miocene (D5 event), when Europe had already collided with Apulia and Pelagonia, extension under brittle conditions took place in the structurally higher Internal Hellenides nappe levels, and ductile deformation dominated in the structurally deeper levels. Ductile deformation was associated with mylonite formation, low- to high-temperature metamorphism, and new magmatic activity and migmatization. In detail, brittle conditions dominate in the upper parts of the Pelagonian nappe pile, while ductile

conditions are recognized in the lowermost parts of the Pelagonian nappe, in the lower Rhodope Pangaion unit, and in the Paleocene–Eocene high-pressure Ampelakia-Cyclades metamorphic belt (Figure 7a,b, Figure 11a,b and Figure 17a,b; [5–7,86,157,158,296]). The former overthickened lithospheric crust collapsed along ductile shear zones and normal detachment faults with a mainly top-to-SW sense of movement (e.g., the Olympos-Ossa and Strymon Valley detachment faults; Figures 3, 4, 19 and 32b,c; [5,48,86,158,208, 212,297]) or with a mainly top-to-N-NE sense of movement (e.g., the Cyclades detachment faults; Figures 9 and 19; [10,89,191,327]). Nevertheless, an opposite sense of movement has also been described in some cases, e.g., in the Olympos-Ossa province from the top to the NE and the Cyclades area from the top to the S-SW, indicating here a bivergent geometry of the extensional tectonics and a bulk coaxial type of deformation. This collapse caused the formation of several tectonic windows and/or metamorphic core complexes, where the upper structural series of the Apulian Plate were exhumed under the Pelagonia and the Internal Hellenides nappe stack (e.g., the Olympos, Rizomata, and Paikon windows and Pangaion and Cyclades metamorphic core complexes; Figures 3, 4, 7, 16 and 32b,c; [6,7,30,38,47,86,89,95,145,157,206,212,297,300,328–330]). In the Olympos-Ossa area, the exhumation was very rapid and took place under an isothermal decompression path, while, in the Rhodope and Cyclades provinces, the exhumation followed a decompression path with an initially increasing temperature gradient (Figure 8a,b; [6,38,47,48,51,88,89,95,208,212]). According to our recent work, a constrictional type deformation (i.e., NW–SE compression along the Y-axis of the strain ellipsoid, $Y < 1$) characterizes, in places, Tertiary tectonic activity in the Internal Hellenides nappes. A flattening type of deformation ($Y > 1$) was also calculated in other places, highlighting this complicated architecture and the evolution of the deformation [7,30,158,200,216,240]. Finally, according to our descriptions concerning the structural and geotectonic evolution of the Olympos-Ossa and Rizomata windows, the lowermost Rhodope Pangaion and Cyclades metamorphic core complexes are joined with the same tectonostratigraphy and composition of their geological units as well as the same structural evolution.

Simultaneously with the Oligocene–Miocene extension, nappe collapse and exhumation processes in the Olympos-Ossa-Cyclades and Serbo-Macedonian/Rhodope provinces, new compression, and SW-wards verging nappe stacking developed at the External Hellenides (Gavrovo and Ionian zones), associated with new subduction processes and the formation of the External Oligocene–Miocene high-pressure belt, visible in the Peloponnese and on Crete island (Figures 3, 4, 6, 26 and 32c). In the Peloponnese and on Crete island, Oligocene–Miocene nappe stacking was progressively followed by new Early–Middle Miocene bulk coaxial extension and nappe denudation along ductile shear zones and normal detachment faults, causing a series of Miocene tectonic windows and metamorphic core complexes, where the Oligocene–Miocene high-pressure rocks of the External Hellenides, represented by the Plattenkalk series (? Ionian zone) and Phyllite-Quartzite series (of unknown origin), were exhumed from under the whole Hellenides nappe stack, and an isothermal decompression P-T metamorphic path (e.g., the Taygetos window, the Leyka Ori window, and the Psiloritis window; Figures 2, 3, 4 and 32c; [31–34,83,96,97,328,331–334]).

During the Neogene–Quaternary, a brittle extensional deformation dominated the entire Hellenides belt. It was associated with high-angle normal and oblique strike-slip faults (D6 event), in some cases expressed by transpressional or transtensional tectonics (Figures 3, 4, 12, 14 and 32c; [7,261,302]), dismembering all pre-Neogene tectonic units and structures. Now, in the present day, convergence and compression have migrated toward the SW, being directed into the active Hellenic subduction zone, where the African plate is subducting under the Hellenides towards the NE, forming the active Hellenic subduction zone and the active volcanic arc of the Aegean sea (Figures 2, 4, 20 and 32c).

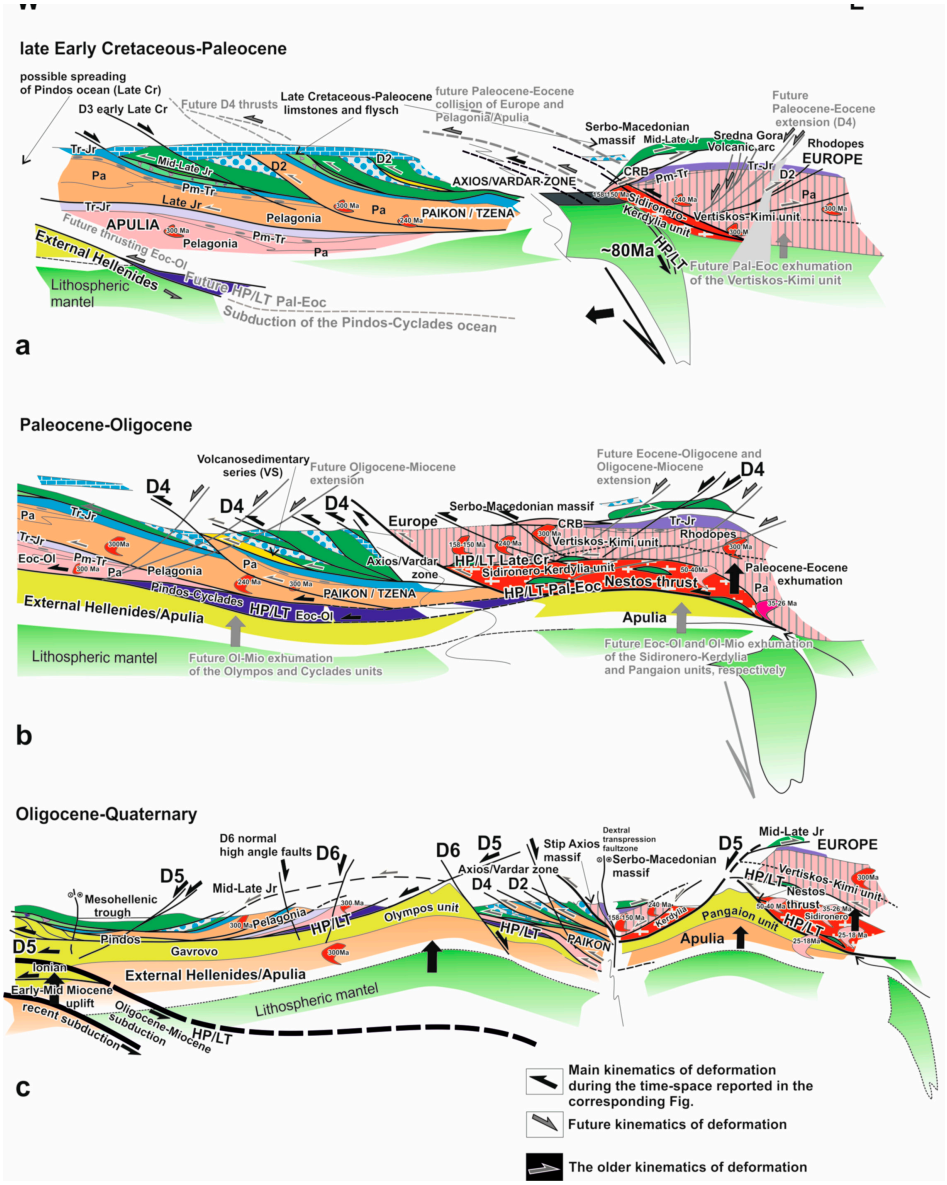

Figure 32. Schematic crustal-scale transects showing the structural evolution of the Hellenides during the Alpine orogeny from the early Late Cretaceous until the Neogene–Quaternary. CRB = Circum-Rhodope belt, granite age of 240 Ma (modified after [6,17,24,123,124,186]). (**a**) late Early Cretaceous–Paleocene extension during the Albian (Late Cretaceous) (D3): Unconformable sedimentation of the Late Cretaceous shallow-water carbonate series terminated with the Early Paleocene Internal Hellenides flysch. Progressively, the development of the Late Cretaceous subduction of the Axios/Vardar ocean remnants under the Serbo-Macedonian margin (Europe) and the formation of Late Cretaceous calc-alkaline, arc-type magmatism at the European margin, as well as the Late Cretaceous high-pressure/high-temperature metamorphic belt (HP/HT). Exhumation of the uppermost Serbo-Macedonian parts during the late Late Cretaceous–Paleocene (parts of the Vertiskos unit). Possible spreading of the ?Pindos/Cyclades small ocean basin, now between the Pelagonian and Apulia. Its future Paleocene–Eocene subduction under the Pelagonian nappe is also indicated by the grey line. (**b**) Paleocene–Eocene/Oligocene (D4): Compression, a W- to SW-ward sense of movement and intense crustal imbrication of the Pelagonian nappe and Axios/Vardar zone. Final collision of Europe (Serbo-Macedonian) with the Pelagonian nappe during the Paleocene–Eocene, simultaneously with extension and the exhumation of the unified Vertiskos-Kimi unit. Formation of

the Internal Hellenides high-pressure belt of the Paleocene–Eocene age (Olympos-Ossa, Cyclades) due to the subduction of the small Pindos/Cyclades ocean under the Pelagonia. Progressive emplacement during the Eocene–Oligocene of the Pelagonian nappe (Apulia) together with the HP/LT Internal Hellenides metamorphic belt on the External Hellenides Olympos-Ossa unit, which constituted the Triassic–Oligocene platform carbonate sequence of the Apulian passive margin. Simultaneously, along the Nestos ductile thrust zone, tectonic emplacement of the Sidironero-Kerdylia unit on the Pangaion unit takes place, considering the latter as equivalent to the Olympos-Ossa unit. In that case, the suture zone between the Pelagonian nappe and Olympos-Ossa unit should be the same as the tectonic contact between the Sidironero-Kerdylia and Pangaion units. This means that the same suture zone continues from the Pelagonian nappe to the Serbo-Macedonian/Rhodope nappe pile. Intense compression and nappe stacking in the External Hellenides Pindos and Gavrovo units. Eocene–Oligocene syn-orogenic extension in the Serbo-Macedonian/Rhodope metamorphic province associated with high-temperature metamorphism, migmatization, and magmatism causes the exhumation of the Sidironero-Kerdylia unit. (**c**) Oligocene–Miocene to Quaternary (D5, D6): HP/LT metamorphism and building of the External Hellenides Oligocene–Miocene high-pressure belt associated with compression and nappe stacking in the External Hellenides. Simultaneous syn-orogenic extension, low- to high-temperature metamorphism and magmatism in the Internal Hellenides (the Olympos-Ossa, Cyclades, and Serbo-Macedonian/Rhodope metamorphic province), and final exhumation of the lowermost Rhodope Pangaion unit in the form of a metamorphic core complex, regarded as part of the External Hellenides Olympos-Ossa unit. (D6). Neogene–Quaternary: active Hellenic subduction and compression associated contemporaneously with extension and rapid exhumation during the Early–Middle Miocene of the External Hellenides Oligocene–Miocene HP/LT belt as a series of tectonic windows in the External Hellenides in the Peloponnese and on Crete island. Finally, high-angle normal and strike-slip faults, some of which are related to intramontagne basin formations and/or recent neo-tectonic activity. Abbreviations as in Figure 3.

However, the evolution of the two syn- to late-orogenic sedimentary basins of the Meso-Hellenic trough and the Thrace basin should also be reported. These are considered very important for the final image of the Alpine Hellenides orogenic belt. They are mentioned as molassic-type basins, filled with turbiditic and clastic sediments, that persisted through the Tertiary deformation history of the Hellenides. The Meso-Hellenic trough is defined as a polyhistory strike-slip and piggy-back basin behind the Tertiary External Hellenides thrust and fold belt. The Thrace basin is described as a supra-detachment basin in the Rhodope province. The deposition history of the Meso-Hellenic trough starts during the Early–Middle Eocene and ends in the Early–Middle Eocene. Respectively, the Thrace basin is filled with Eocene–Oligocene turbidites intercalated with acid to intermediate volcanic products of the same age. Younger Miocene basic magmatic products also intrude into the Paleogene deposits in the basin (Figures 1–4; [60–67,248]).

The described orogenic outward Tertiary W- to SW-ward migration of dynamic peer compression vs. extension, related respectively to nappe stacking vs. crustal uplift or to the contemporaneous action of compressional and extensional tectonics in the several parts of the Hellenic orogenic belt (e.g., the External and Internal Hellenides), can be well explained by a retreating subduction zone and roll-back of the subducted Pindos-Cyclades lithospheric slab and also by lithospheric mantel delamination [4,6,9,18,24,191,221,222,267,335].

6. Conclusions

I. The Alpine structural evolution of the Hellenides starts during the Permo–Triassic with the continental rifting of the Pangea supercontinent and the progressive opening of the Neotethyan Meliata/Maliac-Axios/Vardar ocean realm.

II. Alpine deformation and metamorphism are recorded in a multiphase deformational setting from the Early–Middle Jurassic to the present day. Six main (D1 to D6) deformational events were identified that followed, at their early stages, intra-oceanic subduction and ophiolite obduction. Compression, nappe stacking, crustal thickening and high-pressure metamorphism alternated progressively over

time with extension, orogenic collapse, mylonite formation, and low- to high-temperature metamorphism associated with migmatite formation and granite intrusions in places. Furthermore, the extension leads to crustal thinning, uplift, and the exhumation of deep crustal levels as tectonic windows or metamorphic core complexes (e.g., the Olympos-Ossa window, Cyclades and Rhodope Pangaion metamorphic core complexes, and Cretan and Peloponnese windows). A S-to SW-ward migration of dynamic peer compression vs. extension is clearly recognized during the Tertiary in the Hellenides. In any case, extension and crustal uplift follow compression and nappe stacking or they take place simultaneously in different places in the orogen. Today, compression has migrated along the Hellenic active subduction zone south of Crete island.

III. The ophiolite belts, including the Mid–Late Jurassic ophiolitic mélanges, in the Hellenides are considered far-traveled nappes that originated from a single source ocean, which was the Neotethyan Meliata/Maliac-Axios/Vardar ocean basin. Nappe thrusting and ophiolite overriding started during the Early–Middle Jurassic, related to the evolution of an intra-oceanic E-ward dipping subduction in the Meliata/Maliac ocean. The upper limit of ophiolite emplacement on the Apulian (Pelagonia) and European (Vertiskos-Kimi unit) continental margins is the Callovian–Oxfordian. The Axios/Vardar ocean finally closed during the Paleocene–Eocene, subducting totally under the European continental margin. As a result, the Vertisko-Kimi unit, as part of the European margin, overthrusts during the late Late Cretaceous–Paleocene the Sidironero-Kerdylia unit, composed of imbricated continental parts and pieces of the Axios/Vardar NE-ward-subducted lithosphere. Subsequently, Europe collided with the Pelagonian fragment of Apulian origin.

IV. The Axios/Vardar zone is allochthonous, imbricated intensively SW-ward by the Paleocene–Eocene compressional stage. The Axios/Vardar ophiolites along the Axios/Vardar zone form the exposed surface parts of the deep-seated Axios/Vardar suture, which is traced at depth between the Rhodopes nappes. The Internal Hellenides Serbo-Macedonian/Rhodope thrust stack is rooted along this Axios/Vardar suture.

V. The lower-most Pangaion Rhodope unit should be the Apulian plate's eastern marginal part. It was underthrust along the unified Nestos-Ampelakia-Cyclades ductile thrust zone during the Eocene–Oligocene below the Pelagonian and the Serbo-Macedonian/Rhodope nappe stack, following Paleocene–Eocene subduction of the small Pindos-Cyclades ocean under the Pelagonian fragment. This model, in agreement with Jahn-Awe et al. (2010) [17] and Froitzheim et al. (2014) [24] assumes an E-NE-ward, far-traveled underthrusting of the Apulian Plate below the Pelagonian and the Serbo-Macedonian/Rhodope nappe pile. Finally, the lower-most Pangaion Rhodope unit exhumed as a metamorphic core complex below the Serbo-Macedonian/Rhodope nappe stack during the Oligocene–Miocene extensional tectonics of the Internal Hellenides and the broader Aegean region. Respectively, the Serbo-Macedonian/Rhodope nappes were exhumed progressively under an extensional regime, initially with the exhumation of the Vertiskos-Kimi unit during the Paleocene–Eocene, followed by the exhumation of the Sidironero-Kerdylia unit during the Eocene–Oligocene. In contrast, during the Tertiary in the External Hellenides, compression and nappe thrusting dominate, migrating S-SW-ward to the today-active Hellenic subduction zone, also causing the Oligocene–Miocene subduction processes. Moreover, Oligocene–Miocene HP/LT metamorphism is recognized between the External Hellenides in the southern Peloponnese and Crete island (the Plattenkalk series and the Phyllit-Quartzite unit). Here, the Early–Middle Miocene extension followed, causing a series of tectonic windows and metamorphic core complexes.

VI. During the Eocene–Oligocene, the Pelagonian nappe with obducted ophiolite nappes and the Ampelakia-Cyclades Paleocene–Eocene high-pressure belt were

emplaced on the External Hellenides Gavrovo carbonate platform (the Apulian Plate). The latter exhumed subsequently during the Oligocene–Miocene extension, forming the Olympos-Ossa tectonic window as well as the Cyclades and Pangaion metamorphic core complexes simultaneously with Oligocene–Miocene compression, subduction, and SW-S-ward nappe stacking in the External Hellenides.

VII. A retreating subduction zone and rollback of the subducted Pindos-Cyclades lithospheric slab and/or mantel delamination processes could well explain the Tertiary S- to SW-ward migration of the compressional and extensional tectonics. Compression is related to nappe stack and crustal thickening, extension to nappe denudation, crustal uplift, and crustal thining. Extension normally follows compression.

Funding: This research received no external funding.

Data Availability Statement: Not applicable.

Acknowledgments: Dedicated to my students at the School of Geology of the University of Thessaloniki GR, as well as to my teachers, friends, and colleagues, with whom I have collaborated for a long time of about 50 years. I can't forget the nice fieldwork days and the endless discussions of geological problems and orogenic processes. I would also like to thank three anonymous referees for their critical comments, as well as Ilias Lazos for his editorial assistance.

Conflicts of Interest: The author declares no conflicts of interest.

References

1. Jacobshagen, V.; Dürr, F.; Kockel, K.; Kopp, K.O.; Kowalczyk, G.; Berckhemer, H.; Buttner, D. Structure and Geodynamic Evolution of the Aegean Region. In *Alps, Apennines, Hellenides*; Cloos, H., Roeder, D., Schmidt, K., Eds.; IUGG: Berlin, Germany, 1978; pp. 537–564.
2. Jacobshagen, V. *Geologie von Griechenland. Beiträge zur Regionalen Geologie der Erde, Band 19*; Gebrüder Bornträger: Berlin, Germany, 1986; p. 363.
3. Mountrakis, D. The Pelagonian Zone in Greece: A Polyphase-Deformed Fragment of the Cimmerian Continent and Its Role in the Geotectonic Evolution of the Eastern Mediterranean. *J. Geol.* **1986**, *94*, 335–347. [CrossRef]
4. Ricou, L.-E.; Burg, J.-P.; Godfriaux, I.; Ivanov, Z. Rhodope and Vardar: The metamorphic and the olistostromic paired belts related to the Cretaceous subduction under Europe. *Geodin. Acta* **1998**, *11*, 285–309. [CrossRef]
5. Kilias, A.; Tranos, M.D.; Orozco, M.; Alonso-Chaves, F.M.; Soto, J.I. Extensional collapse of the Hellenides: A review. *Rev. La Soc. Geol. Espana* **2002**, *15*, 129–139.
6. Kilias, A.; Frisch, W.; Avgerinas, A.; Dunkl, I.; Falalakis, G.; Gawlick, H.-J. Alpine architecture and kinematics of de-formation of the northern Pelagonian nappe pile in the Hellenides. *Austrian J. Earth Sci.* **2010**, *103*, 4–28.
7. Kilias, A.; Falalakis, G.; Sfeikos, A.; Papadimitriou, E.; Vamvaka, A.; Gkarlaouni, C. The Thrace basin in the Rhodope province of NE Greece — A tertiary supradetachment basin and its geodynamic implications. *Tectonophysics* **2013**, *595–596*, 90–105. [CrossRef]
8. Stampfli, G.M.; Borel, G.D. A plate tectonic model for the Paleozoic and Mesozoic constrained by dynamic plate boundaries and restored synthetic oceanic isochrons. *Earth Planet. Sci. Lett.* **2002**, *196*, 17–33. [CrossRef]
9. Jolivet, L.; Rimmelé, G.; Oberhënsli, R.; Goffé, B.; Candan, O. Correlation of syn-orogenic tectonic and metamorphic events in the Cyclades, the Lycian nappes and the Menderes massif. Geodynamic implications. *Bull. Soc. Geol. Fr.* **2004**, *175*, 217–238. [CrossRef]
10. Jolivet, L.; Brun, J.-P. Cenozoic geodynamic evolution of the Aegean. *Int. J. Earth Sci.* **2010**, *99*, 109–138. [CrossRef]
11. Schmid, S.M.; Bernoulli, D.; Fügenschuh, B.; Matenco, L.; Schefer, S.; Schuster, R.; Tischler, M.; Ustaszewski, K. The Alpine-Carpathian-Dinaridic orogenic system: Correlation and evolution of tectonic units. *Swiss J. Geosci.* **2008**, *101*, 139–183. [CrossRef]
12. Schmid, S.; Fügenschuh, B.; Kounov, A.; Maţenco, L.; Nievergelt, P.; Oberhänsli, R.; Pleuger, J.; Schefer, S.; Schuster, R.; Tomljenović, B.; et al. Tectonic units of the Alpine collision zone between Eastern Alps and western Turkey. *Gondwana Res.* **2020**, *78*, 308–374. [CrossRef]
13. Gawlick, H.-J.; Frisch, W.; Hoxha, L.; Dumitrica, P.; Krystyn, L.; Lein, R.; Missoni, S.; Schlagintweit, F. Mirdita Zone ophiolites and associated sediments in Albania reveal Neotethys Ocean origin. *Int. J. Earth Sci.* **2008**, *97*, 865–881. [CrossRef]
14. Dilek, Y.; Furnes, H.; Shallo, M. Geochemistry of the Jurassic Mirdita Ophiolite (Albania) and the MORB to SSZ evolution of a marginal basin oceanic crust. *Lithos* **2008**, *100*, 174–209. [CrossRef]
15. Dilek, Y.; Altunkaynak, S.; Öner, Z. Syn-extensional granitoids in the Menderes core complex and the late Cenozoic extensional tectonics of the Aegean province. *Geol. Soc. Lond. Speéc. Publ.* **2009**, *321*, 197–223. [CrossRef]
16. Saccani, E.; Bortolotti, V.; Marroni, M.; Pandolfi, L.; Photiades, A.; Principi, G. The Jurassic association of backarc basin ophiolites and calc-alkaline volcanics in the Guevgueli Complex (NorthernGreece): Implication for the evolution of the Vardar Zone. *Ofioliti* **2008**, *33*, 209–227.

17. Jahn-Awe, S.; Froitzheim, N.; Nagel, T.J.; Frei, D.; Georgiev, N.; Pleuger, J. Structural and geochronological evidence for Paleogene thrusting in the western Rhodopes, SW Bulgaria: Elements for a new tectonic model of the Rhodope Metamorphic Province. *Tectonics* **2010**, *29*, 1–30. [CrossRef]
18. Burg, J.-P. Rhodope: From Mesozoic convergence to Cenozoic extension. Review of petro-structural data in the geochronological frame. *J. Virtual Explor.* **2012**, *42*, 1–44. [CrossRef]
19. Robertson, A.H. Late Palaeozoic–Cenozoic tectonic development of Greece and Albania in the context of alternative reconstructions of Tethys in the Eastern Mediterranean region. *Int. Geol. Rev.* **2013**, *54*, 373–454. [CrossRef]
20. Bortolotti, V.; Chiari, M.; Marroni, M.; Pandolfi, L.; Principi, G.; Saccani, E. Geodynamic evolution of ophiolites from Albania and Greece (Dinaric-Hellenic belt): One, two, or more oceanic basins? *Int. J. Earth Sci.* **2013**, *102*, 783–811. [CrossRef]
21. Robertson, A.H.; Trivić, B.; Đerić, N.; Bucur, I.I. Tectonic development of the Vardar ocean and its margins: Evidence from the Republic of Macedonia and Greek Macedonia. *Tectonophysics* **2012**, *595–596*, 25–54. [CrossRef]
22. Papanikolaou, D. Timing of tectonic emplacement of the ophiolites and terrane paleogeography in the Hellenides. *Lithos* **2009**, *108*, 262–280. [CrossRef]
23. Papanikolaou, D. Tectonostratigraphic models of the Alpine terranes and subduction history of the Hellenides. *Tectonophysics* **2013**, *595–596*, 1–24. [CrossRef]
24. Froitzheim, N.; Jahn-Awe, S.; Frei, D.; Wainwright, A.N.; Maas, R.; Georgiev, N.; Nagel, T.J.; Pleuger, J. Age and composition of meta-ophiolite from the Rhodope Middle Allochthon (Satovcha, Bulgaria): A test for the maximum-allochthony hypothesis of the Hellenides. *Tectonics* **2014**, *33*, 1477–1500. [CrossRef]
25. Brunn, J.H. Contribution à l'étude géologique du Pinde septentrional et d' une partie de la Macédoine occidnetale. *Ann. Géol. Pays Helléniques* **1956**, *7*, 1–358.
26. Aubouin, J. Contribution a l' étude géologique de la Grèce septentrional: Les confins de l' Epire et de la Thessaly. *Ann. Géol. Pays Helléniques* **1959**, *10*, 1–525.
27. Mercier, J. Étude géologique des zones internes des Hellénides en Macédoine centrale (Grèce). Contribution é l' étude du métamorphisme et de l' évolution magmatique des zones internes des Hellénides. *Ann. Géol. Pays Helléniques* **1968**, *20*, 1–792.
28. Zouros, N.; Mountrakis, D. The thrusting of the Pindos zone and the relationship between the External geotectonic zones in Metsovo-eastern Zagori area (NW Greece). *Bull. Geol. Soc. Greece* **1991**, *25*, 245–262.
29. Zouros, N. Study of the Tectonic Structures Connected with the Pindos Nappe in Epirus (NW Greece). Ph.D. Thesis, University of Thessaloniki, Thessaloniki, Greece, 1993; p. 630.
30. Kilias, A.; Thomaidou, E.; Katrivanos, E.; Vamvaka, A.; Fassoulas, C.; Pipera, K.; Falalakis, G.; Avgerinas, S.; Sfeikos, A. A geological cross-section through northern Greece from Pindos to Rhodope Mountain Ranges: A field guide accross the Ex-ternal and Internal Hellenides. *J. Virtual Explor.* **2016**, *50*, 1–107.
31. Seidel, E.; Kreuzer, H.; Harre, W. A Late Oligocene/Early Miocene high pressure belt in the external Hellenides. *Geol. Jahrb.* **1982**, *23*, 165–206.
32. Kilias, A.; Fassoulas, C.; Mountrakis, D. Tertiary extension of continental crust and uplift of Psiloritis metamorphic core complex in the central part of the Hellenic Arc (Crete, Greece). *Geol. Rundschau* **1994**, *83*, 417–430. [CrossRef]
33. Fassoulas, C.; Kilias, A.; Mountrakis, D. Postnappe stacking extension and exhumation of high-pressure/low-temperature rocks in the island of Crete, Greece. *Tectonics* **1994**, *13*, 127–138. [CrossRef]
34. Jolivet, L.; Goffé, B.; Monié, P.; Truffert-Luxey, C.; Patriat, M.; Bonneau, M. Miocene detachment in Crete and exhumation P-T-t paths of high-pressure metamorphic rocks. *Tectonics* **1994**, *15*, 1129–1153. [CrossRef]
35. Stöckhert, B.; Wachmann, M.; Küster, M.; Bimmermann, S. Low effective viscosity during high pressure metamorphism due to dissolution precipitation creep: The record of HP–LT metamorphic carbonates and siliciclastic rocks from Crete. *Tectonophysics* **1999**, *303*, 299–319. [CrossRef]
36. Godfriaux, I. Étude géologique de la region de l'Olympe (Grèce). *Ann. Géolog. Pays Helléniques* **1968**, *19*, 1–281.
37. Vergely, P. Tectoniques des Ophiolites Dans les Hellénides Internes Déformation, Métamorphisme et Phénomènes Sédi-Mentaires. Conséquences sur l' Évolution des Région Téthysiennes Occidentales. Ph.D. Thesis, University Paris-Sud, Orsay, Paris, France, 1984; pp. 1–560.
38. Schermer, E.R. Mechanisms of blueschist creation and preservation in an A-type subduction zone, Mount Olympos region, Greece. *Geology* **1990**, *18*, 1130–1133. [CrossRef]
39. Schermer, E. Geometry and kinematics of continental basement deformation during the Alpine orogeny, Mt. Olympos region, Greece. *J. Struct. Geol.* **1993**, *15*, 571–591. [CrossRef]
40. Bonev, N.; Burg, J.-P.; Ivanov, Z. Mesozoic–Tertiary structural evolution of an extensional gneiss dome—the Kesebir–Kardamos dome, eastern Rhodope (Bulgaria–Greece). *Int. J. Earth Sci.* **2006**, *95*, 318–340. [CrossRef]
41. Bonev, N.; Marchev, P.; Moritz, R.; Collings, D. Jurassic subduction zone tectonics of the Rhodope Massif in the Thrace region (NE Greece) as revealed by new U–Pb and 40Ar/39Ar geochronology of the Evros ophiolite and high-grade basement rocks. *Gondwana Res.* **2015**, *27*, 760–775. [CrossRef]
42. Bonev, N.; Moritz, R.; Borisova, M.; Filipov, P. Therma–Volvi–Gomati complex of the Serbo-Macedonian Massif, northern Greece: A Middle Triassic continental margin ophiolite of Neotethyan origin. *J. Geol. Soc.* **2018**, *176*, 931–944. [CrossRef]
43. Schenker, F.L.; Fellin, M.G.; Burg, J.-P. Polyphase evolution of Pelagonia (northern Greece) revealed by geological and fission-track data. *Solid Earth* **2015**, *6*, 285–302. [CrossRef]

44. Altherr, R.; Schliestedt, M.; Okrusch, M.; Seidel, E.; Kreuzer, H.; Harre, W.; Lenz, H.; Wendt, I.; Wagner, G. Geochro-nology of high- pressure rocks on Sifnos (Greece, Cyclades). *Contrib. Miner. Petrol.* **1979**, *70*, 245–255. [CrossRef]
45. Wijbrans, J.R.; McDougall, I. 40Ar/39Ar dating of white micas from an Alpine high-pressure metamorphic belt on Naxos (Greece): The resetting of the argon isotopic system. *Contrib. Miner. Pet.* **1986**, *93*, 187–194. [CrossRef]
46. Okrusch, M.; Broecker, M. Eclogites associated with highgrade blueschists in the Cycladic archipelago, Greece: A review. *Eur. J. Mineral.* **1990**, *2*, 451–478. [CrossRef]
47. Schermer, E.R.; Lux, D.R.; Burchfiel, B.C. Temperature-time history of subducted continental crust, Mount Olympos Region, Greece. *Tectonics* **1990**, *9*, 1165–1195. [CrossRef]
48. Kilias, A.; Fassoulas, C.; Priniotakis, M.; Frisch, W.; Sfeikos, A. Deformation and HP/LT metamorphic condition at the tectonic window of Kranea (W. Thessaly, N. Greece). *Z. Dtsch. Geol. Ges.* **1991**, *142*, 87–96. [CrossRef]
49. Broecker, M.; Kreuzer, H.; Matthews, A.; Okrusch, M. 40Ar/39Ar and oxygen isotope studies of polymetamorphism from Tinos Island, Cycladic blueschist belt, Greece. *J. Metamorph. Geol.* **1993**, *11*, 223–240. [CrossRef]
50. Wawrzenitz, N.; Mposkos, E. First evidence for Lower Cretaceous HP/HT-Metamorphism in the Eastern Rhodope, North Aegean Region, North-East Greece. *Eur. J. Miner.* **1997**, *9*, 659–664. [CrossRef]
51. Liati, A.; Gebauer, D. Constraining the prograde and retrograde P-T-t path of Eocene HP rocks by SHRIMP dating of different zircon domains: Inferred rates of heating, burial, cooling and exhumation for central Rhodope, northern Greece. *Contrib. Miner. Pet.* **1999**, *135*, 340–354. [CrossRef]
52. Mposkos, E.D.; Kostopoulos, D.K. Diamond, former coesite and supersilicic garnet in metasedimentary rocks from the Greek Rhodope: A new ultrahigh-pressure metamorphic province established. *Earth Planet. Sci. Lett.* **2001**, *192*, 497–506. [CrossRef]
53. Liati, A. Identification of repeated Alpine (ultra) high-pressure metamorphic events by U–Pb SHRIMP geochronology and REE geochemistry of zircon: The Rhodope zone of Northern Greece. *Contrib. Miner. Pet.* **2005**, *150*, 608–630. [CrossRef]
54. Krenn, K.; Bauer, C.; Proyer, A.; Klötzli, U.; Hoinkes, G. Tectonometamorphic evolution of the Rhodope orogen. *Tectonics* **2010**, *29*. [CrossRef]
55. Schmidt, S.; Nagel, T.J.; Froitzheim, N. A new occurrence of microdiamond-bearing metamorphic rocks, SW Rhodopes, Greece. *Eur. J. Miner.* **2010**, *22*, 189–198. [CrossRef]
56. Nagel, T.J.; Schmidt, S.; Janák, M.; Froitzheim, N.; Jahn-Awe, S.; Georgiev, N. The exposed base of a collapsing wedge: The Nestos Shear Zone (Rhodope Metamorphic Province, Greece). *Tectonics* **2011**, *30*, 1–17. [CrossRef]
57. Kirchenbaur, M.; Münker, C.; Schuth, S.; Garbe-Schönberg, D.; Marchev, P. Tectonomagmatic Constraints on the Sources of Eastern Mediterranean K-rich Lavas. *J. Pet.* **2012**, *53*, 27–65. [CrossRef]
58. Collings, D.; Savov, I.; Maneiro, K.; Baxter, E.; Harvey, J.; Dimitrov, I. Late Cretaceous UHP metmorphism recorded in kyanite–garnet schists from the Central Rhodope Mountains, Bulgaria. *Lithos* **2016**, *246–247*, 165–181. [CrossRef]
59. Miladinova, I.; Froitzheim, N.; Nagel, T.J.; Janák, M.; Georgiev, N.; Fonseca, R.O.C.; Sandmann, S.; Münker, C. Late Cretaceous eclogite in the Eastern Rhodopes (Bulgaria): Evidence for subduction under the Sredna Gora magmatic arc. *Int. J. Earth Sci.* **2018**, *107*, 2083–2099. [CrossRef]
60. Doutsos, T.; Koukouvelas, J.; Zelilidas, A.; Kontopoulos, N. Intracontinental wedging and post-orogenic collapse in the mesohellenic trough. *Geol. Rundschau* **1994**, *83*, 257–275. [CrossRef]
61. Ferrière, J.; Reynaud, J.-Y.; Migiros, G.; Proust, J.-N.; Bonneau, M.; Pavlopoulos, A.; Houze, A. Initiation d 'un bassin transporté: L' exemple du "sillon meso-hellénique" au Tertiaire (Grèce). *Comptés Rendus l'Académie Sci. Ser. IIa, Sci. la Terre des Planètes* **1998**, *326*, 567–574. [CrossRef]
62. Ferrière, J.; Reynaud, J.-Y.; Pavlopoulos, A.; Bonneau, M.; Migiros, G.; Chanier, F.; Proust, J.-N.; Gardin, S. Geologic evolution and geodynamic controls of the Tertiary intramontane piggyback Meso-Hellenic basin, Greece. *Bull. De La Sociète Gèologique De Fr.* **2004**, *175*, 361–381. [CrossRef]
63. Zelilidis, A.; Piper, D.J.W.; Kontopoulos, N. Sedimentation and basin evolution of the Oligocene–Miocene Mesohellenic basin. *Am. Assoc. Pet. Geol. Bull.* **2002**, *86*, 161–182.
64. Vamvaka, A.; Kilias, A.; Mountrakis, D.; Papaoikonomou, J. Geometry and structural evolution of the Mesohellenic Trough (Greece): A new approach. *Geol. Soc. Lond. Speéc. Publ.* **2006**, *260*, 521–538. [CrossRef]
65. Vamvaka, A.; Spiegel, C.; Frisch, W.; Danišík, M.; Kilias, A. Fission track data from the Mesohellenic Trough and the Pel-agonian zone in NW Greece: Cenozoic tectonics and exhumation of source areas. *Int. Geol. Rev.* **2009**, *52*, 223–249. [CrossRef]
66. Maravelis, A.; Konstantopoulos, P.; Pantopoulos, G.; Zelilidis, A. North Aegean sedimentary basin during te Late Eocene to Early Oligocene based on sedimentological studies on Limnos island (NE Greece). *Geol. Carpathica* **2007**, *58*, 455–464.
67. Kilias, A.D.; Vamvaka, A.; Falalakis, G.; Sfeikos, A.; Papadimitriou, E.; Gkarlaouni, C.H.; Karakostas, B. The Mesohellenic Trough and the Paleogene Thrace Basin on the Rhodope Massif, their Structural Evolution and Geotectonic Significance in the Hellenides. *J. Geol. Geosci.* **2015**, *4*, 1–17. [CrossRef]
68. Kockel, F.; Mollat, H.; Walther, H.W. *Erläuterungen zur Geologischen Karte der Chalkidhiki und angrenzender Gebiete 1:100.000 (Nord-Griechenland)*; Bundesanstalt fuer Geowissenschaften und Rohstoffe: Hannover, Germany, 1977; p. 119.
69. Psilovikos, A. Paleogeographic Evolution of the Mygdonia Basin and Lake (Lagada-Volvi). Ph.D. Thesis, University Thessaloniki, Thessaloniki, Greece, 1977; pp. 1–156, (In Greek with English Abstract).
70. Pavlides, S.; Mountrakis, D. Extensional tectonics of northwestern Macedonia, Greece, since the late Miocene. *J. Struct. Geol.* **1987**, *9*, 385–392. [CrossRef]

71. Koufos, G.; Pavlides, S. Correlation between the continental deposits of the Lower Axios Valley and Ptolemais Basin. *Bull. Soc. Geol. Greece* **1988**, *20*, 9–19.
72. Syrides, G. Lithostratigraphical, Biostratigraphical and Paleographical study of the Neogene-Quaternary sedimentary Formations of the Chalkidiki Peninsula. Ph.D. Thesis, University Thessaloniki, Thessaloniki, Greece, 1990; pp. 1–241, (In Greek with English Abstract).
73. Ioakim, C.; Rondoyianni, T.; Mettos, A. The Miocene basins of Greece from a paleoclimatic prospective. *Rev. De Paleobiol.* **2005**, *24*, 735–748.
74. Aubouin, J.; Blanchet, R.; Cadet, J.-P.; Celet, P.; Charvet, J.; Chorowicz, J.; Cousin, M.; Rampnoux, J.P. Essai sur la géologie des Dinarides. *Bull. De La Société Géologique De Fr.* **1970**, *7*, 1060–1095. [CrossRef]
75. Bernoulli, D.; Laubscher, H. The palinspastic problem of the Hellenides. *Eclogae Geologicae Helvetiae* **1972**, *65*, 107–118.
76. Papanikolaou, D. The tectonostratigraphic terranes of the Hellenides. *Ann. Geol. Pays Helleniques* **1997**, *37*, 33–48.
77. Zoumpoulis, E.; Pomoni-Papaioannou, F.; Zelilidis, A. Studying in the Paxos Zone the carbonate depositional environment changes during upper Cretaceous, in Sami area of Kefallinia Island, Greece. *Bull. Geol. Soc. Greece* **2017**, *43*, 793–801. [CrossRef]
78. Zoumpouli, E.; Pomoni-Papaioannou, F.; Zelilidis, A.; Iliopoulos, G. Biostratigraphical and sedimentological study of an Upper Cretaceous succession in the Sami area (central area of Kefallinia, W. Greece). *Bull. Geol. Soc. Greece* **2016**, *47*, 226. [CrossRef]
79. Zoumpouli, E. Carbonate Sedimentation in Kephalonia Island, Paxi Zone, during Mesozoic. Ph.D. Thesis, University Patras, Patras, Greece, 2016; pp. 1–227.
80. Bonneau, M. Correlation of the Hellenide nappes in the south-east Aegean and their tectonic reconstruction. *Geol. Soc. Lond. Speéc. Publ.* **1984**, *17*, 517–527. [CrossRef]
81. Skourtsos, E.; Lekkas, S. Extensional tectonics in Mt Parnon (Peloponnesus, Greece). *Int. J. Earth Sci.* **2010**, *100*, 1551–1567. [CrossRef]
82. Seybold, L.; Trepmann, C.A.; Janots, E. A ductile extensional shear zone at the contact area between HP-LT metamorphic units in the Talea Ori, central Crete, Greece: Deformation during early stages of exhumation from peak metamorphic conditions. *Int. J. Earth Sci.* **2018**, *108*, 213–227. [CrossRef]
83. Theye, T.; Seidel, E. Petrology of low-grade high-pressure metapelites from the External Hellenides (Crete, Peloponnese) A case study with attention to sodic minerals. *Eur. J. Miner.* **1991**, *3*, 343–366. [CrossRef]
84. Theye, T.; Seidel, E.; Vidal, O. Carpholite, sudoite and chloritoid in low-grade high-pressure metapelites from Crete and the Peloponnese. *Eur. J. Mineral.* **1992**, *4*, 487–507. [CrossRef]
85. Godfriaux, I.; Ricou, L.E. The Paikon, a tectonic window within the Internal Hellenides, Macedonia, Greece. *Comptes Rendus Acad. Sci. Ser. II* **1991**, *313*, 1479–1484.
86. Kilias, A. Emplacement of the blueschists unit in eastern Thessaly and (central Greece). *Miner. Wealth* **1995**, *96*, 7–22.
87. Lips, A.L.; White, W.S.H.; Wijbccrans, J.R. 40Ar/39Ar laser probe direct dating of discrete deformational events: A con-tinuous record of early Alpine tectonics in the Pelagonian Zone, NW Aegean area, Greece. *Tectonophysics* **1998**, *298*, 133–153. [CrossRef]
88. Altherr, R.; Kreuzer, H.; Wendt, I.; Lenz, H.; Wagner, G.-A.; Keller, J.; Harre, W.; Hohndorf, A. A late Oligocene/early Miocene high temperature belt in the Attico-Cycladic crystalline complex (SE Pelagonian, Greece). *Geol. Jahrb.* **1982**, *23*, 97–164.
89. Lister, G.S.; Banga, G.; Feenstra, A. Metamorphic core complexes of Cordilleran type in the Cyclades, Aegean Sea, Greece. *Geology* **1984**, *12*, 221–225. [CrossRef]
90. Keay, S.; Lister, G.; Buick, I. The timing of partial melting, Barrovian metamorphism and granite intrusion in the Naxos metamorphic core complex, Cyclades, Aegean Sea, Greece. *Tectonophysics* **2001**, *342*, 275–312. [CrossRef]
91. Grasemann, B.; Petrakakis, K. Evolution of the Serifos Metamorphic Core Complex. *J. Virtual Explor.* **2007**, *27*. [CrossRef]
92. Iglseder, C.; Grasemann, B.; Rice, A.H.N.; Petrakakis, K.; Schneider, D.A. Miocene south directed low-angle normal fault evolution on Kea Island (West Cycladic Detachment System, Greece). *Tectonics* **2011**, *30*, TC4013. [CrossRef]
93. Roche, V.; Laurent, V.; Cardello, G.L.; Jolivet, L.; Scaillet, S. Anatomy of the Cycladic Blueschist Unit on Sifnos Island (Cyclades, Greece). *J. Geodyn.* **2016**, *97*, 62–87. [CrossRef]
94. Ring, U.; Glodny, J.; Peillod, A.; Skelton, A. The timing of hightemperature conditions and ductile shearing in the footwall of the Naxos extensional fault system, Aegean Sea, Greece. *Tectonophysics* **2018**, *745*, 366–381. [CrossRef]
95. Linnros, H.; Hansman, R.; Ring, U. The 3D geometry of the Naxos detachment fault and the three-dimensional tectonic architecture of the Naxos metamorphic core complex, Aegean Sea, Greece. *Int. J. Earth Sci.* **2019**, *108*, 287–300. [CrossRef]
96. Thomson, S.N.; Stöckhert, B.; Brix, M.R. Thermochronology of the high-pressure metamorphic rocks of Crete, Greece: Implications for the speed of tectonic processes. *Geology* **1998**, *26*, 259–262. [CrossRef]
97. Thomson, S.N.; Stöckhert, B.; Brix, M.R. Miocene high-pressure metamorphic rocks of Crete, Greece: Rapid exhuma-tion by buoyant escape. *Geol. Soc. Lond.Spec. Publ.* **1999**, *154*, 87–107. [CrossRef]
98. Kilias, A.; Mountrakis, D. The Pelagonian nappe. Tectonics, metamorphism and magmatism (In Greek with English abstract). *Bull. Soc. Geol. Greece* **1989**, *20*, 29–46.
99. Schenker, F.L.; Burg, J.; Kostopoulos, D.; Moulas, E.; Larionov, A.; von Quadt, A. From Mesoproterozoic magmatism to collisional Cretaceous anatexis: Tectonomagmatic history of the Pelagonian Zone, Greece. *Tectonics* **2014**, *33*, 1552–1576. [CrossRef]
100. Engel, M.; Reischmann, T. Single zircon geochronology of orthogneisses from Paros, Greece. *Bull. Geol. Soc. Greece* **1998**, *32*, 91–99.
101. Reischmann, T. Pre-Alpine origin of tectonic units from the metamorphic complex of Naxos, Greece, identified by single zircon Pb/Pb dating. *Bull. Geol. Soc. Greece* **1998**, *32*, 101–111.

102. Ring, U.; Layer, P.W.; Reischmann, T. Miocene high-pressure metamorphism in the Cyclades and Crete, Aegean Sea, Greece: Evidence for large-magnitude displacement on the Cretan detachment. *Geology* **2001**, *29*, 395–398. [CrossRef]
103. Baran, Z.O.; Dilek, Y.; Stockli, D. Diachronous uplift and cooling history of the Menderes core complex, western Anatolia (Turkey), based on new Zircon (U-Th)/He ages. *Tectonophysics* **2017**, *694*, 181–196. [CrossRef]
104. Lamont, T.N.; Searle, M.P.; Waters, D.J.; Roberts, N.M.; Palin, R.M.; Smye, A.; Dyck, B.; Gopon, P.; Weller, O.M.; St-Onge, M.R. Compressional origin of the Naxos metamorphic core complex, Greece: Structure, petrography, and thermobarometry. *GSA Bull.* **2019**, *132*, 149–197. [CrossRef]
105. Hetzel, R.; Ring, U.; Akal, C.; Troesch, M. Miocene NNE-directed extensional unroofing in the Menderes massif, western Turkey. *J. Geol. Soc.* **1995**, *152*, 639–654. [CrossRef]
106. Hetzel, R.; Romer, R.L.; Candan, O.; Passchier, C.W. Geology of the Bozdag area, central Menderes massif, SW Turkey: Pan-African basement and Alpine deformation. *Geol. Rundschau* **1998**, *87*, 394–406. [CrossRef]
107. Kilias, A.; Mountrakis, D.; Tranos, M.; Pavlides, S. The prevolcanic metamorphic rocks of Santorini island: Structural evolution and kinematics during the Tertiary (South Aegean, Greece). In *Volcanic Risk. The European Laboratory Volcanoes, Proceedings of the 2nd workshop. EUR18161-The European Laboratory Volcanos/Volcanic Risc, Santorini, Greece, 2–4 May 1996*; European Commision: Luxembourg, 1996; pp. 23–36.
108. Ring, U.; Gessner, K.; Güngör, T.; Passchier, C.W. The Menderes Massif of western Turkey and the Cycladic Massif in the Aegean—Do they really correlate? *J. Geol. Soc. Lond.* **1999**, *156*, 3–6. [CrossRef]
109. Hetzel, R.; Reischmann, T. Intrusion age of Pan-African augen gneisses in the southern Menderes Massif and the age of cooling after Alpine ductile extensional deformation. *Geol. Mag.* **1996**, *133*, 565–572. [CrossRef]
110. Partzsch, J.H.; Oberhansli, R.; Candan, O.; Warkus, F. The evolution of the central Menderes massif, West Turkey: A complex nappe pile recording 1.0Ga of geological history. *Freib. Forsch* **1998**, *C-471*, 166–168.
111. Gessner, K.; Piazolo, S.; Güngör, T.; Ring, U.; Kröner, A.; Passchier, C.W. Tectonic significance of deformation patterns in granitoid rocks of the Menderes nappes, Anatolide belt, southwest Turkey. *Int. J. Earth Sci.* **2001**, *89*, 766–780. [CrossRef]
112. Bozkurt, E.; Oberhaensli, R. Menderes Massif (western Turkey): Structural metamorphic and magmatic evolution-a synthesis. *Int. J. Earth Sci.* **2001**, *89*, 679–708. [CrossRef]
113. Altherr, R.; Siebel, W. I-type plutonism in a continental back-arc setting: Miocene granitoids and monzonites from the central Aegean Sea, Greece. *Contrib. Miner. Pet.* **2002**, *143*, 397–415. [CrossRef]
114. Ring, U.; Thomson, S.N.; Bröcker, M. Fast extension but little exhumation: The Vari detachment in the Cyclades, Greece. *Geol. Mag.* **2003**, *140*, 245–252. [CrossRef]
115. Glodny, J.; Ring, U. The Cycladic Blueschist Unit of the Hellenic subduction orogen: Protracted high-pressure meta-morphism, decompression and reimbrication of a diachronous nappe stack. *Earth-Sci. Rev.* **2021**, *224*, 103883. [CrossRef]
116. Brunn, J.H.; Argyriadis, I.; Ricou, L.E.; Poisson, A.; Marcoux, J.; de Graciansky, P.C. Elements majeurs de liaison entre Taurides et Hellenides. *Bull. Soc. Géol. Fr.* **1976**, *7*, 481–497. [CrossRef]
117. Robertson, A.H.F.; Dixon, J.E.; Brown, S.; Collins, A.; Morris, A.; Pickett, E.; Sharp, I.; Ustaömer, T. Alternative tectonic models for the Late Palaeozoic-Early Tertiary development of Tethys in the Eastern Mediterranean region. *Geol. Soc. Lond. Speéc. Publ.* **1996**, *105*, 239–263. [CrossRef]
118. Dinter, D.A. Late Cenozoic extension of the Alpine collisional orogen, northeastern Greece: Origin of the north Aegean basin. *Bull. Geol. Soc. Am.* **1998**, *110*, 1208–1230. [CrossRef]
119. Rassios, A.H.E.; Moores, E.M. Heterogeneous mantle complex, crustal processes, and obduction kinematics in a unified Pindos-Vourinos ophiolitic slab (northern Greece). *Geol. Soc. Lond. Speéc. Publ.* **2006**, *260*, 237–266. [CrossRef]
120. Rassios, A.E.; Dilek, Y. Rotational deformation in the Jurassic Mesohellenic ophiolites, Greece, and its tectonic significance. *Lithos* **2009**, *108*, 207–223. [CrossRef]
121. Petrík, I.; Janák, M.; Froitzheim, N.; Georgiev, N.; Yoshida, K.; Sasinková, V.; Konečný, P.; Milovská, S. Triassic to Early Jurassic (c. 200 Ma) UHP metamorphism in the Central Rhodopes: Evidence from U–Pb–Th dating of monazite in dia-mondbearing gneiss from Chepelare (Bulgaria). *J. Metamorph. Geol.* **2016**, *34*, 265–291. [CrossRef]
122. Papanikolaou, D. Tectonic evolution of the Cycladic blueschist belt (Aegean Sea, Greece). In *Chemical Transport in Metasomatic Processes: NATO ASI Series*; Helgeson, H.C., Ed.; Springer: Dordrecht, The Netherlands, 1987; pp. 429–450.
123. Kilias, A. The Hellenides: A complicated, multiphase deformed Alpine orogenic belt. Compression vs. extension, the dynamic peer for the orogen making. In Proceedings of the 9th International INQUA Meeting on Paleoseismology, Active Tec-tonics and Archeoseismology (PATA), Possidi, Greece, 25–27 June 2018; pp. 119–123.
124. Killias, A. The Hellenides, a complicated, multiphase Alpine orogenic belt. New aspects for the geotectonic evolution of the Hellenides: A review. In Proceedings of the XXI International Congress of the CBGA, Salzburg, Austria, 10–13 September 2018. Abstract.
125. Stampfli, G.M.; Vavassis, I.; De Bono, A.; Rosselet, F.; Matti, B.; Bellini, M. Remnants of the paleotethys oceanic su-ture-zone in the western Tethyan area. *Bull. Soc. Geol. Italia* **2003**, *2*, 1–23.
126. Savoyat, E.; Lalechos, N. *Geological Map of Greece, Scale 1:50.000, Kalampaka Sheet*; Institute of Geology and Mineral Exploration: Athens, Greece, 1972.
127. Lekkas, E. Geological structure and geodynsmic evolution of the Koziakas Mountain (western Thessaly, Greece). Ph.D. Thesis, University Athens, Athens, Greece, 1987; pp. 1–280, (In Greek with English Abstract).

128. Karfakis, I.; Skourtsi-Koroneou, B.; Kanaki-Mavridou, I.C. *Geological Map of Greece, Scale 1:50,000, Moyzakion Sheet*; Institute of Geology and Mineral Exploration: Athens, Greece, 1993.
129. Nirta, G.; Moratti, G.; Piccardi, L.; Montanari, D.; Catanzariti, R.; Carras, N.; Papini, M. The boeotian flysch revisited: New constraints on ophiolite obduction in central Greece. *Ofioliti* **2015**, *40*, 107–123. [CrossRef]
130. Ghon, G. Mikrofazielle Untersuchung einer Karbonatklastischen Beckenfüllung im Hangenden der Ophiolitführenden Koziakas Mélange in Kori, Nordgriechenland. Bachelor's Thesis, University Leoben, Leoben, Austria, 2017; pp. 1–20.
131. Ghon, G.; Gawlick, H.J.; Missoni, S.; Djeric, N.; Kilias, A.; Goričan, Š. Age and microfacies of a carbonate-clastic radio-laritic basin fill above the Koziakas Mélange (Hellenides, Greece). In Proceedings of the XXI International Congress of the CBGA, (abstract), Salzburg, Austria, 10–13 September 2018.
132. Chiari, M.; Bortolotti, V.; Marcucci, M.; Photiades, A.; Principi, G.; Saccani, E. Radiolarian biostratigraphy and geochemistry of the Koziakas massif ophiolites (Greece). *Bull. Soc. Géol. Fr.* **2012**, *183*, 287–306. [CrossRef]
133. Yarwood, G.A.; Aftalion, M. Field relations and U-Pb geochronology of a granite from the Pelagonian zone of the Hel-lenides (High Pieria, Greece). *Bull. Soc. Géol. Fr.* **1976**, *18*, 259–264. [CrossRef]
134. Mountrakis, D.; Sapountzis, E.; Kilias, A.; Eleftheriadis, G.; Christofides, G. Paleogeographic conditions in the western Pelagonian margin in Greece during the initial rifting of the continental area. *Can. J. Earth Sci.* **1983**, *20*, 1673–1681. [CrossRef]
135. Koroneos, A.; Christofides, G.; Del Moro, A.; Kilias, A. Rb-Sr geochronology and geochemical aspects of the Eastern Varnountas plutonite (NW Macedonia, Greece). *Neues Jahrb. Fur Mineral. Abhandlungen* **1993**, *165*, 297–315.
136. Koroneos, A.; Kilias, A.; Avgerinas, A. Hercynian plutonic rocks of Voras Mountain, Macedonia, Northern Greece: Their structure, petrogenesis, and tectonic significance. *Int. Geol. Rev.* **2013**, *55*, 994–1016. [CrossRef]
137. Poli, G.; Christophidis, G.; Koroneos, A.; Soldatos, T.; Perugini, D. Langone AEarly Triassic granitic magmatism—Arnea Kerkini granitic complexes—In the Vertiskos unit (Serbo-macedonian massif, north-eastern Greece) and its signifi-cance in the geodynamic evolution of the area. *Acta Vulcanol.* **2009**, *21*, 47–70.
138. Michard, A.; Feinberg, H.; Montigny, R. Supra-ophiolitic formations from the Thessaloniki nappe (Greece), and associated magmatism: An intra-oceanic subduction predates the Vardar obduction. *Comptes Rendus l'Academie Sci. Ser. IIa Sci. Terre Planetes* **1998**, *327*, 493–499. [CrossRef]
139. Kilias, A.; Tranos, M.; Mountrakis, D.; Shallo, M.; Marto, A.; Turku, I. Geometry and kinematics of deformation in the Albanian orogenic belt during the Tertiary. *J. Geodyn.* **2001**, *31*, 169–187. [CrossRef]
140. Gawlick, H.-J.; Missoni, S. Middle-Late Jurassic sedimentary mélange formation related to ophiolite obduction in the Alpine-Carpathian-Dinaridic Mountain Range. *Gondwana Res.* **2019**, *74*, 144–172. [CrossRef]
141. Reinecke, T.; Altherr, R.; Hartung, B.; Hatzipanagiotou, K.; Kreuzer, H.; Harre, W.; Klein, H.; Keller, J.; Geenen, E.; Boeger, H. Remnants of Late Cretaceous high temperature belt on the island of Anafi (Cyclades, Greece). *Neus Jahrb. Mineral. Abh.* **1982**, *145*, 157–182.
142. Sánchez-Gómez, M.; Avigad, D.; Heimann, A. Geochronology of clasts in allochthonous Miocene sedimentary sequences on Mykonos and Paros Islands: Implications for back-arc extension in the Aegean Sea. *J. Geol. Soc.* **2002**, *159*, 45–60. [CrossRef]
143. Kruckenberg, S.C.; Ferré, E.C.; Teyssier, C.; Vanderhaeghe, O.; Whitney, D.L.; Seaton, N.C.A.; Skord, J.A. Viscoplastic flow in migmatites deduced from fabric anisotropy: An example from the Naxos dome, Greece. *J. Geophys. Res. Solid Earth* **2010**, *115*. [CrossRef]
144. Cao, S.; Neubauer, F.; Bernroider, M.; Liu, J. The lateral boundary of a metamorphic core complex: The Moutsounas shear zone on Naxos, Cyclades, Greece. *J. Struct. Geol.* **2013**, *54*, 103–128. [CrossRef] [PubMed]
145. Katrivanos, E.; Kilias, A.; Mountrakis, D. Kinematics of deformation and structural evolution of the Paikon Massif (Central Macedonia, Greece): A Pelagonian tectonic window? *Neues Jahrb. Für Geol. Und Paläontologie Abh.* **2013**, *269*, 149–171. [CrossRef]
146. Galeos, A.; Pomoni-Papaioannou, F.; Tsaila-Monopolis, S.; Turnsek, D.; Ioakim, C. Upper Jurassic-Lower Cretaceous molassic-type sedimentation in the western part of the Almopias subzone, Aridhea Loutra unit (northern Greece). *Bull. Geol. Soc. Greece* **1994**, *30*, 171–184.
147. Photiades, A.; Skourtsi-Coroneou, V.; Grigoris, P. The stratigraphic and paleogeographic evolution of the eastern Pelagonian margin during the Late Jurassic—Cretaceous interval (Western Vermion Mountain—Western Macedonia, Greece). *Bull. Geol. Soc. Greece* **1998**, *32*, 71–77.
148. Bortolotti, V.; Fazzuoli, M.; Principi, G. The late Early Cretaceous transgression on the laterites in Vourinos and Vermion massifs (western Macedonia, Greece). *Bull. Geol. Soc. Greece* **2007**, *40*, 182–190.
149. Bortolotti, V.; Carras, N.; Chiari, M.; Fazzuoli, M.; Photiades, A.; Principi, G. Sedimentary evolution of the Upper Jurassic Zyghosti platform, Kozani, Northern Greece. In Proceedings of the International Symposium on Earth System Sciences (ISES) 2004, Istanbul, Turkey, 8–10 September 2004; pp. 705–712.
150. Gawlick, H.-J.; Sudar, M.; Missoni, S.; Aubrecht, R.; Schlagintweit, F.; Jovanović, D.; Mikuš, T. Formation of a Late Jurassic carbonate platform on top of the obducted Dinaridic ophiolites deduced from the analysis of carbonate pebbles and ophiolitic detritus in southwestern Serbia. *Int. J. Earth Sci.* **2020**, *109*, 2023–2048. [CrossRef]
151. Schlagintweit, F.; Gawlick, H.-J.; Missoni, S.; Hoxha, L.; Lein, R.; Frisch, W. The eroded Late Jurassic Kurbnesh carbonate platform in the Mirdita Ophiolite Zone of Albania and its bearing on the Jurassic orogeny of the Neotethys realm. *Swiss J. Geosci.* **2008**, *101*, 125–138. [CrossRef]

152. Kostaki, G.; Kilias, A.; Gawlick, H.J.; Schlagintweit, F. Kimmeridgian-Tithonian shallow- water platform clasts from mass flows on top of the Vardar/Axios ophiolites. *Bull. Geol. Soc. Greece* **2016**, *47*, 184. [CrossRef]
153. Kostaki, G.; Kilias, A.; Gawlick, H.-J.; Schlagintweit, F. Component analysis in the vardar/Axios zone of northern Greece reveals an eroded Late Jurassic carbonate platform comparable to those of the Eastern Alps/Western Carpathian, Dinarides, Albanides and Hellenides. *Bul. Shk. Gjeol.* **2014**, *1*, 85–88.
154. Most, T.; Frisch, W.; Dunkl, I.; Kodosa, B.; Boev, B.; Avgerinas, A.; Kilias, A. Geochonological and structural investigation of the Northern Pelagonian crystalline zone. Constraints from K/Ar and zircon and apatite fission track dating. *Bull. Geol. Soc. Greece* **2001**, *34*, 91–95. [CrossRef]
155. Mposkos, E.; Kostopoulos, D.; Krohe, A. Low-P/High-T prealpine metamorphism and medium-P alpine overprint of the Pelagonian zone documented in high-alumina metapelites from the Vernon massif, Western Macedonia, Northern Greece. *Bull. Geol. Soc. Greece* **2001**, *34*, 949–958. [CrossRef]
156. Mposkos, E.; Krohe, A. New Evidences of the Low-P/High-T Pre-Alpine Metamorphism and Medium-P Alpine Overprint of the Pelagonia Zone Documented in Metapelites and Orthogneisses from the Voras Massif, Macedonia, Northern Greece. *Bull. Geol. Soc. Greece* **2004**, *34*, 558–567. [CrossRef]
157. Kilias, A. Transpressive tektonik in den zentralen Helleniden. Aenderung der translations pfade durch die transpression (Nord-zentral Griechenland). *Neues Jahrb. Geol. Paläentologie Monatshefte* **1991**, *20*, 291–306. [CrossRef]
158. Sfeikos, A.; Böhringer, C.; Frisch, W.; Kilias, A.; Ratschbacher, L. Kinematics of the Pelagonian nappes in the Kranea area, N. Thessaly (Greece). *Bull. Geol. Soc. Greece* **1991**, *25*, 101–115.
159. Frisch, W. Plate motions in the Alpine region and their correlation to the opening of the Atlantic ocean. *Geol. Rundschau* **1981**, *70*, 402–411. [CrossRef]
160. Tremblay, A.; Meshi, A.; Deschamps, T.; Goulet, F.; Goulet, N. The Vardar zone as a suture for the Mirdita ophiolites, Albania: Constraints from the structural analysis of the Korabi-Pelagonia zone. *Tectonics* **2015**, *34*, 352–375. [CrossRef]
161. Hoxha, L. The Jurassic-Cretaceous orogenic event and its effects in the exploration of sulphide ores, Albanian ophiolites, Albania. *Eclogae Geol. Helv.* **2001**, *94*, 339–350.
162. Michail, M.; Pipera, K.; Koroneos, A.; Kilias, A.; Ntaflos, T. New perspectives on the origin and emplacement of the Late Jurassic Fanos granite, associated with an intra-oceanic subduction within the Neotethyan Axios-Vardar Ocean. *Int. J. Earth Sci.* **2016**, *105*, 1965–1983. [CrossRef]
163. Robertson, A.; Shallo, M. Mesozoic–Tertiary tectonic evolution of Albania in its regional Eastern Mediterranean context. *Tectonophysics* **2000**, *316*, 197–254. [CrossRef]
164. Sharp, I.R.; Robertson, A.H.F. Tectonic-sedimentary evolution of the western margin of the Mesozoic Vardar Ocean: Evidence from the Pelagonian and Almopias zones, northern Greece. *Geol. Soc. Lond. Speéc. Publ.* **2006**, *260*, 373–412. [CrossRef]
165. Ferrière, J. Étude géologique d'un sectuer des zones Helléniques internes subpelagonienne et pélagonienne (massif de l'Othrys, Grèce continental). Importance et signification de l période orogénique ante-Cretacé superieur. *Bul. Soc. Géol. France* **1974**, *7*, 543–562. [CrossRef]
166. Carras, N. La piattaforma carbonatica del Parnasso durante il Guirassico Superiore—Cretaceo inferiore. Ph.D. Thesis, University Athens, Athens, Greece, 1995; p. 232, (In Greek with Italian Abstract).
167. Celet, P. Contribution a l' étude géologique du Parnasse-Gkiona et d' une partie des régions méridionales de la Grèce continental. *Ann. Géol. Pays Hellén.* **1962**, *13*, 1–360.
168. Celet, P. *Les Bordures de la Zone du Parnasse. 'Evolution Paleogéographique au Mésozoique et Caractères Structuraux*; VI Coll. Aegean; Pascal and Francis: Athens, Greece, 1977; pp. 725–740.
169. Clement, B. *Relations Structurales Entre la Zone du Parnasse et la Zone Pelagonienne en Beotie*; VI Coll. Aegean; Pascal and Francis: Athens, Greece, 1977; pp. 237–251.
170. Carras, N.; Fazzuoli, M. La Formation des "Calcaires de Amfissa" ("Intermediate Limestones Auctt."), Cretacé inferieur, Zone du Parnasse (Grèce continentale). *Ann. Géol. des Pays Helléniques* **1992**, *35*, 43–101.
171. Anders, B.; Reischmann, T.; Poller, U.; Kostopoulos, D. Age and origin of granitic rocks of the eastern Vardar Zone, Greece: New constraints on the evolution of the Internal Hellenides. *J. Geol. Soc. Lond.* **2005**, *162*, 857–870. [CrossRef]
172. Šarić, K.; Cvetković, V.; Romer, R.L.; Christofides, G.; Koroneos, A. Granitoids associated with East Vardar ophiolites (Serbia, F.Y.R. of Macedonia and northern Greece): Origin, evolution and geodynamic significance inferred from major and trace element data and Sr–Nd–Pb isotopes. *Lithos* **2009**, *108*, 131–150. [CrossRef]
173. Brown, S.A.; Robertson, A.H. Evidence for Neotethys rooted within the Vardar suture zone from the Voras Massif, northernmost Greece. *Tectonophysics* **2004**, *381*, 143–173. [CrossRef]
174. Brown, S.A.; Robertson, A.H. Sedimentary geology as a key to understanding the tectonic evolution of the Mesozoic–Early Tertiary Paikon Massif, Vardar suture zone, N Greece. *Sediment. Geol.* **2003**, *160*, 179–212. [CrossRef]
175. Bonneau, M.; Godfriaux, I.; Moulas, Y.; Fourcade, E.; Masse, J. Stratigraphie et structure de la bordure orientale de la double fenêtre du Paikon (Macédoine, Grèce). *Bull. Geol. Soc. Greece* **1994**, *30*, 105–114.
176. Danelian, T.; Robertson, A.H.F.; Dimitriadis, S. Age and significance of radiolarian sediments within basic extrusives of the marginal basin Guevgueli Ophiolite (northern Greece). *Geol. Mag.* **1996**, *133*, 127–136. [CrossRef]
177. Zachariadis, P. Ophiolites of the Eastern Vardar Zone. Ph.D. Thesis, Johannes Gutenberg Universität, Mainz, Germany, 2007; p. 125.

178. Chiari, M.; Bortolotti, V.; Marcucci, M.; Photiades, A.; Principi, G. The Middle jurassic siliceous sedimentary cover at the top of the vourinos ophiolite (Greece). *Ophioliti* **2003**, *28*, 95–103.
179. Most, T. Geodynamic Evolution of the Eastern Pelagonian Zone in Northwestern Greece and the Republic of Macedonia: Implications from U/Pb, Rb/Sr, K/Ar, 40Ar/39Ar Geochronology and Fission TRACK thermochronology. Ph.D. Thesis, Eberhardt-Karls-Universität, Tübingen, Germany, 2003; p. 198.
180. Frisch, W.; Meschede, M. *Plattentektonik: Kontinentverschiebung und Gebirgsbildung. 2., Aktualisierte Auflage*; WBG: Darmstad, Germany, 2007; p. 196.
181. Ferrière, J.; Chanier, F.; Ditbanjong, P. The Hellenic ophiolites: Eastward or westward obduction of the Maliac Ocean, a discussion. *Geol. Rundschau* **2012**, *101*, 1559–1580. [CrossRef]
182. Bonev, N.G.; Stampfli, G.M. New structural and petrologic data on Mesozoic schists in the Rhodope (Bulgaria): Geodynamic implications. *Comptes Rendus Geosci.* **2003**, *335*, 691–699. [CrossRef]
183. Bonev, N.; Stampfli, G. Petrology, geochemistry and geodynamic implications of Jurassic island arc magmatism as revealed by mafic volcanic rocks in the Mesozoic low-grade sequence, eastern Rhodope, Bulgaria. *Lithos* **2008**, *100*, 210–233. [CrossRef]
184. Bonev, N.; Stampfli, G. Alpine tectonic evolution of a Jurassic subduction-accretionary complex: Deformation, kinematics and 40Ar/39Ar age constraints on the Mesozoic low-grade schists of the Circum-Rhodope Belt in the eastern Rhodope–Thrace region, Bulgaria–Greece. *J. Geodyn.* **2011**, *52*, 143–167. [CrossRef]
185. Koglin, N.; Kostopoulos, D.; Reischmann, T. Geochemistry, petrogenesis and tectonic setting of the Samothraki mafic suite, NE Greece: Trace-element, isotopic and zircon age constraints. *Tectonophysics* **2009**, *473*, 53–68. [CrossRef]
186. Kilias, A. Architecture of the Alpine Deformation and Geotectonic Setting of the Hellenides. A synthesis. In Proceedings of the 15th International Congress of the Geological Society of Greece, Athens, Greece, 22–24 May 2019; Volume 7, pp. 158–159.
187. Robertson, A.H. Overview of the genesis and emplacement of Mesozoic ophiolites in the Eastern Mediterranean region. *Lithos* **2002**, *65*, 1–67. [CrossRef]
188. Ustaszewski, K.; Schmid, S.M.; Lugović, B.; Schuster, R.; Schaltegger, U.; Bernoulli, D.; Hottinger, L.; Kounov, A.; Fügenschuh, B.; Schefer, S. Late Cretaceous intra-oceanic magmatism in the internal Dinarides (northern Bosnia and Herzegovina): Implications for the collision of the Adriatic and European plates. *Lithos* **2009**, *108*, 106–125. [CrossRef]
189. Ustaszewski, K.; Kounov, A.; Schmid, S.M.; Schaltegger, U.; Krenn, E.; Frank, W.; Fügenschuh, B. Evolution of the Adria-Europe plate boundary in the northern Dinarides: From continent-continent collision to back-arc extension. *Tectonics* **2010**, *29*, TC6017. [CrossRef]
190. Medwenitsch, W. *Zur Geologie Vardarisch-Makedoniens (Jugoslawien), zum Problem der Pelagoniden*; Oestereichische Akademie der Wissenschaften, Sitzungsberichte der mathematisch naturwissenschaftlichen Klasse, Abteilung 1; Springer: Berlin/Heidelberg, Germany, 1956; Volume 165, pp. 397–473.
191. Ring, U.; Glodny, J.; Will, T.; Thomson, S. The Hellenic Subduction System: High-Pressure Metamorphism, Exhumation, Normal Faulting, and Large-Scale Extension. *Annu. Rev. Earth Planet. Sci.* **2010**, *38*, 45–76. [CrossRef]
192. Ring, U.; Will, T.; Glodny, J.; Kumerics, C.; Gessner, K.; Thomson, S.; Güngör, T.; Monié, P.; Okrusch, M.; Drüppel, K. Early exhumation of high-pressure rocks in extrusion wedges: Cycladic blueschist unit in the eastern Aegean, Greece, and Turkey. *Tectonics* **2007**, *26*, TC2001. [CrossRef]
193. Keay, S. The Geological Evolution of the Cyclades, Greece: Constraints from SHRIMP U-Pb Geochronology. Ph.D. Thesis, Australian National University, Canberra, Australia, 1998; pp. 1–335.
194. Tomaschek, F.; Kennedy, A.K.; Villa, I.M.; Lagos, M.; Ballhaus, C. Zircons from Syros, Cyclades, Greece--Recrystallization and Mobilization of Zircon During High-Pressure Metamorphism. *J. Pet.* **2003**, *44*, 1977–2002. [CrossRef]
195. Ring, U.; Layer, P.W. High-pressure metamorphism in the Aegean, eastern Mediterranean: Underplating and exhuma-tion from the Late Cretaceous until the Miocene to recent above the retreating Hellenic subduction zone. *Tectonics* **2003**, *22*, 1022. [CrossRef]
196. Jolivet, L.; Lecomte, E.; Huet, B.; Denèle, Y.; Lacombe, O.; Labrousse, L.; Le Pourhiet, L.; Mehl, C. The North Cycladic Detachment System. *Earth Planet. Sci. Lett.* **2010**, *289*, 87–104. [CrossRef]
197. Avigad, D.; Garfunkel, Z.; Jolivet, L.; Azañón, J.M. Back arc extension and denudation of Mediterranean eclogites. *Tectonics* **1997**, *16*, 924–941. [CrossRef]
198. Meinhold, G.; Kostopoulos, D.; Reischmann, T.; Frei, D.; BouDagher-Fadel, M.K. Geochemistry, provenance and stratigraphic age of metasedimentary rocks from the eastern Vardar suture zone, northern Greece. *Palaeogeogr. Palaeoclim. Palaeoecol.* **2009**, *277*, 199–225. [CrossRef]
199. Meinhold, G.; Kostopoulos, D.K. The Circum-Rhodope Belt, northern Greece: Age, provenance, and tectonic setting. *Tectonophysics* **2013**, *595-596*, 55–68. [CrossRef]
200. Kilias, A.; Mountrakis, D. Kinematics of the crystalline sequences in the western Rhodope massif. *Geol. Rhodopica* **1990**, *2*, 100–116.
201. Brun, J.-P.; Sokoutis, D. Kinematics of the Southern Rhodope Core Complex (North Greece). *Int. J. Earth Sci.* **2007**, *96*, 1079–1099. [CrossRef]
202. Turpaud, P.; Reischmann, T. Characterization of igneous terranes by zircon dating: Implications for UHP occurrences and suture identification in the Central Rhodope, northern Greece. *Int. J. Earth Sci.* **2010**, *99*, 567–591. [CrossRef]
203. Kronberg, P.; Meyer, W.; Pilger, A. Geologie der Rila-Rhodope-Masse zwischen Strimon und Nestos (Nordgriechenland). *Geol. Jahrb.* **1970**, *88*, 133–180.

204. Kronberg, P.; Raith, M. Tectonics and metamorphism of the Rhodope Crystalline Complex in Eastern Greek Macedonia and parts of Western Thrace. *N. Jb. Geol. Paläont. Mh.* **1977**, *11*, 697–704.
205. Zagorchev, I.; Dinkova, I. *Geological Map of Bulgaria on the Scale 1:100.000. Map Sheet Strumitsa, Petrich, Gevgeli, Sidirocastron*; Geology and Geophysics Ltd.: Sofia, Bulgaria, 1989.
206. Zagorchev, I. Geological Heritage of the Balkan Peninsula: Geological setting (an overview). *Geol. Balc.* **1996**, *26*, 3–10. [CrossRef]
207. Zagorchev, I. Introduction to the geology of SW Bulgaria. *Geol. Balc.* **2001**, *31*, 3–52. [CrossRef]
208. Dinter, D.A.; Macfarlane, A.; Hames, W.; Isachsen, C.; Bowring, S.; Royden, L. U-Pb and $^{40}Ar/^{39}Ar$ geochronology of the Symvolon granodiorite: Implications for the thermal and structural evolution of the Rhodope metamorphic core complex, northeastern Greece. *Tectonics* **1995**, *14*, 886–908. [CrossRef]
209. Massonne, H.-J. Tertiary high-pressure metamorphism recorded in andalusite-bearing mica-schist, southern Pirin Mts., SW Bulgaria. *Eur. J. Miner.* **2016**, *28*, 1187–1202. [CrossRef]
210. Burg, J.P.; Ricou, L.E.; Ivano, Z.; Godfriaux, I.; Dimov, D.; Klain, L. Syn-metamorphic nappe complex in the Rhodope Massif. Structure and kinematics. *Terra Nova* **1996**, *8*, 6–15. [CrossRef]
211. Sokoutis, D.; Brun, J.P.; Driessche, J.V.D.; Pavlides, S. A major Oligo-Miocene detachment in southern Rhodope controlling north Aegean extension. *J. Geol. Soc. Lond.* **1993**, *150*, 243–246. [CrossRef]
212. Dinter, D.A.; Royden, L. Late Cenozoic extension in northeastern Greece: Strymon Valley detachment system and Rhodope metamorphic core complex. *Geology* **1993**, *21*, 45–48. [CrossRef]
213. Kydonakis, K.; Moulas, E.; Chatzitheodoridis, E.; Brun, J.-P.; Kostopoulos, D. First-report on Mesozoic eclogite-facies metamorphism preceding Barrovian overprint from the western Rhodope. *Lithos* **2015**, *220–223*, 147–163. [CrossRef]
214. Peytcheva, I.; von Quadt, A. U–Pb zircon dating of metagranites from Byala Reka region in the east Rhodopes, Bulgaria. *Geol. Soc. Greece Spec. Publ.* **1995**, *4*, 637–642.
215. Peytcheva, I.; von Quadt, A.; Kouzmanov, K.; Bogdanov, K. Elshitsa and Vlaykov Vruh epithermal and porphyry Cu (–Au) deposits of central Srednogorie, Bulgaria: Source and timing of magmatism and mineralisation. In *Mineral Exploration and Sustainable Development*; Eliopoulos, D., Ed.; Millpress: Rotterdam, The Netherlands, 2003; pp. 371–374.
216. Kilias, A.; Mountrakis, D. Tertiary extension of the Rhodope massif associated with granite emplacement (Northern Greece). *Acta Vulcanol.* **1998**, *10*, 331–337.
217. Christofides, G.; Koroneos, A.; Soldatos, T.; Eleftheriadis, G.; Kilias, A. Eocene magmatism (Sithonia and Elatia plutons) in the Internal Hellenides and implications for Eocene-Miocene geological evolution of the Rhodope massif (Northern Greece). *Acta Vulcanol.* **2001**, *13*, 73–89.
218. Soldatos, T.; Koroneos, A.; Christofides, G.; Del Moro, A. Geochronology and origin of the Elatia plutonite (Hellenic Rhodope Massif, N. Greece) constrained by new Sr isotopic data. *N. Jb. Mineral. Abh.* **2001**, *176*, 179–209. [CrossRef]
219. Soldatos, T.; Koroneos, A.; Del Moro, A.; Christophidis, G. Evolution of the Elatia plutonite (Hellenic Rhodope Massif, N. Greece). *Chem. Der Erde* **2001**, *61*, 92–116.
220. Soldatos, T.; Koroneos, A.; Kamenov, B.K.; Peytcheva, I.; von Quadt, A.; Christofides, G.; Zheng, X.; Sang, H. New U–Pb and Ar–Ar mineral ages for the Barutin-Buynovo-Elatia-Skaloti-Paranesti batholith (Bulgaria and Greece): Refinement of its debatable age. *Geochem. Miner. Pet.* **2008**, *46*, 85–102.
221. Marchev, P.; Raicheva, R.; Downes, H.; Vaselli, O.; Chiaradia, M.; Moritz, R. Compositional diversity of Eocene–Oligocene basaltic magmatism in the Eastern Rhodopes, SE Bulgaria: Implications for genesis and tectonic setting. *Tectonophysics* **2004**, *393*, 301–328. [CrossRef]
222. Marchev, P.; Kaiser-Rohrmeier, M.; Heinrich, C.; Ovtcharova, M.; von Quadt, A.; Raicheva, R. 2: Hydrothermal ore deposits related to post-orogenic extensional magmatism and core complex formation: The Rhodope Massif of Bulgaria and Greece. *Ore Geol. Rev.* **2005**, *27*, 53–89. [CrossRef]
223. Marchev, P.; Georgiev, S.; Raicheva, R.; Peytcheva, I.; von Quadt, A.; Ovtcharova, M.; Bonev, N. Adakitic magmatism in post-collisional setting: An example from the Early–Middle Eocene Magmatic Belt in Southern Bulgaria and Northern Greece. *Lithos* **2013**, *180–181*, 159–180. [CrossRef]
224. Georgieva, M.; Cherneva, Z.; Kolcheva, K.; Sarov, S.; Gerdjikov, I.; Voinova, E. P-T metamorphic path of sillimanite-bearing schists in an extensional shear zone, Central Rhodopes, Bulgaria. *Geochem. Mineral. Petrol.* **2002**, *39*, 95–106.
225. Georgieva, M.; Bosse, V.; Cherneva, Z.; Kirilova, M. Products of HP melting in Chepelare shear zone, Central Rhodope, Bulgaria: Petrology, P–T estimates and U–Th–Pb dating. In Proceedings of the Bulgarian Geological Society Annual Conference 'Geosciences', Sofia, Bulgaria, 8–9 December 2011; pp. 55–56.
226. Gautier, P.; Bosse, V.; Cherneva, Z.; Didier, A.; Gerdjikov, I.; Tiepolo, M. Polycyclic alpine orogeny in the Rhodope metamorphic core complex: The record in migmatites from the Nestos shear zone (N. Greece). *Bull. Soc. Géol. Fr.* **2017**, *188*, 36. [CrossRef]
227. Wuethrich, E.D. Low Temperature Thermochronology of the Northern Aegean Rhodope Massif. Ph.D. Thesis, ETH Zurich, Zurich, Switzerland, 2009; pp. 1–209.
228. Mposkos, E.; Krohe, A. Pressure–temperature–deformation paths of closely associated ultra-high-pressure (diamond-bearing) crustal and mantle rocks of the Kimi complex: Implications for the tectonic history of the Rhodope Mountains, northern Greece. *Can. J. Earth Sci.* **2006**, *43*, 1755–1776. [CrossRef]
229. Liati, A.; Seidel, E. Metamorphic evolution and geochemistry of kyanite eclogites in central Rhodope, northern Greece. *Contrib. Miner. Pet.* **1996**, *123*, 293–307. [CrossRef]

230. Carrigan, C.W.; Mukasa, S.B.; Haydoutov, I.; Kolcheva, K. Ion microprobe U–Pb zircon ages of pre-Alpine rocks in the Balkan, Sredna Gora and Rhodope terranes of Bulgaria: Constraints on Neoproterozoic and Variscan tectonic evolution. *J. Czech Geol. Soc.* **2003**, *48*, 32–33.
231. Himmerkus, F.; Reischmann, T.; Kostopoulos, D. Serbo-Macedonian revisited: A Silurian basement terrane from northern Gondwana in the Internal Hellenides, Greece. *Tectonophysics* **2009**, *473*, 20–35. [CrossRef]
232. Peytcheva, I.; Macheva, L.; von Quadt, A.; Zidarov, N. Gondwana derived units in Ograzhden and Belasitsa Mountains, SerboMacedonian Massif (SW Bulgaria): Combined geochemical, petrological and U–Pb zircon-xenotime age constraints. *Geol. Balc.* **2015**, *44*, 51–84.
233. Gorinova, T.; Georgiev, N.; Cherneva, Z.; Naydenov, K.; Grozdev, V.; Lazarova, A. Kinematics and time of emplacement of the Upper Allochthon of the Rhodope Metamorphic Complex: Evidence from the Rila Mountains, Bulgaria. *Int. J. Earth Sci.* **2019**, *108*, 2129–2152. [CrossRef]
234. Bauer, C.; Rubatto, D.; Krenn, K.; Proyer, A.; Hoinkes, G. A zircon study from the Rhodope metamorphic complex, N-Greece: Time record of a multistage evolution. *Lithos* **2007**, *99*, 207–228. [CrossRef]
235. Liati, A.; Gebauer, D.; Wysoczanski, R. U–Pb SHRIMP-dating of zircon domains from UHP garnet-rich mafic rocks and late pegmatoids in the Rhodope zone (N Greece); evidence for Early Cretaceous crystallization and Late Cretaceous metamorphism. *Chem. Geol.* **2002**, *184*, 281–299. [CrossRef]
236. Liati, A.; Theye, T.; Fanning, C.M.; Gebauer, D.; Rayner, N. Multiple subduction cycles in the Alpine orogeny, as recorded in single zircon crystals (Rhodope zone, Greece). *Gondwana Res.* **2016**, *29*, 199–207. [CrossRef]
237. Moritz, R.; Jacquat, S.; Chambefort, I.; Fontignie, D.; Petrunov, R.; Georgieva, S.; von Quadt, A. Controls on ore formation at the high-sulphidation Au–Cu Chelopech deposit, Bulgaria: Evidence from infrared fluid inclusion microthermometry of enargite and isotope systematics of barite. In *Mineral Exploration and Sustainable Development*; Eliopoulos, D., Ed.; Millpress: Rotterdam, The Netherlands, 2003; pp. 1209–1212.
238. von Quadt, A.; Peytcheva, I.; Cvetkovic, V. Geochronology, geochemistry and isotope tracing of the Cretaceous mag-matism of east-Serbia and Panagyurishte District (Bulgaria) as part of the Apuseni–Timok–Srednogorie metallogenic belt in eastern Europe. In *Mineral Exploration and Sustainable Development*; Eliopoulos, D., Ed.; Millpress: Rotterdam, The Netherlands, 2003; pp. 407–410.
239. von Quadt, A.; Moritz, R.; Peytcheva, I.; Heinrich, C.A. Geochronology and geodynamics of Late Cretaceous magmatism and Cu–Au mineralization in the Panagyurishte region of the Apuseni–Banat–Timok–Srednogorie belt, Bulgaria. *Ore Geol. Rev.* **2005**, *27*, 95–126. [CrossRef]
240. Kilias, A.; Falalakis, G.; Mountrakis, D. Cretaceous-Tertiary structures and kinematics of the Serbomacedonian metamorphic rocks and their relation to the exhumation of the Hellenic hinterland (Macedonia, Greece). *Int. J. Earth Sci.* **1999**, *88*, 513–531. [CrossRef]
241. Krohe, A.; Mposkos, E. Multiple generations of extensional detachments in the Rhodope Mountains (northern Greece): Evidence of episodic exhumation of high-pressure rocks. *Geol. Soc. Lond. Speéc. Publ.* **2002**, *204*, 151–178. [CrossRef]
242. Kockel, F.; Mollat, H.; Walther, H.W. Geologie des Serbo-Mazedonischen Massivs und seines mesozoischen Rahmens (Nordgriechenland). *Geol. Jahrb.* **1971**, *89*, 529–551.
243. Chatzidimitriadis, E.; Kilias, A.; Staikopoulos, G. Nouvi aspetti petrologici e tettonici del massiccio serbomacedonne e delle regioni adiacenti, della Grecia del Nortd. *Boll. Soc. Geol. Italia* **1985**, *104*, 515–526.
244. Kockel, F.; Walther, H. Die Strimonlinie als Grenze zwischen Serbo-Mazedonischem und Rila-Rhodope Massiv in Ost Mazedonien. *Geol. Jahrb.* **1965**, *83*, 575–602.
245. Koukouzas, C. Le chévauchement de Strymon dans la région de la frontiere Grecobulgare. *Z. Dtsch. Geol. Gesell.* **1972**, *123*, 343–348.
246. Dixon, J.E.; Dimitriadis, S. Metamorphosed ophiolitic rocks from the Serbo-Macedonian Massif, near Lake Volvi, North-east Greece. *Geol. Soc. Lond. Speéc. Publ.* **1984**, *17*, 603–618. [CrossRef]
247. Papadopoulos, C.; Kilias, A. Altersbeziehungen zwischen Metamorphose und Deformation im zentralen Teil des Serbomazedonischen Massivs (Vertiskos Gebirge, Nord-Griechenland). *Geol. Rundschau* **1985**, *74*, 77–85. [CrossRef]
248. Brun, J.; Sokoutis, D. Core Complex Segmentation in North Aegean, A Dynamic View. *Tectonics* **2018**, *37*, 1797–1830. [CrossRef]
249. Janák, M.; Froitzheim, N.; Georgiev, N.; Nagel, T.J.; Sarov, S. P-T evolution of kyanite eclogite from the Pirin Mountains (SW Bulgaria): Implications for the Rhodope UHP Metamorphic Complex. *J. Metamorph. Geol.* **2011**, *29*, 317–332. [CrossRef]
250. Himmerkus, F.; Reischmann, T.; Kostopoulos, D. Gondwana-derived terranes in the northern Hellenides. 4-D Framew. *Cont. Crust* **2007**, *200*, 379–390. [CrossRef]
251. Himmerkus, F.; Reischmann, T.; Kostopoulos, D. Triassic rift-related meta-granites in the Internal Hellenides, Greece. *Geol. Mag.* **2009**, *146*, 252–265. [CrossRef]
252. Macheva, L.; Peytcheva, I.; von Quadt, A.; Zidarov, N.; Tarassova, E. Petrological, geochemical and isotope features of Lozen metagranite, Belasitza Mountain—Evidence for widespread distribution of Ordovician metagranitoids in the Serbo-Macedonian Massif, SW Bulgaria. In Proceedings of the National Conference "GEOSCIENCES 2006", Sofia, Bulgaria, 30 November–1 December 2006; pp. 209–212.
253. Dimitriadis, S.; Godelitsas, A. Evidence for high pressure metamorphism in the Vertiskos group of the Serbomacedonian massif. The eclogite of Nea Roda, Chalkidiki. *Bull. Geol. Soc. Greece* **1991**, *25*, 67–80.

254. Dimitriadis, S.; Kondopoulou, D.; Atzemoglou, A. Dextral rotations and tectonomagmatic evolution of the southern Rhodope and adjacent regions (Greece). *Tectonophysics* **1998**, *299*, 159–173. [CrossRef]
255. Bonev, N.; Filipov, P. From an ocean floor wrench zone origin to transpressional tectonic emplacement of the Sithonia ophiolite, eastern Vardar Suture Zone, northern Greece. *Int. J. Earth Sci.* **2017**, *107*, 1689–1711. [CrossRef]
256. Kostopoulos, D.K.; Ioannidis, N.M.; Sklavounos, S.A. A New Occurrence of Ultrahigh-Pressure Metamorphism, Central Macedonia, Northern Greece: Evidence from Graphitized Diamonds? *Int. Geol. Rev.* **2000**, *42*, 545–554. [CrossRef]
257. De Wet, A.P. Geology of a Part of the Chalkidiki Peninsula, Northern Greece. Ph.D. Thesis, University of Cabridge, Cambridge, UK, 1989; pp. 1–245.
258. Antić, M.; Peytcheva, I.; von Quadt, A.; Kounov, A.; Trivić, B.; Serafimovski, T.; Tasev, G.; Gerdjikov, I.; Wetzel, A. Pre-Alpine evolution of a segment of the North-Gondwanan margin: Geochronological and geochemical evidence from the central Serbo-Macedonian Massif. *Gondwana Res.* **2015**, *36*, 523–544. [CrossRef]
259. Kydonakis, K.; Gallagher, K.; Brun, J.-P.; Jolivet, M.; Gueydan, F.; Kostopoulos, D. Upper Cretaceous exhumation of the western Rhodope Metamorphic Province (Chalkidiki Peninsula, northern Greece). *Tectonics* **2014**, *33*, 1113–1132. [CrossRef]
260. Kaufmann, G.; Kockel, F.; Mollat, H. Notes on the stratigraphic palaeogeographical position of the Svoula Formation in the innermost zone of the Hellenides, Northern Greece. *Bull. La Société Géologique Fr.* **1976**, *18*, 225–230. [CrossRef]
261. Tranos, M.; Kilias, A.; Mountrakis, D. Geometry and kinematics of the Tertiary post-metamorphic Circum Rhodope Belt Thrust System (CRBTS), Northern Greece. *Bull. Soc. Geol. Greece* **1999**, *33*, 5–16.
262. Pe-Piper, G.; Doutsos, T.; Mijara, A. Petrology and regional significance of the Hercynian granitoid rocks of the Olympiada area, northern Thessaly, Greece. *Chem. Der Erde Geochem.* **1993**, *53*, 21–36.
263. Pe-Piper, G.; Doutsos, T.; Mporonkay, C. Structure, geochemistry and mineralogy of Hercynian granitoid rocks of the Verdikoussa area, northern Thessaly, Greece and their regional significance. *Neues Jahrb. Mineral. Abhandlungen* **1993**, *165*, 267–296.
264. Mountrakis, D.; Eleftheriadis, G.; Christofides, G.; Kilias, A.; Sapountzis, E. Silicic metavolcanics in the western Pelago-nian margin of Greece, related to the opening of Neo-Tethys. *Chemie Erde* **1987**, *47*, 167–179.
265. Koroneos, A. Petrogenesis of the Upper Jurassic Monopigadon pluton related to the Vardar/Axios ophiolites (Macedonia, northern Greece) and its geotectonic significance. *Chemie Erde Geochem.* **2010**, *70*, 221–241. [CrossRef]
266. Boccaletti, M.; Manetti, P.; Peccerillo, A.; Stanisheva-Vasileva, G. Late Cretaceous high-potassium volcanism in eastern Srednogorie, Bulgaria. *Geol. Soc. Am. Bull.* **1978**, *89*, 439–447. [CrossRef]
267. Royden, L.H. Evolution of retreating subduction boundaries formed during continental collision. *Tectonics* **1993**, *12*, 629–638. [CrossRef]
268. Georgiev, N.; Henry, B.; Jordanova, N.; Froitzheim, N.; Jordanova, D.; Ivanov, Z.; Dimov, D. The emplacement mode of Upper Cretaceous plutons from the southwestern part of the Sredna Gora Zone (Bulgaria): Structural and AMS study. *Geol. Carpathica* **2009**, *60*, 15–33. [CrossRef]
269. Robertson, A.H.F.; Karamata, S.; Šarić, K. Overview of ophiolites and related units in the Late Paleozoic-Early Cenozoic magmatic and tectonic developmemt of Tethys in the northern part of the Balkan region. *Lithos* **2009**, *72*, 1–36. [CrossRef]
270. Seward, D.; Vanderhaeghe, O.; Siebenaller, L.; Thomson, S.; Hibsch, C.; Zingg, A.; Duchêne, S. Cenozoic tectonic evo-lution of Naxos Island through a multi-faceted approach of fission-track analysis. *Geol. Soc. Lond. Spec. Publ.* **2009**, *321*, 179–196. [CrossRef]
271. Soldatos, K. The Volcanics of the Almopias Area. Ph.D. Thesis, University of Thessaloniki, Thessaloniki, Greece, 1955; p. 120.
272. Eleftheriades, G. Contribution to the Study of the Volcanic Rocks of the Southern Almopia. Ph.D. Thesis, University of Thessaloniki, Thessaloniki, Greece, 1977; p. 120, (In Greek with English Abastract).
273. Fytikas, M.; Innocenti, F.; Manetti, P.; Peccerillo, A.; Mazzuoli, R.; Villari, L. Tertiary to Quaternary evolution of volcanism in the Aegean region. *Geol. Soc. Lond. Speéc. Publ.* **1984**, *17*, 687–699. [CrossRef]
274. Vougioukalakis, G. The Pliocene volcanites of the Voras mountain, Central Macedonia, Greece. *Bull. Geol. Soc. Greece* **1994**, *30*, 223–240.
275. Pe-Piper, G.; Piper, D.J.W. *The Igneous Rocks of Greece: The Anatomy of an Orogen*; Gebrüder Borntraeger: Berlin, Germany, 2002; p. 280.
276. Vougioukalakis, G.E.; Satow, C.G.; Druitt, T.H. Volcanism of the South Aegean Volcanic Arc. *Elements* **2019**, *15*, 159–164. [CrossRef]
277. Gawlick, H.J.; Missoni, S.; Sudar, N.M.; Suzuki, H.; Meres, S.; Lein, R.; Jovanovic, D. The Jurassic Hallstatt Melange of the Inner Dinarides (SW Serbia): Implications for Triassic-Jurassic geodynamic and paleogeographic reconstructions of the Western Tethyan realm. *N. Jb. Geol. Palaeont. Abh.* **2018**, *288*, 1–47. [CrossRef]
278. Jones, G.; Robertson, A.H.F. Tectono-stratigraphy and evolution of the Mesozoic Pindos ophiolite and related units, northwestern Greece. *J. Geol. Soc. Lond.* **1991**, *148*, 267–288. [CrossRef]
279. Gawlick, H.-J.; Missoni, S.; Suzuki, H.; Sudar, M.; Lein, R.; Jovanović, D. Triassic radiolarite and carbonate components from a Jurassic ophiolitic mélange (Dinaridic Ophiolite Belt). *Swiss J. Geosci.* **2016**, *109*, 473–494. [CrossRef]
280. Jones, G.; Robertson, A.H.F. Rift-drift-subduction and empacement historyof the Early Mesozoic Pindos ocean: Evidence from the Avdella melange, Northern Greece. *Bull. Geol. Soc. Greece* **1994**, *30*, 45–58.
281. Chiari, M.; Bortolotti, V.; Marcousi, M.; Principi, G. New data on the age of the Simoni Mélange, northern Mirdita ophiolite nappe, Albania. *Ophioliti* **2007**, *32*, 53–56.
282. Ghikas, C.; Dilek, Y.; Rassios, A.E. Structure and tectonics of subophiolitic mélanges in the western Hellenides (Greece): Implications for ophiolite emplacement tectonics. *Int. Geol. Rev.* **2009**, *52*, 423–453. [CrossRef]

283. Mercier, J.; Vergely, P. Les mélanges ophiolitiques de Macédonie (Grèce): Décrochements d'âge anté Cretacé supérieur. *Z. Der Dtsch. Geol. Gessellschaft* **1972**, *123*, 469–489.
284. Vergely, P. Chevauchement vers l' ouest et retrochariage vers l'est des ophiolites: Deux phases tectoniques au course du Jurassique supérier-Cretacé dans les Hellénides internes. *Bul. Soc. Geol. France* **1976**, *18*, 231–244. [CrossRef]
285. Mountrakis, D.; Kilias, A.; Zouros, N. Kinematic analysis and Tertiary evolution of the Pindos-Vourinos ophiolites (Epirus-Western Macedonia, Greece). *Bull. Geol. Soc. Greece* **1993**, *28*, 111–124.
286. Nirta, G.; Bortolotti, V.; Chiari, M.; Menna, F.; Saccani, E.; Principi, G.; Vannucchi, P. Ophiolites from the Gram-mos-Arrenes area, northern Greece:geological, paleontological and geochemical data. *Ofioliti* **2010**, *35*, 103–115.
287. Nirta, G.; Moratti, G.; Piccardi, L.; Montanari, D.; Carras, N.; Catanzariti, R.; Chiari, M.; Marcucci, M. From obduction to continental collision: New data from Central Greece. *Geol. Mag.* **2018**, *155*, 377–421. [CrossRef]
288. Spray, J.G.; Roddick, J.C. Petrology and 40Ar/39Ar geochronology of some hellenic sub-ophiolite metamorphic rocks. *Contrib. Miner. Pet.* **1980**, *72*, 43–55. [CrossRef]
289. Spray, J.G.; Bébien, J.; Rex, D.C.; Roddick, J.C. Age constraints on the igneous and metamorphic evolution of the Hellenic-Dinaric ophiolites. *Geol. Soc. Lond. Speéc. Publ.* **1984**, *17*, 619–627. [CrossRef]
290. Gawlick, H.-J.; Frisch, W. The Middle to Late Jurassic carbonate clastic radiolaritic flysch sediments in the Northern Calcareous Alps: Sedimentology, basin evolution, and tectonics—An overview. *Neues Jahrb. Geol. Paläontologie Abh.* **2003**, *230*, 163–213. [CrossRef]
291. Marku, D. Report of the Projekt V1b Cretaceous of the Zepe-Guri i Nuses area. *Cent. Arch. Albanian Geol. Surv.* **2002**, 1–62.
292. Bortolotti, V.; Kodra, A.; Marroni, M.; Mustafa, F.; Pandolfi, L.; Principi, G.; Saccani, E. Geology and Petrology of ophiolitic sequences in the Mirdita region (Northern Albania). *Ofioliti* **1996**, *21*, 3–20.
293. Peza, L.H.; Markou, D. *Lower Cretaceous in the Munella Mountain (Mirdita Zone, northeastern Albania)*; Oester-reichische Akademie der Wissenschaften, Schriftenreihe der Erdwissenschaftlichen Kommission: Wien, Austria, 2002; Volume 15, pp. 365–372.
294. Mercier, J.; Vergely, P. *Geological Map of Greece, 1:50.000, Edhessa Sheet*; Institute of Geology and Mineral Exploration: Athens, Greece, 1984.
295. Pavlides, S.; Kilias, A. Neotectonic and active faults along the Serbomacedonian zone (Chalkidiki, N. Greece). *Ann. Tectonicae* **1987**, *1*, 97–104.
296. Katrivanos, E.; Kilias, A.; Mountrakis, D. Deformation history and correlation of Paikon & Tzena terranes (Axios zone, central Macedonia, Greece). *Bull. Geol. Soc. Greece* **2016**, *50*, 34–45.
297. Kilias, A. Late orogenic extension in Hellenides (In Greek with English abstract). *Bull. Soc. Geol. Greece* **2001**, *34*, 149–156. [CrossRef]
298. Michard, A.; Goffe, B.; Liati, A.; Mountrakis, D. First evidence of blueschist-facies metamorphism in the Circum-Rhodope nappes. Internal Hellenides, Greece. *Comptes Rendus Acad. Sci. Comptes Rendus Acad. Sci. Ser. II Sci. Terre Planetes* **1994**, *318*, 1535–1542.
299. Baroz, F.; Bebien, J.; Ikenne, M. An example of high-pressure low-temperature metamorphic rocks from an island-arc: The Paikon Series (Innermost Hellenides, Greece). *J. Metamorph. Geol.* **1987**, *5*, 509–527. [CrossRef]
300. Ozsvárt, P.; Kovács, S. Revised Middle and Late Triassic radiolarian ages for ophiolite mélanges: Implications for the geodynamic evolution of the northern part of the early Mesozoic Neotethyan subbasins. *Bull. Soc. Geol. Fr.* **2012**, *183*, 273–286. [CrossRef]
301. Mountrakis, D.; Tranos, M.; Papazachos, C.; Thomaidou, E.; Karagianni, E.; Vamvakaris, D. Neotectonic and seismological data concerning major active faults, and the stress regimes of Northern Greece. *Geol. Soc. Lond. Speéc. Publ.* **2006**, *260*, 649–670. [CrossRef]
302. Pavlides, S.; Mountrakis, D.; Kilias, A.; Tranos, M. The role of strike-slip movements in the extensional area of the northern Aegean (Greece). A case of transtetional tectonics. *Ann. Tectonicae* **1990**, *4*, 196–211.
303. Orozco, M.; Alonso-Chaves, F.M.; Nieto, F. Development of large north-facing folds and their relation to crustal exten-sion in the Albora´n domain (Alpujarras region, Betic Cordilleras, Spain). *Tectonophysics* **1998**, *298*, 271–295. [CrossRef]
304. Orozco, M.; Alonso-Chaves, F.M. Kilometre-scale sheath folds in the western Betics (south of Spain). *Int. J. Earth Sci.* **2011**, *101*, 505–519. [CrossRef]
305. Froitzheim, N. Formation of recumbent folds during synorogenic crustal extension (Austroalpine nappes, Switzerland). *Geology* **1992**, *20*, 923–926. [CrossRef]
306. Froitzheim, N.; Weber, S.; Nagel, T.J.; Ibele, T.; Furrer, H. Late Cretaceous extension overprinting a steep belt in the Northern Calcareous Alps (Schesaplana, Rätikon, Switzerland and Austria). *Int. J. Earth Sci.* **2012**, *101*, 1315–1329. [CrossRef]
307. Georgiev, N.; Pleuger, J.; Froitzheim, N.; Sarov, S.; Jahn-Awe, S.; Nagel, T.J. Separate Eocene–Oligocene and Miocene stages of extension and core complex formation in the Western Rhodopes, Mesta Basin, and Pirin Mountains (Bulgaria). *Tectonophysics* **2010**, *487*, 59–84. [CrossRef]
308. Georgiev, N.; Henry, B.; Jordanova, N.; Jordanova, D.; Naydenov, K. Emplacement and fabric-forming conditions of plutons from structural and magnetic fabric analysis: A case study of the Plana pluton (Central Bulgaria). *Tectonophysics* **2014**, *629*, 138–154. [CrossRef]
309. Ring, U.; Glodny, J. Geometry and Kinematics of Bivergent Extension in the Southern Cycladic Archipelago: Constraining an Extensional Hinge Zone on Sikinos Island, Aegean Sea, Greece. *Tectonics* **2021**, *40*, e2020TC006641. [CrossRef]
310. Thiebault, F. 'Evolution géodynamique des Hellénides externes en Péloponnèse méridional (Grèce). *Soc. Géol. Nord Publ.* **1982**, *6*, 574–596.

311. Thiebault, F.; Triboulet, T. Alpine metamorphism and deformation in Phyllite nappes (External Hellenides, southern Peloponnesus, Greece): Geodynamic implication. *J. Geol.* **1984**, *92*, 185–199. [CrossRef]
312. Doutsos, T.; Koukouvelas, I.; Poulimenos, G.; Kokkalas, S.; Xypolias, P.; Skourlis, K. An Exhumation model for the south Pelopenessus, Greece. *Int. J. Earth Sci.* **2000**, *89*, 350–365. [CrossRef]
313. Papazachos, B.; Delibasis, N. Tectonic stress field and seismic faulting in the area of Greece. *Tectonophysics* **1969**, *7*, 231–255. [CrossRef]
314. Papanikolaou, D.; Lykousis, V.; Chronis, G.; Pavlakis, P. A comparative study of neotectonic basins across the Hellenic arc: The Messiniakos, Argolikos, Saronikos and Southern Evoikos Gulfs. *Basin Res.* **1988**, *1*, 167–176. [CrossRef]
315. Pavlides, S.; Kondopoulou, D.; Kilias, A.; Westphal, M. Complex rotational deformations in the Serbo-Macedonian massif (north Greece): Structural and paleomagnetic evidence. *Tectonophysics* **1988**, *145*, 329–335. [CrossRef]
316. Meulenkamp, J.-E.; Jonkers, A.; Sppak, P. *Late Miocene to Early Pliocene Development of Crete*; VI Col Geol Aegean region; Pascal and Francis: Athens, Greece, 1977; pp. 269–280.
317. Hatzfeld, D.; Kassaras, I.; Panagiotopoulos, D.; Amorese, D.; Makropoulos, K.; Karakaisis, G.; Coutant, O. Microseimicity and strain pattern in northwestern Greece. *Tectonics* **1995**, *14*, 773–785. [CrossRef]
318. Papazachos, B.C.; Papazachou, C.C. *The Earthquakes of Greece: Thessaloniki*; Ziti publications: Thessaloniki, Greece, 2002; p. 315.
319. Tranos, M.D.; E Papadimitriou, E.; Kilias, A.A. Thessaloniki–Gerakarou Fault Zone (TGFZ): The western extension of the 1978 Thessaloniki earthquake fault (Northern Greece) and seismic hazard assessment. *J. Struct. Geol.* **2003**, *25*, 2109–2123. [CrossRef]
320. Sengör, A.M.C.; Yilmaz, Y. Tethyan evolution of Turkey: A plate tectonic approach. *Tectonophysics* **1981**, *75*, 181–241. [CrossRef]
321. Sengör, A.M.C.; Yılmaz, Y.; Sungurly, O. Tectonics of the Mediterranean Cimmerides: Nature and evolution of the western termination of Paleo-Tethys. *Geol. Soc. Lond. Spec. Publ.* **1984**, *17*, 77–112. [CrossRef]
322. Akal, C.; Koralay, O.E.; Candan, O.; Roland, O.; Chen, F. Geodynamic Significance of the Early Triassic Karaburun Granitoid (Western Turkey) for the Opening History of Neo-Tethys. *Turk. J. Earth Sci.* **2011**, *20*, 255–271. [CrossRef]
323. Akal, C.; Candan, O.; Koralay, O.E.; Oberhänsli, R.; Chen, F.; Prelević, D. Early Triassic potassic volcanism in the Afyon Zone of the Anatolides/Turkey: Implications for the rifting of the Neo-Tethys. *Int. J. Earth Sci.* **2012**, *101*, 177–194. [CrossRef]
324. Candan, O.; Akal, C.; Koralay, O.; Okay, A.; Oberhänsli, R.; Prelević, D.; Mertz-Kraus, R. Carboniferous granites on the northern margin of Gondwana, Anatolide-Tauride Block, Turkey – Evidence for southward subduction of Paleotethys. *Tectonophysics* **2016**, *683*, 349–366. [CrossRef]
325. Carras, N.; Fazzuali, M.; Photiades, A. Transition from carbonate platform to pelagic deposition (Mid Jurassic to Late Cretaceous), Vourinos massif, Northern Greece. *Riv. Ital. Paleontol. Stratigr.* **2004**, *110*, 345–355.
326. Kolokotroni, C.N.; Dixon, J.E. The origin and emplacement of the Vrondou granite, NE Greece. *Bull. Geol. Soc. Greece* **1991**, *25*, 469–483.
327. Gautier, P.; Brun, J.P. Crustal-scale geometry and kinematics of late-orogenic extension in the central Aegean (Cyclades and Evvia island). *Tectonophysics* **1994**, *238*, 399–424. [CrossRef]
328. van Hinsbergen DJ, J.; Zachariasse, W.J.; Wortel MJ, R.; Meulenkamp, J.E. Underthrusting and exhumation: A comparison between the External Hellenides and the "hot" Cycladic and "cold" South Aegean core complexes (Greece). *Tectonics* **2005**, *24*, 1–19. [CrossRef]
329. Xypolias, P.; Spanos, D.; Chatzaras, V.; Kokkalas, S.; Koukouvelas, I. Vorticity of flow in ductile thrust zones: Examples from the Attico-Cycladic Massif (Internal Hellenides, Greece). *Geol. Soc. Lond. Spec. Publ.* **2010**, *335*, 687–714. [CrossRef]
330. Xypolias, P.; Iliopoulos, I.; Chatzaras, V.; Kokkalas, S. Subduction- and exhumation-related structures in the Cycladic Blueschists: Insights from south Evia Island (Aegean region, Greece). *Tectonics* **2012**, *31*. [CrossRef]
331. Schwartz, S.; Stoeckhert, B. Pressure solution in siliciclastic HP-LT metamorphic rocks -constraints on the state of stress in deep levels of accretionary complexes. *Tectonophysics* **1996**, *255*, 203–209. [CrossRef]
332. Xypolias, P.; Doutsos, T. Kinematics of rock flow in a crustal-scale shear zone: Implication for the orogenic evolution of the southwestern Hellenides. *Geol. Mag.* **2000**, *137*, 81–96. [CrossRef]
333. Xypolias, P.; Kokkalas, S. Heterogeneous ductile deformation along a mid-crustal extruding shear zone: An example from the External Hellenides (Greece). *Geol. Soc. Lond. Spec. Publ.* **2006**, *268*, 497–516. [CrossRef]
334. Papanikolaou, D.; Vassilakis, E. Thrust faults and extensional detachment faults in Cretan tectono-stratigraphy: Impli-cations for Middle Miocene extension. *Tectonophysics* **2010**, *488*, 233–247. [CrossRef]
335. Brun, J.-P.; Faccenna, C. Exhumation of high-pressure rocks driven by slab rollback. *Earth Planet. Sci. Lett.* **2008**, *272*, 1–7. [CrossRef]